THREE-STATE SENTIMENT DYNAMICS

Inaugural-Dissertation
zur Erlangung des akademischen Grades einer Doktorin
der Wirtschafts- und Sozialwissenschaften
der Wirtschafts- und Sozialwissenschaftlichen Fakultät
der Christian-Albrechts-Universität zu Kiel

vorgelegt von
DIPL. MATH. VERONIKA PENNER
aus Petrowka, Russland

Kiel, 2020

Erstbegutachtung: Prof. Dr. Thomas Lux
Zweitbegutachtung: Prof. Dr. Uwe Jensen

Tag der mündlichen Prüfung: 20. Dezember 2019

Table of Contents

List of Tables

List of Figures

1 Introductory Remarks

The expectations about the development of a single selected variable, e.g. price or return rate, in the next period influences long-term decisions of economic agents. While homogeneous rational expectations are still the ruling paradigm in economic theory, expectations in reality are more diversified. Among others, Akerlof and Shiller (2009) state that agents making economic decisions are often emotional and intuitive and they tend toward irrational decisions. Therefore an alternative approach needs to be considered. It should incorporate that these decisions are based on an opinion index which captures a 'market mood' or 'sentiment'.

One approach to formalize this idea in a canonical framework goes back to the work of Weidlich and Haag (1983). They assume that agents can choose between two opinions in a probabilistic manner. Models incorporating sentiment dynamics mostly focus on two attitudes, i.e. positive/negative, optimistic/pessimistic or bullish/bearish. There exists a large variety of economic related models incorporating the idea of a sentiment index. The modeling of opinion formation, based on interactions between two groups has attracted the interest of an increasing number of researchers, cf. Franke (2007), Toscani (2006), Düring et al. (2009) and Lux (2012).

The main objective of this thesis is a more plausible modeling of the dynamic components, i.e. sentiment dynamics, in a stochastic framework. Therefore it is necessary to review the existing definitions of sentiment variables by extending the possible set of attitudes of the agents. Let us consider a boom phase of the economy in which most of the agents are optimistic. These agents will become sceptical if bad news arrive. However, this does not imply that they immediately adopt the opposite extreme attitude, i.e. the pessimistic attitude. Instead, many situations are conceivable where these optimistic agents first wait and check if there are any changes regarding their objective function. In a formal model this behavior could be represented by letting part of the agents first switch from optimism to neutrality. One may hope that additional phenomena might emerge in the new framework that could not possibly occur previously.

There are already models in the literature which contain three or even more attitudes in a setup of opinion dynamics, see Hohnisch et al. (2005), Gomes and Sprott (2017) and Franke and Westerhoff (2019). We follow the latter contribution and include the neutral sentiment into different versions of stochastic models. This is partially motivated by the fact that most surveys include data on neutrality but in the empirical literature it is often neglected in favor of the two extreme attitudes. These models have no neutral sentiment incorporated and therefore they ignore the corresponding data or redistribute the relevant shares. At best the neutral attitude is understood as intermediate state.

Empirical literature on investor sentiment related to financial markets can be found for several data providers: *ZEW* (Lahl and Hüfner (2003), Franke (2007)), *sentix* (Hengelbrock et al. (2013), Menkhoff et al. (2010), Heiden et al. (2013), Schmeling (2007)), *animusX (Lux (2010))* and *AAII* (Fisher and Statman (2000), Brown and Cliff (2004)) and other providers (Akhtar et al. (2011), Entorf et al. (2012)).

There is also literature on macroeconomic applications of such sentiment models, cf. Franke and Westerhoff (2017) and Franke (2012). These contributions use two approaches which equip the agents with time-varying probabilities for switches between alternatives. One approach introduces the concept of transition probabilities and the second one uses logit probabilities from discrete choice theory. In both cases, the probabilities are functions of other variables in the model. The transition probability approach typically includes a majority index in a way that makes it possible to capture herding, while applications of the discrete choice approach mostly refer to the current utility of two options. However, in both approaches the probabilities can depend on the same set of variables.

Both approaches are pursued in this thesis. They lead to three-state models of sentiment dynamics with attitudes bold, cautious and neutral. Individual transition probabilities cause shifts in the shares of these three groups of agents. Additionally an embedded 'herding' component allows for behavioral changes.

This thesis is organized as follows. In Section 2, we introduce the agents' feedback-guided transition probabilities that govern their switches between three attitudes and

two deterministic adjustment equations for the aggregated attitudes are presented. The stability and bifurcation behavior of the system are analyzed. We consider a version with modified feedback index in terms of included weight and the corresponding dynamical system is subject to a bifurcation analysis. The next section deals with a discrete-choice version of the original model. The stability and bifurcation behavior are analyzed. In Section 4 a three-state stochastic model of investor sentiment is presented and the parameters are estimated via maximum likelihood. Details on the data and estimation methodology are provided. Additionally, several parameter restricted models are analyzed and their out-of-sample forecasts are compared. Concluding Remarks are given in Section 5. Additional figures, respectively proofs of some technical results and mathematical derivations are provided in the Graphical Appendix, respectively Mathematical Appendix.

2 Transition Probability Approach

This chapter presents a three-state model of sentiment dynamics with attitudes bold, cautious and neutral. Individual transition probabilities cause shifts in the shares of these three groups of agents, an embedded herding component allows for behavioral changes.

2.1 Introduction

Transition probabilities are incorporated in several models of investor sentiment. In Barberis et al. (1998) probabilities are assigned to two states by one single agent. These states differ in their process of governing earnings. A more traditional definition of transition probabilities refers to the change of attitudes between groups. This is possible for more than two sentiments, cf. Gomes and Sprott (2017). They formulate a model with five categories of agents and their transition probabilities are not individual but uniform for all categories.

Franke and Westerhoff (2019) have designed a macroeconomic agent-based model with three-state sentiment dynamics. They also use the framework of transition probabilities for changes between attitudes and they include a Goodwinian augmentation of these sentiment dynamics which has not been considered in the macroeconomic literature so far. In a similar way Franke (2018) presents a two-state approach and a three-state approach which are separately integrated into a macroeconomic framework.

We also apply the extension of these latter contributions and include the neutral sentiment into two versions of a transition probability approach. Each group of agents is equipped with their own set of individual transition probabilities. The definition of these probabilities hinges on the specification of sentiment indices; or broader feedback indices. Here a rare sentiment ratio including the neutral attitude is defined and extended such that we obtain feedback indices. Furthermore we present an augmented feedback component which gives rise to more complex dynamics. In this second scenario agents use a linear combination of the traditional sentiment variable, i.e. the difference of the

two extreme attitudes, and the novel sentiment variable including neutrality. This second version tries to mimic the considerations taken into account by agents in more detail.

Assume there is a small-sized share of bearish traders on a financial market during a period of rising stock prices. The share of inactive traders holding stocks, i.e. neutral traders, is small-sized as well. It is obvious that the large-sized share of bullish traders has an influence on the other groups of traders and this scenario is captured by the augmented version.

It needs to be mentioned that this chapter contains purely theoretical considerations and an extensive analysis of the resulting nonlinear dynamical systems.[1]

2.2 Sentiment Dynamics

Let the business sector be populated by N firms, or more general, agents, whose number remains invariant. At each point in time a single agent can be characterized as having one of three attitudes: optimistic or bold (b), pessimistic or cautious (c), and neutral (0). Correspondingly, let n_t^b, n_t^c and n_t^0 be the number of bold, cautious and neutral agents, respectively, and $b_t = n_t^b/N,\ c_t = n_t^c/N$ the fractions of bold and cautious agents. The fraction of neutral agents is expressed in terms of the residual $1 - b_t - c_t$.

Agents may change their attitude over time. For the moment being, we consider this process in discrete time with adjustment periods of length $\Delta t > 0$. The changes will depend on a great variety of macroscopic aspects and idiosyncratic circumstances, which one will not want to specify in all of their details. It rather seems suitable to introduce random elements in this respect, in order to keep the modeling simple and to avoid arbitrary assumptions. Therefore, the basic concept to describe the changes in the business climate are the transition probabilities of the individual agents: at time t, let π_t^{rs} be the probability *per unit of time* that an agent changes from attitude r to attitude s with $r, s \in \{b, c, 0\}$, $r \neq s$. More precisely, $\Delta t\, \pi_t^{rs}$ is the probability that an agent with attitude r at time t will have turned to attitude s at the end of the period at

[1] In Medio (1992) and Medio and Lines (2003) several applications of nonlinear dynamical systems in the field of economics can be found.

$t+\Delta t$. These probabilities are predetermined and fixed within that period, though they will endogenously evolve over time in response to the evolution of other variables in the economy.

With more information the behavior of individual agents could be described in terms of probabilities, conditional on events at the micro level, or each agent could be equipped with transition probabilities of its own. Hence, being interested in the macroscopic adjustments, we can abstract from the idiosyncratic circumstances of the agents that are currently entertaining attitude r and view π_t^{rs} as their representative transition probability of switching to attitude s, given the realizations of the aggregate variables considered below.

To derive a law of motion for the macroscopic population shares b_t and c_t, we draw on an elementary argument put forward by Alfarano and Lux (2005).[2] For simplicity, we assume that the agents do not directly switch from one extreme to the other; only neutral agents can become bold or cautious within an adjustment period. Hence, the number of bold agents evolves over time

$$n^b_{t+\Delta t} \;=\; n^b_t \;+\; k^{0b}_t \;-\; k^{b0}_t, \tag{1}$$

where k^{0b}_t is the number of originally neutral agents that have turned bold by the end of period, and k^{b0}_t is the number of agents that have switched from bold to neutral.

The number k^{0b}_t arises from n^0_t random draws, one for each neutral agent, with probability $\Delta t\, \pi^{0b}_t$ for the event that the agent switches to bold. That is, k^{0b}_t is the sum of the cases when this event occurs. Accordingly, when viewed as a random variable, k^{0b}_t has a binomial distribution $B(n^0_t, \Delta t\, \pi^{0b}_t)$.[3] By the same token, the number of agents k^{b0}_t converting from bold to neutral is distributed as $B(n^b_t, \Delta t\, \pi^{b0}_t)$.

[2]They present it in Appendix A1 and A2 because the apparatus of statistical mechanics is needed for their analysis.

[3]A binomial distribution $B(m, \pi)$ is the probability distribution for the number of successes (k) in a sequence of m independent success/failure experiments, each of which yields success with probability π. The probability of getting exactly k successes is given by $\binom{m}{k} \pi^k (1-\pi)^{m-k}$, the mean of the distribution is $m\pi$, and the variance $m\pi(1-\pi)$.

The expected values of these variables are

$$\begin{aligned} E(k_t^{0b}) &= (1 - b_t - c_t)\, N\, \Delta t\, \pi_t^{0b}, \\ E(k_t^{b0}) &= b_t\, N\, \Delta t\, \pi_t^{b0} \end{aligned}$$

and their variances amount to

$$\begin{aligned} Var(k_t^{0b}) &= (1 - b_t - c_t)\, N\, \Delta t\, \pi_t^{0b}\, (1 - \Delta t\, \pi_t^{0b}), \\ Var(k_t^{b0}) &= b_t\, N\, \Delta t\, \pi_t^{b0}\, (1 - \Delta t\, \pi_t^{b0}). \end{aligned}$$

If the expected values are large enough, the two binomial distributions are well approximated by the Gaussian distributions with the same first and second moments. This is ensured if there are sufficiently many agents and the population shares are not too close to the boundaries, i.e. $b_t \gg 0$ and $1 - b_t - c_t \gg 0$. We assume that the following conditions hold

$$k_t^{0b} = E(k_t^{0b}), \qquad k_t^{b0} = E(k_t^{b0}).$$

Furthermore, the difference of two normally distributed random variables is normally distributed as well, its mean being the difference between the two single means and its variance the sum of the two single variances. For the random variable $k_t = k_t^{0b} - k_t^{b0}$, we thus have

$$\begin{aligned} E(k_t) &= \Delta t \cdot [(1 - b_t - c_t)\, \pi_t^{0b} - b_t\, \pi_t^{b0}] \cdot N \\ Var(k_t) &= \Delta t \cdot [(1 - b_t - c_t)\, \pi_t^{0b}\, (1 - \Delta t\, \pi_t^{0b}) + b_t\, \pi_t^{b0}\, (1 - \Delta t\, \pi_t^{b0})] \cdot N \end{aligned}$$

To derive the law governing the adjustments of b_t a sufficiently large population is assumed, so that the intrinsic noise from different realizations can be neglected. By dividing Eq. (1) by N and the changes in the number of groups are directly given by the product of size and transition probability. The fraction of bold agents decreases by

$\Delta t\, b_t\, \pi_t^{b0}$ due to the agents leaving this group, and it increases by $\Delta t\,(1-b_t-c_t)\,\pi_t^{0b}$ because of the neutral agents who newly join in. We thus arrive at a deterministic adjustment equation that governs the changes in the fraction b_t of bold agents,

$$b_{t+\Delta t} \;=\; b_t \;+\; \Delta t \cdot [(1-b_t-c_t)\,\pi_t^{0b} - b_t\,\pi_t^{b0}] \tag{2}$$

As in the derivation of Eq. (2) the population size N was supposed to be large. Furthermore, the process of letting the adjustment period shrink to zero is well defined in the limit $\Delta t \to 0$ and allows for a continuous time setting. Since the changes in the fraction c_t of cautious agents can be derived analogously to Eq. (2), the analysis so far can thus be summarized by the following two differential equations

$$\begin{aligned} \dot{b} &= (1-b-c)\,\pi^{0b} - b\,\pi^{b0}, \\ \dot{c} &= (1-b-c)\,\pi^{0c} - c\,\pi^{c0}. \end{aligned} \tag{3}$$

The further exploration of system (3) hinges on the specification of the transition probabilities $\pi^{0b}, \pi^{b0}, \pi^{0c}$ and π^{c0}.

2.2.1 Feedback-based Transition Probabilities

The transition probabilities change in response to the variations of a set of several variables that the agents observe. These effects can generally be summarized in a single feedback index f_b when we consider the flux of agents towards and out of a bold attitude. The index is allowed to attain positive and negative values in different stages the economy goes through. Let positive and negative values of f_b be related to the probability π^{0b} of switching from neutral to bold. That is, an increase in the feedback index increases π^{0b} and decreases the probability π^{b0}.

In the concept of Weidlich and Haag (1983) it is assumed that the changes of the transition probabilities depend on the changes of the index f_b in a linear way. More precisely, they assume that the relative changes are linear in f_b, so that we have $d\pi^{0b}/\pi^{0b} = A\,df_b$ for some constant A. Without loss of generality, A can be taken to be unity. Symmetry

is another natural assumption to make. Here, we refer to symmetry of transition probabilities, which gives us $d\pi^{b0}/\pi^{b0} = -df_b$. Note that possible risk aversion, according to which the agents show a greater tendency to switch to neutral rather than to one of the extreme attitudes, can be captured by a suitable specification of the feedback index.

The transition probabilities of switches in and out of a cautious attitude can be similarly treated by referring to a feedback index f_c. Introducing $\nu > 0$ as constant for the speed of adjustment, the functional specification of the four transition probabilities reads,

$$\begin{aligned} \pi^{0b} = \pi^{0b}(f_b) &= \nu \exp(f_b), & \pi^{b0} = \pi^{b0}(f_b) &= \nu \exp(-f_b), \\ \pi^{0c} = \pi^{0c}(f_c) &= \nu \exp(f_c), & \pi^{c0} = \pi^{c0}(f_c) &= \nu \exp(-f_c). \end{aligned} \tag{4}$$

Certainly, employing the exponential function ensures positive values of the probabilities. The complementary condition that the feedback index is bounded in order to ensure that the probabilities in terms of the fixed time unit are bounded, too, should be a property of the model into which the specifications in (4) are incorporated. Using the transition probabilities in (4), the two differential equations in (3) for the evolution of the population shares b and c become

$$\begin{aligned} \dot{b} &= \nu\,[\,(1-b-c)\,\exp(f_b) \;-\; b\,\exp(-f_b)\,], \\ \dot{c} &= \nu\,[\,(1-b-c)\,\exp(f_c) \;-\; c\,\exp(-f_c)\,]. \end{aligned} \tag{5}$$

The variables b and c are supposed to take values within the co-domain of the unit simplex

$$S \;:=\; \{(b,c) \in [0,1]^2 |\; b + c \;\leq\; 1\}.$$

For carefully chosen feedback indices f_b and f_c, it is immediately observed that the pair (b, c) does not leave the unit simplex. Additionally, the pair (b, c) is also repelled from its boundary. In fact, when the fraction of bold agents b (or cautious agents c)

tends toward unity, the second term in the square bracket of system (5) will eventually dominate the first one, so that the derivative of b will become negative from then on (or $\dot{c} < 0$, respectively). On the other hand, when the neutral attitude tends to attract all of the agents, such that $b + c \to 0$, the right-hand side of system (5) will eventually turn positive and we have $\dot{b} > 0$ as well as $\dot{c} > 0$.

The exponential function in the specification of the transition probabilities in (4) has been introduced to make their relative changes linearly dependent on the changes in the feedback index, thus preventing the probabilities from falling down to zero. It bears emphasizing that apart from the exponential function no further nonlinearity is required for this global self-stabilization mechanism to work out. As far as the adjustments of the population shares of bold and cautious agents and their impact on the macroeconomy are concerned, there is no need for additional restrictions on the model parameters.

While the equations in (4) provide a first and useful organizational device, the meaningfulness of the model rests on the variables that make up the feedback indices. Here we first concentrate on the interactions of the agents without a feedback from fundamental macroeconomic data.

2.2.2 Pure Sentiment Dynamics

A key word to describe pure sentiment dynamics is herding.[4] Literally taken, a single firm asks other firms, e.g. friends, business partners and competitors for their opinion about the future, and it may then show a certain tendency to join the majority. The channels of opinion propagation may, however, also be more indirect, through the media or more specialized sources from which the firms can derive information about the distribution of current attitudes. In any case, the basic concept is that a widely disseminated attitude will attract further adherents. This is in line with the previous literature, such as Düring et al. (2009), Lux and Marchesi (1999) and Toscani (2006).

[4]Lux (1995) analyzes herding in speculative markets and the emergence of bubbles due to contagion of opinions. A business sentiment variable with a herding component in a macroeconomic framework is defined in Franke (2012).

Considering the probability π^{0b} (π^{0c}) of switching from neutral to bold (cautious), the concept implies that π^{0b} (π^{0c}) increases if the number of bold (cautious) agents rises relative to the number of neutral agents. The differences between the adherents of the two attitudes enter the feedback indices f_b and f_c, respectively, where they are expressed as percentage ratios,

$$\begin{aligned} \frac{n^b - n^0}{N} &= b - (1-b-c) = 2b + c - 1\,, \\ \frac{n^c - n^0}{N} &= c - (1-b-c) = 2c + b - 1\,. \end{aligned} \tag{6}$$

The intensity of this herding is measured by two positive coefficients ϕ_{hb} and ϕ_{hc}. To account for a possible risk aversion of agents we introduce two coefficients α_b and α_c. The two feedback indices are thus given by

$$\begin{aligned} f_b &= -\alpha_b + \phi_{hb}\,(2b + c - 1) \\ f_c &= -\alpha_c + \phi_{hc}\,(2c + b - 1) \end{aligned} \tag{7}$$

Positive coefficients α_b and α_c express a risk aversion of the agents to switch from neutral to a bold or cautious attitude rather than into the opposite direction. This is most clearly seen when the other term in the feedback index vanishes, in which case, according to specifications in (4), $\pi^{0r} = \nu \exp(-\alpha_r) < \nu \exp(\alpha_r) = \pi^{r0}$ for $r = b, c$. Different coefficients allow for the possibility that the agents' risk aversion may be different for turning bold and cautious. Of course, a negative coefficient α_b or α_c can be interpreted as risk-seeking behavior.

To sum up, the pure sentiment dynamics is constituted by the two differential equations in (5) together with the specification of the feedback indices in (7). The basic properties to which this dynamical system gives rise will already be seen from the case of neutral risk aversion and uniform herding, i.e., $\alpha_b = \alpha_c = 0$ and $\phi = \phi_{hb} = \phi_{hc}$.[5]

[5] A similar model, which likewise can exhibit multiple equilibria, is Foster and Flieth (2002).

2.3 Stability Analysis

After establishing the basic principles of the dynamical system, the following analysis focuses on the analytical calculation of the explicit solutions of the two differential equations given by the nonlinear system (5), if possible, and on the numerical derivation of solutions.[6]

Stability analysis exhibits what will happen if the system starts not exactly at the equilibrium point, but in the neighborhood of it. It is not only crucial to know whether the system will converge to the equilibrium or diverge from it but also the nature of the dynamic paths, when the dynamical system is perturbed and moves away from the equilibrium.

The analysis takes place in the (b, c)-phase plane and concentrates on the qualitative properties of isoclines which are level curves of the differential equations $\dot{b}$ and $\dot{c}$ with a fixed slope m. In order to determine the equilibria of system (5), and check their stability behavior, the dynamics need to come to rest, i.e. $m = 0$ or more precisely $\dot{b} = 0$ and $\dot{c} = 0$. When using the expression isoclines in the following it is done with reference to these identities.

It is possible to show that for each ordinary differential equation $\dot{b}$ and $\dot{c}$ with a fixed herding parameter ϕ two types of isoclines occur, more precisely the first isocline has a linear structure for all values of ϕ while the second isocline, emerging for $\phi > 1$, is of nonlinear parabolic form.

Additionally this model has no natural time unit incorporated and that is the reason why without loss of generality the parameter regulating the speed of adjustment can be set equal to unity, i.e. $\nu = 1$, since only qualitative properties are of interest. This results in the following system of ordinary differential equations[7]

[6] See Khalil (2002) and Seydel (1988) for more information on the stability analysis for nonlinear systems.

[7] For a subsequent investigation of occurring phenomena related to the herding parameter ϕ it is useful to transform the two differential equations in (5) expressed in terms of the exponential function into a system using hyperbolic functions, see Appendix B.1.1.1 for the derivation.

$$\begin{aligned} \dot{b} &= [\,(1-c)\,\tanh(f_b)\, -(\,2b+c-1)]\,\cosh(f_b) \\ &=: F_b(b,c;\phi) \\ \dot{c} &= [\,(1-b)\,\tanh(f_c)\, -(\,2c+b-1)]\,\cosh(f_c) \\ &=: F_c(b,c;\phi)\,, \end{aligned} \tag{8}$$

with feedback indices f_b and f_c containing a neutrality in risk aversion and uniform herding given by

$$f_b = \phi\,(2b+c-1) \quad , \qquad f_c = \phi\,(2c+b-1). \tag{9}$$

These feedback indices lead to symmetric transition probabilities $\pi^{0b} = \pi^{b0}$ and $\pi^{0c} = \pi^{c0}$ if the share of agents with neutral attitude and the share of bold, respectively cautious agents are equal. Hence the feedback components in (6) are zero, i.e. $2b+c-1=0$ and $2c+b-1=0$. These identities lead to vanishing feedback effects, i.e. $f_b = f_c = 0$. Thus, rearranging the two homogeneous differential equations $F_b(b,c)=0$ and $F_c(b,c)=0$ results in two linear isoclines LI_b and LI_c

$$\begin{aligned} c &= LI_b(b) := -2b+1 \\ &:\Rightarrow \quad \dot{b} = F_b(b,c) = 0, \\ c &= LI_c(b) := -\tfrac{1}{2}b + \tfrac{1}{2} \\ &:\Rightarrow \quad \dot{c} = F_c(b,c) = 0\,. \end{aligned} \tag{10}$$

It is obvious that both linear isoclines are decreasing functions in c and intersect in $(b^s, c^s) = (\frac{1}{3}, \frac{1}{3})$ which is denoted by the *symmetric equilibrium* since the fractions of bold, cautious and neutral agents are divided equally. Additionally it is crucial to mention that both linear isoclines are actually independent of the uniform herding parameter ϕ.

In order to analyze the stability behavior of the underlying dynamical system it is

necessary to determine its Jacobian matrix. Denoting the first-order partial derivatives of (8) by $F_{bb} = \frac{\partial F_b}{\partial b}$, $F_{bc} = \frac{\partial F_b}{\partial c}$, $F_{cb} = \frac{\partial F_c}{\partial b}$ and $F_{cc} = \frac{\partial F_b}{\partial c}$ the corresponding Jacobian,

$$J = \begin{bmatrix} F_{bb} & F_{bc} \\ F_{cb} & F_{cc} \end{bmatrix}, \tag{11}$$

has the following entries:

$$\begin{aligned} F_{bb} &= \big[\, 2\phi(1-c) - 2 - 2\phi(\,2b + c - 1\,)\tanh(f_b)\,\big]\cosh(f_b), \\ F_{cc} &= \big[\, 2\phi(1-b) - 2 - 2\phi(\,2c + b - 1\,)\tanh(f_c)\,\big]\cosh(f_c), \\ \\ F_{bc} &= \big[\, \phi(1-c) - 1 - \big(\,1 + \phi(\,2b + c - 1\,)\big)\tanh(f_b)\,\big]\cosh(f_b), \\ F_{cb} &= \big[\, \phi(1-b) - 1 - \big(\,1 + \phi(\,2c + b - 1\,)\big)\tanh(f_c)\,\big]\cosh(f_c). \end{aligned}$$

Both the main diagonal elements, F_{bb} and F_{cc}, as well as both off-diagonal elements, F_{bc} and F_{cb}, are symmetric with respect to the representation of the underlying nonlinear equations in the state variables b and c. Therefore this matrix has a symmetric structure. The trace $tr(J)$ and determinant $det(J)$ of the Jacobian J,

$$\begin{aligned} tr(J) &= F_{bb} + F_{cc} \\ &= \big[\, 2\phi(1-c) - 2 - 2\phi(\,2b + c - 1\,)\tanh(f_b)\,\big]\cosh(f_b) \\ &\quad + \big[\, 2\phi(1-b) - 2 - 2\phi(\,2c + b - 1\,)\tanh(f_c)\,\big]\cosh(f_c), \\ \\ det(J) &= F_{bb}F_{cc} - F_{bc}F_{cb} \\ &= \cosh(f_b)\cosh(f_c)\Big[\big[\, 2\phi(1-c) - 2 - 2\phi(\,2b + c - 1\,)\tanh(f_b)\,\big] \\ &\quad \cdot\big[\, 2\phi(1-b) - 2 - 2\phi(\,2c + b - 1\,)\tanh(f_c)\,\big] \\ &\quad - \big[\, \phi(1-c) - 1 - \big(\,1 + \phi(\,2b + c - 1\,)\big)\tanh(f_b)\,\big] \\ &\quad \cdot\big[\, \phi(1-b) - 1 - \big(\,1 + \phi(\,2c + b - 1\,)\big)\tanh(f_c)\,\big]\Big], \end{aligned}$$

lead to this discriminant[8]

$$\begin{aligned}\Delta &= tr(J)^2 - 4\,det(J) \\ &= \big[\big(\,2\phi(1-c) - 2 - 2\phi(\,2b + c - 1\,)\tanh(f_b)\,\big)\cosh(f_b) \\ &\quad -\big(\,2\phi(1-b) - 2 - 2\phi(\,2c + b - 1\,)\tanh(f_c)\,\big)\cosh(f_c)\big]^2 \\ &\quad + \cosh(f_b)\cosh(f_c) \\ &\quad \cdot\big[\,2\phi(1-c) - 2 - \big(\,2\phi(\,2b + c - 1\,) + 2\,\big)\tanh(f_b)\,\big] \\ &\quad \cdot\big[\,2\phi(1-b) - 2 - \big(\,2\phi(\,2c + b - 1\,) + 2\,\big)\tanh(f_c)\,\big].\end{aligned} \tag{12}$$

The sign of Δ of the corresponding Jacobian J is fundamental for the determination of the limit behavior type.
Two cases depending on the herding component ϕ are considered hereafter.

2.3.1 Herding Intensity $\phi < 1$

The linear isoclines LI_b and LI_c are given explicitly, and as long as the herding component ϕ does not exceed unity the phase plane representation restricted to the co-domain of the unit simplex S remains unaltered.[9]

The following proposition contains a basic conclusion.

Proposition 1: [The analogous statement holds for LI_c and $F_c(b, c, \phi) = 0$]

If $\phi < 1$, then the linear isocline LI_b is the only isocline of $\dot{b} = 0$,
i.e. $\dot{b} = F_b(b, c) = 0 \quad \Rightarrow \quad c = LI_b(b)$.

Taken together, LI_b and LI_c imply the following statement:

[8] See Appendix B.1.1.2 for the derivation.

[9] See Cooper (2001) and Shone (2002) for comments on the setup of phase plane representations.

Corollary 1:

If $\phi < 1$, then the symmetric equilibrium $(b^s, c^s) = (\frac{1}{3}, \frac{1}{3})$ is the only equilibrium.

We turn to the local stability properties of the system. The resulting Jacobian evaluated at the symmetric equilibrium is given by

$$J_{|(b^s,c^s)} = \begin{bmatrix} -2 + \frac{4}{3}\phi & -1 + \frac{2}{3}\phi \\ \\ -1 + \frac{2}{3}\phi & -2 + \frac{4}{3}\phi \end{bmatrix}.$$

The Jacobian J is a function of the herding intensity ϕ. $J(\phi)$ is real and symmetric and therefore a Hermitian matrix with real eigenvalues only, for all values of ϕ.

The symmetric equilibrium $(b^s, c^s) = (\frac{1}{3}, \frac{1}{3})$ is at least a locally stable node for all herding intensities $\phi < \frac{3}{2}$. This equilibrium is even globally stable for a herding parameter $\phi < 1$ since only linear isoclines occur and a single symmetric equilibrium point is given (cf. Proposition 1 and Corollary 1).

Figure 1 shows the phase plane representation of the isoclines $F_b = 0$ and $F_c = 0$. The b-axis, respectively c-axis, displays the share of bold agents b, respectively the share of cautious agents c. Additionally trajectory dynamics for $\phi < 1$ are depicted. The intersection point of both isoclines constitutes the equilibrium which is stable. From the trajectories in Fig. 1 and the local stability properties it can be concluded that the boundaries of the unit simplex are repelling.

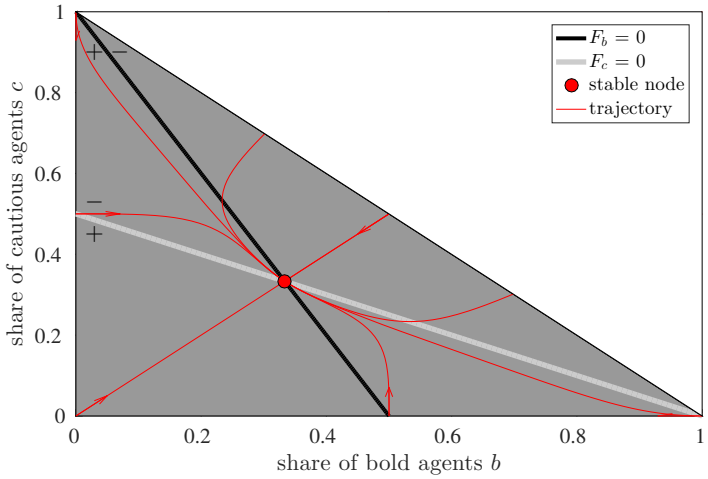

Figure 1: Phase plane representation of isoclines $F_b = 0$ (black) and $F_c = 0$ (white), trajectory dynamics for $\phi < 1$ (red) with stable equilibrium (red dot). $+/-$ indicate $F_b \gtrless 0$, respectively $F_c \gtrless 0$.

Before we proceed with additional nonlinear dynamics and a global stability analysis a summary of the fundamental results is provided.

Proposition 2:

With respect to a herding parameter $\phi < 1$ the following holds for system (8), cf. Fig. 1:

1. The unique symmetric equilibrium $(b^s, c^s) = (\frac{1}{3}, \frac{1}{3})$ exhibits global asymptotic stability (see stable node in Fig. 1) and is approached monotonically (see trajectories in Fig. 1).
2. For all values of ϕ two isoclines LI_b and LI_c are located in the phase plane, they are linear and strictly decreasing.
3. The linear isoclines LI_b and LI_c can be computed explicitly and are given by the equations in (10).

2.3.2 Herding Intensity $\phi \geq 1$

So far the focus has been on linear isoclines which lead to simple dynamics only. If nonzero feedback effects are considered, additional parabolic isoclines PI_b and PI_c emerge in the phase plane:

$$\begin{aligned} c &= PI_b(b;\phi) \quad \Rightarrow \quad \dot{b} = F_b(b,c;\phi) = 0, \\ c &= PI_c(b;\phi) \quad \Rightarrow \quad \dot{c} = F_c(b,c;\phi) = 0\,. \end{aligned} \tag{13}$$

Unlike the linear isoclines LI_b and LI_c, which can be computed explicitly, it needs to be mentioned that PI_b and PI_c are implicit functions.[10] Due to their nonlinear form complex dynamics are possible. Figure 2 shows the phase plane evolution of $F_b = 0$ for increasing values of ϕ.[11]

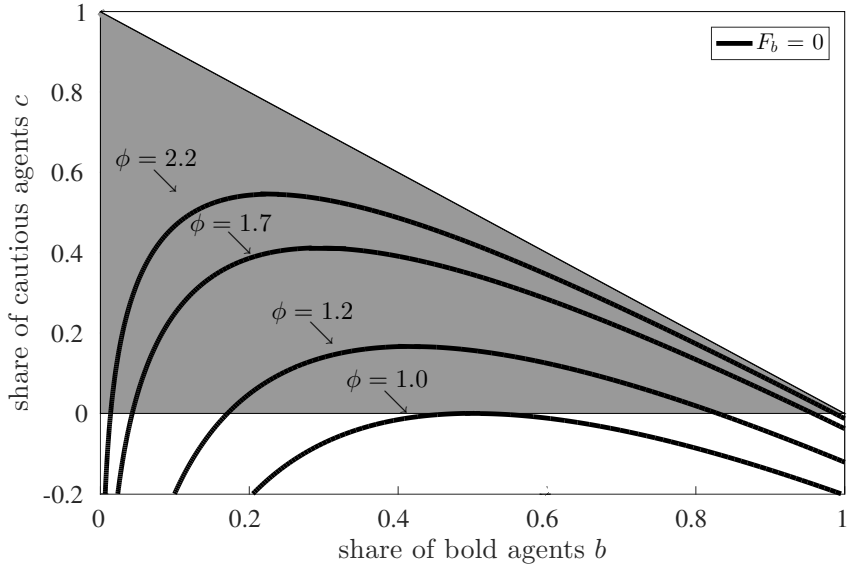

Figure 2: Phase plane representation of upward moving parabolic isoclines $F_b = 0$ for increasing $\phi = 1.0, 1.2, 1.7$ and 2.2. Axis of ordinates is extended to show the first appearance of parabolic isocline for $\phi = 1.0$.

[10] Numerical solution methods of ordinary differential equations equations can be found in Stanoyevitch (2005), Zwillinger (1989), Jordan and Smith (2007a) and Jordan and Smith (2007b).

[11] Lynch (2004) provides an introduction to the theory of dynamical systems with the aid of MATLAB, especially the Symbolic Toolbox. It is needed for the graphical representation of implicit functions.

The parabolic isoclines for different values of the herding component ϕ arise from the b-axis and their peaks stretch in the direction of the upper left corner of the phase plane. At some point these isoclines adapt completely to the boundaries of the unit simplex. The very same evolution can be observed for the second parabolic isocline $F_c = 0$ but the isoclines are mirrored at the symmetry line. So they arise from the c-axis and their peaks stretch in the direction of the lower right corner of the unit simplex, cf. Fig. 3 and Fig. 4.

In general, for a fixed herding parameter ϕ equilibrium points are identified as intersection points of two different isoclines $F_b = 0$ and $F_c = 0$, i.e. intersections of LI_b with LI_c and PI_c, respectively intersections of PI_b with LI_c and PI_c. Due to the symmetric structure of the underlying dynamic system these points of intersection are either arranged on the symmetry line, i.e. for the intersection points of the parabolic isoclines, or they emerge pairwise in the phase plane. One equilibrium point can be reflected with respect to the symmetry line to obtain the second equilibrium point. There points originate from intersections of parabolic and linear isoclines.

Besides the two additional parabolic isoclines PI_b and PI_c no further points of intersection and no change in the system's dynamics occur for $\phi = 1.2$ in Fig. 3a.

Figure 3b shows the scenario for $\phi = 1.373$. When different parabolic isoclines are tangent to each other and intersect on the symmetry line, they are tangent to the opposing linear isoclines as well. Here three new equilibrium points are created at once.

For increasing $\phi \in (1.373, 1.5)$ six equilibria are generated due to additional intersections. Three of these new equilibria are stable nodes and each located closely to one of the vertices of the unit simplex S, hence the system exhibits multistability. Three inner intersection points, which indicate instability, more specifically saddle node stability, are located in the immediate neighborhood of the stable node $(b^s, c^s) = (\frac{1}{3}, \frac{1}{3})$. They collide into the symmetric equilibrium for $\phi = 1.5$ which becomes an unstable node thereafter, see Fig. 4a.

The stability behavior of all seven equilibria persists for increasing values of the herding parameter $\phi > 1.5$, i.e. three outer stable nodes and three inner saddle points

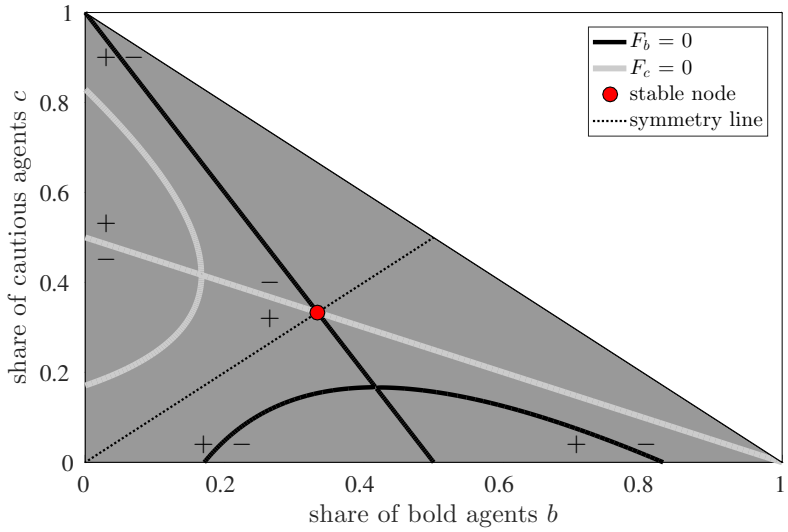

(a) $\phi = 1.2$, one stable equilibrium (red dot). $+/-$ indicate $F_b \gtrless 0$, respectively $F_c \gtrless 0$.

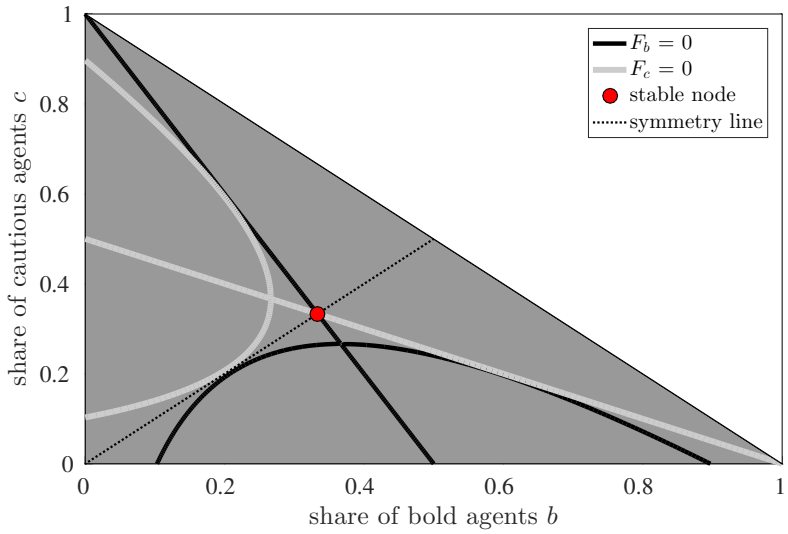

(b) $\phi = 1.373$, one stable equilibrium (red dot)

Figure 3: Phase plane representation of $F_b = 0$ (black) and $F_c = 0$ (white) for $\phi = 1.2$ and $\phi = 1.373$.

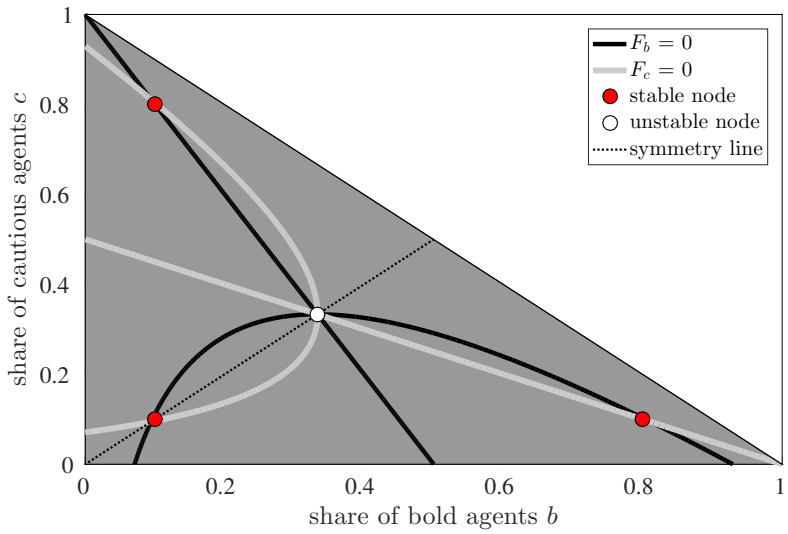

(a) $\phi = 1.5$, three stable equilibria (red dots), one unstable equilibrium (white dot).

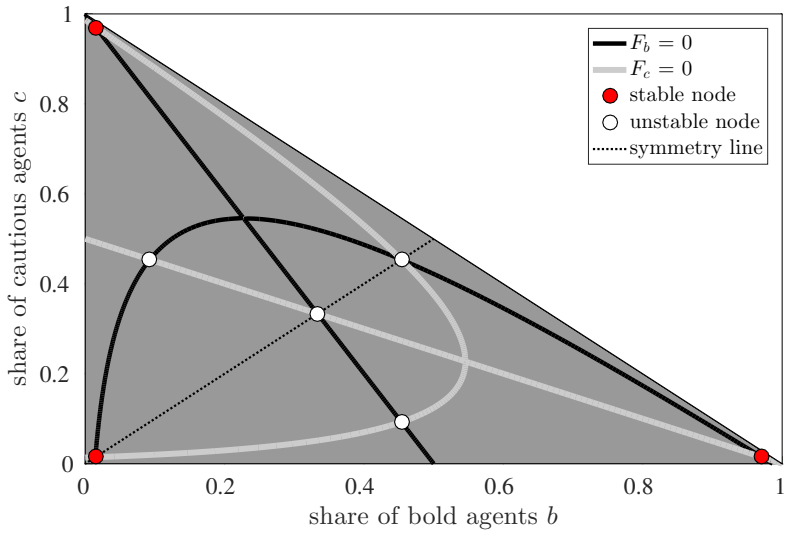

(b) $\phi = 2.2$, three stable equilibria (red dots), four unstable equilibrium (white dots).

Figure 4: Phase plane representation of $F_b = 0$ (black) and $F_c = 0$ (white) for $\phi = 1.5$ and $\phi = 2.2$. Evolution from four equilibria in (a) to seven equilibria in (b).

which are all scattered symmetrically around the unstable symmetric equilibrium $(b^s, c^s) = (\frac{1}{3}, \frac{1}{3})$. Exemplified by $\phi = 2.2$, Fig. 4b exhibits the further evolution of the parabolic isoclines and the points of intersection.

Vector field dynamics for $\phi = 1.7$ are depicted in Fig. 5a. As mentioned above, they show three attracting points located in the vertices of the simplex. These points are stable nodes and each represents the majority of one attitude, i.e. bold, cautious or neutral.

For $\phi = 1.7$ Fig. 5b additionally illustrates the partition of the phase plane into three stability regions via separatrices. Within each stabilty region, the so called basins of attraction, all initial points converge to the associated aforementioned stable node located within the very same phase plane region. Solely initial values located directly on the separatrices allow for convergence towards one of the three saddle points, which have been characterized as (inner) unstable nodes so far. Only a strong shock affecting the herding component and/or the attitudes of the agents can lead to a shift of an equilibrium, i.e. a shift in the configuration of attitudes of the whole population, from one basin of attraction to another.

Each linear isocline, i.e. LI_b and LI_c, has only one b-axis intercept for all herding intensities ϕ. Due to the appearance of the parabolic isoclines PI_b and PI_c for $\phi > 1$ additional b-axis intercepts can be detected. The following proposition summarizes all b-axis intercept characteristics of the isocline LI_b.

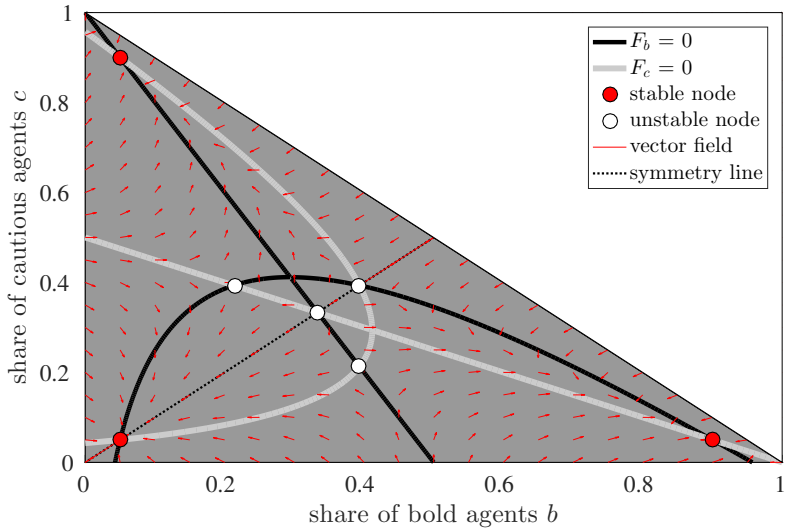

(a) Vector field dynamics pointing towards three attracting nodes in the vertices of the simplex.

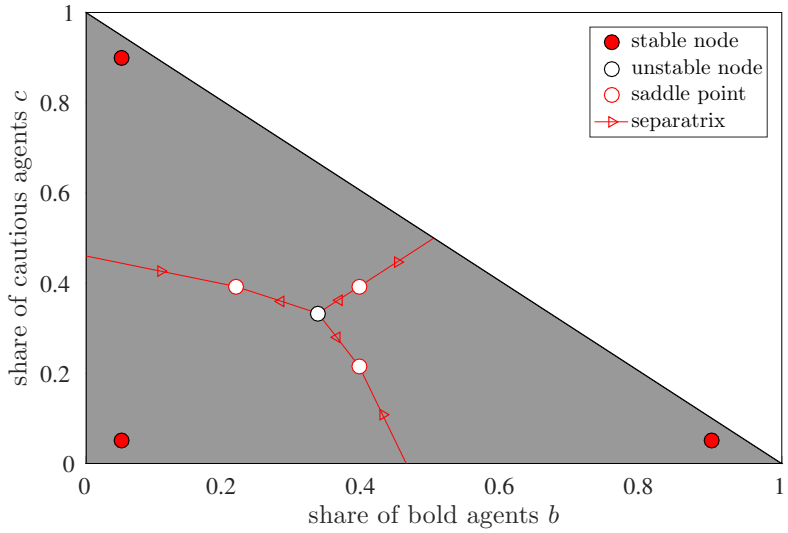

(b) Three stability regions with separatrices and corresponding stable equilibria (red dots). Three saddle points on separatrices (white dots with red frame).

Figure 5: Phase plane representation of $F_b = 0$ (black) and $F_c = 0$ (white) for $\phi = 1.7$ in (a), including vector field dynamics (red arrows). Three stability regions are visible in (b), including three separatrices (red lines).

Proposition 3:

1. For all values of ϕ the linear isocline LI_b has one b-axis intercept, i.e. $b_0 = 0.5$.
2. The parabolic isocline PI_b appears for $\phi = 1$ at $b_0 = 0.5$.
3. If $\phi > 1$ the parabolic isocline PI_b has two symmetric b-axis intercepts,
   i.e. b_1 is a b-axis intercept of $PI_b \Rightarrow b_2 = 1 - b_1$ is a b-axis intercept of PI_b.
4. For increasing ϕ the b-axis intercept $b_1 > 0.5$ converges to 1, respectively $\lim_{\phi \to \infty} b_2 = 0$
5. Statement 2 - 4 hold for c-axis intercepts c_i of PI_c, $i \in \{0, 1, 2\}$.

From subsection 2.3.1 we can conclude that the symmetric equilibrium $(b^s, c^s) = (\frac{1}{3}, \frac{1}{3})$ is repelling for $\phi > \frac{3}{2}$. For $\phi \neq \frac{3}{2}$ it is approached in a monotonic manner, cf. Proposition 2.

2.3.3 Bifurcation Analysis

In general a dynamical system is called structurally stable if the qualitative dynamic properties of the system persist with small variations in its structure.

In the following, structural changes of the system due to the variation of the herding parameter ϕ are under investigation. We want to determine how the qualitative behavior of the dynamical system evolves under variations of the herding parameter. Thus, the results of bifurcation theory are especially important to dynamic modeling in economics.[12]

Once the system passes through a critical value the stability behavior changes. These specific parameter values of ϕ are called bifurcation values. The parametric sphere

[12]For an application of stochastic bifurcation theory to the detection of economic bubbles via a nonlinear dynamical system see Dmitriev et al. (2017). Additional applications in economics are presented in Zhang (2005).

together with its characteristic phase space sphere constitute a bifurcation diagram which is desirable as a result of the qualitative analysis of the given dynamical system (8). A bifurcation diagram categorizes all possible modes of behavior of the dynamical system and transitions between these modes, indicated by bifurcation values, under parameter variations in a very consolidated manner.[13]

Bifurcations do not necessarily imply a shift between stability and instability, but they do imply a change in the nature of the disequilibrium dynamics. As a result, if a confidence region around parameter estimates includes a bifurcation point, various kinds of dynamics can be consistent with the parameters being within this confidence region.

Possible candidates for bifurcation values ϕ can be obtained from the set of equilibrium points. These are intersection points of all isoclines of the two differential equations. Due to the homogeneous structure of the differential equations the multidimensional intersection point problem is equivalent to a multidimensional root problem.

Root detection methods in multidimensional nonlinear systems are far from trivial and not analog to one-dimensional numerical methods. Without further insight, i.e. additional information on the structure of the isoclines of the nonlinear equations, it is a time-consuming process to accurately track all roots of the underlying system. This is also due to the large parameter range for the herding component ϕ which leads to innumerable many roots depending on the step size for each parameter of the routine. As pointed out in Press et al. (2007) the multidimensional numerical algorithm by *Newton-Raphson* is an efficient method to find multiple roots. This rather simple method heavily relies on initial values close to the actual root therefore the step size needs to be chosen carefully as roots might be omitted otherwise.

In case of this scenario it is possible to take advantage of the symmetric setup of the dynamical system, see Fig. 3 and Fig. 4. The intersection points of the linear isoclines LI_b and LI_c, the parabolic isoclines PI_b and PI_c and intersection points of LI_b and PI_c, respectively LI_c and PI_b are of interest.

The inspection of the intersection points of the linear isoclines is simple due to the

[13] See Kuznetsov (2004), Strogatz (1994) and Wiggins (2003) for details on bifurcation theory.

	Brute-force	**Newton-Raphson**	**Bisection**
intersection points	993	989	1030
computing time	< 1 s	4533 s	143 s

Table 1: Comparison of computing time of three root detection methods. Number of intersection points chosen ≈ 1000.

linearity of the equations from system (10). It is obvious that additional intersection points of LI_b and PI_c, respectively LI_c and PI_b are located on the linear isoclines as well. However the intersection points of the parabolic isoclines PI_b and PI_c are arranged on the symmetry line. Including this information into the algorithm decreases the computing time immensely; from more than one hour when applying the advanced Newton-Raphson method to only one second using this information-backed Brute-force method to find a sufficient amount of intersection points (≈ 1000 points) to construct a bifurcation diagram. Additionally the *Bisection method* has been applied to find the most efficient algorithm for root detection, cf. Tab. 1. It turns out that this method is as well far more efficient than the Newton-Raphson method.
The reduction to four single multidimensional root problems is less demanding than the suggested calculation of the Jacobian matrix evaluated at each coordinate $(b, c; \phi)$ in the Newton-Raphson method. The resulting simplified algorithm is sufficiently effective and allows for a rapid determination of equilibrium points.

In order to check the stability properties of the dynamical system these points need to be explored and possible bifurcation values ϕ need to be detected. Due to the sensitivity of the dynamical system regarding the herding parameter ϕ all changes in the system behavior occur only within a narrow range of this parameter. Therefore all types of bifurcations introduced subsequently are local bifurcations in the sense that only the behavior of the dynamical system in the neighborhood of single steady states is affected.

For the purpose of classifying and visualizing the different modes of stability be-

havior the corresponding direct product of a one-dimensional phase space and the one-dimensional parameter space is considered. Due to an adjustment of the two phase plane components b and c which originates from the symmetric setup of the dynamical system an easily accessible and comprehensible two-dimensional illustration is chosen.[14]

Figure 6 shows the bifurcation diagram, including the bifurcation route which indicates the number of equilibria obtained for fixed values of the herding parameter ϕ. The bifurcation diagram is adjusted due to the overlapping of two parabolas which have identical (ϕ, b)-coordinates and differ only in their c-coordinate. Therefore an augmented phase space coordinate has been introduced which includes a weight $\epsilon \in (0, 1)$ for all c-coordinates. The qualitative behavior of the equilibrium points is not affected by this transformation.

Three symmetric parabolas are visible and with increasing herding component ϕ the stability behavior varies. For $\phi = 1.373$ three supercritical saddle-node bifurcations occur at $(b_1^{sn}, c_1^{sn}) = (0.5702, 0.2145)$, $(b_2^{sn}, c_2^{sn}) = (0.2145, 0.5702)$ and $(b_3^{sn}, c_3^{sn}) = (0.2145, 0.2145)$ where (b^{sn}, c^{sn}) denote the (b, c)-coordinates of the saddle-node bifurcations.[15] These are non-adjusted (b, c)-coordinates which coincide with the symmetric structure of the equilibria distribution in the phase plane representation. An additional hyperbolic fixed point occurs for $\phi = 1.5$ and three equilibria collide into the symmetric equilibrium which undergoes a bifurcation and becomes unstable. Furthermore a Hopf bifurcation cannot occur for any value of the herding intensity ϕ since the eigenvalues of the corresponding Jacobian are real.

A non-monotonic sequence of steady-states is created, e.g. from $1 - 4 - 7 - 4 - 7$ equilibria. This step function exhibits two jumps for $\phi = 1.5$ from seven to four and back to seven.

[14] See Appendix A.1.1 for a three-dimensional illustration.

[15] Saddle-node bifurcations can occur in simple partial-analytical models of the labor market where the change in the real wage rate is assumed to depend on the excess demand for labor in this market. The supply of labor and demand for labor, respectively, depend on the real wage. See Lorenz (2012) for more details.

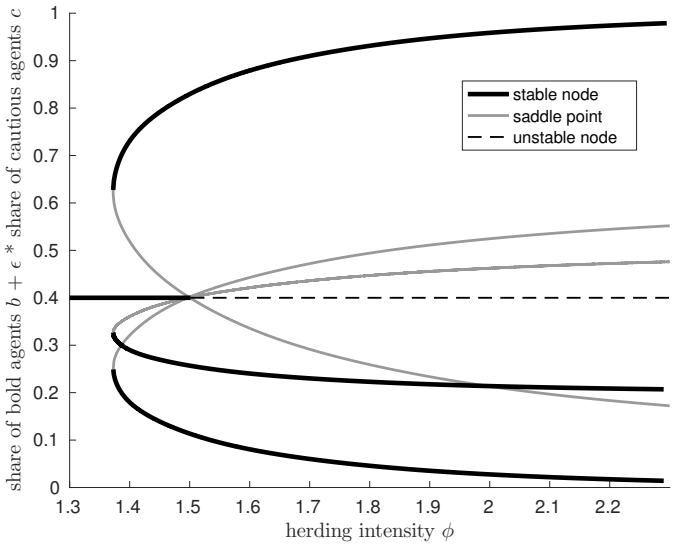

(a) Bifurcation diagram with augmented coordinate $b+\epsilon c$ and $\epsilon = 0.2$.

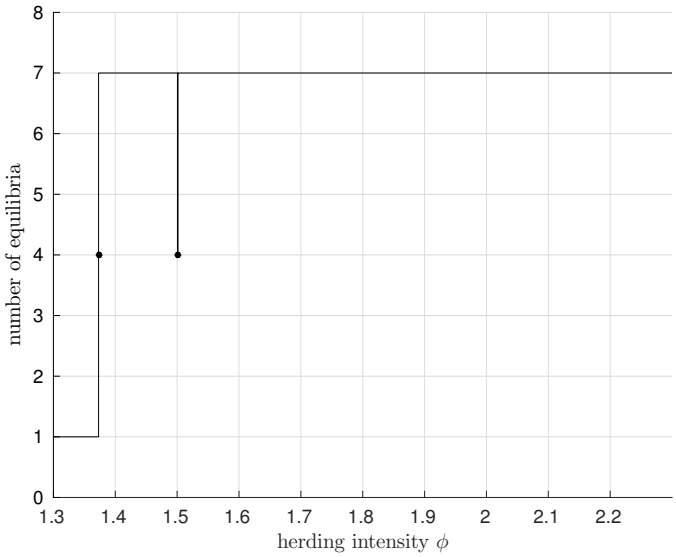

(b) Diagram with number of equilibria and jump at $\phi = 1.5$.

Figure 6: Adjusted bifurcation diagram in (a) and illustration showing the development for number of equilibria in (b) with herding intensity $\phi \in [1.3, 2.3]$.

2.4 Augmented Feedback

While the previous feedback components f_b and f_c take into account the attitude of agents in immediate proximity only, i.e. the differences between the percentage ratios of bold, respectively cautious, agents and neutral agents, the novel feedback components incorporate a distant effect which preponderates with increasing weight factor. Direct switches between the extreme attitude, i.e. from b to c, respectively from c to b, are still not incorporated.

The augmented feedback indices contain a weighted influence of extreme attitudes, constituted by the deviation $b - c$ for the feedback index f_b and the difference $c - b$, respectively for the feedback index f_c:

$$\begin{aligned} f_b &= \phi[\,(1-\omega)(2b+c-1) + \omega(b-c)] \\ f_c &= \phi[\,(1-\omega)(2c+b-1) + \omega(c-b)]\,. \end{aligned} \tag{14}$$

The weight is denoted by ω and takes values within $[0, 1]$. For $\omega = 0$ the original setup of feedback indices in (7) is ensured. With a weighting component $\omega = 1$ the fraction of neutral agents is not taken into consideration and the feedback on the transition probabilities entirely depends on the extreme attitudes and their deviations. If $b - c$ is denoted by x, and $c - b$ by $-x$ respectively, these feedback indices lead back to the opinion index introduced in Lux (1995) with binary choice in a transition probability approach.

2.4.1 Stability Analysis for Augmented Feedback

Figure 7, Fig. 8 and Fig. 9 display phase plane representations for three fixed herding components ϕ which exhibit the evolution of the parabolic isoclines of F_b, with varying weight $\omega = 0.2, 0.5, 0.8$. Apparently linear isoclines do not emerge as in the unweighted feedback scenario.

For the combination of herding and weight $(\phi = 1.8, \omega = 0.2)$ two types of parabolic isoclines are visible, cf. Fig. 7. With an increasing weight these two nonlinear isoclines

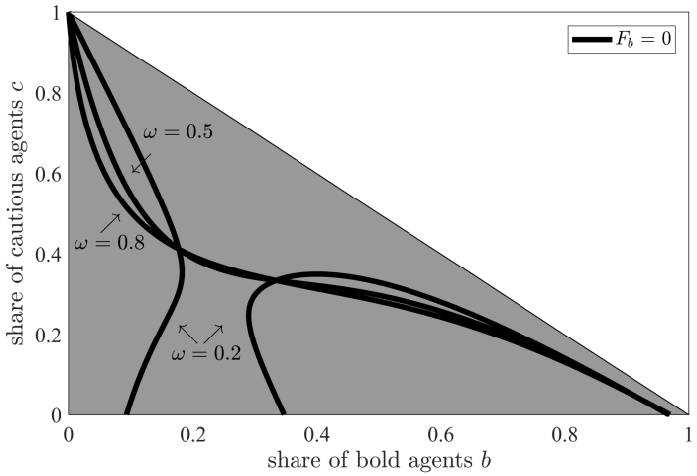

Figure 7: Phase plane representation of $F_b = 0$ for herding intensity $\phi = 1.8$ and weight $\omega = 0.2, 0.5, 0.8$. Two nonlinear isoclines for $\omega = 0.2$ and one nonlinear isocline for $\omega = 0.5, 0.8$ are visible.

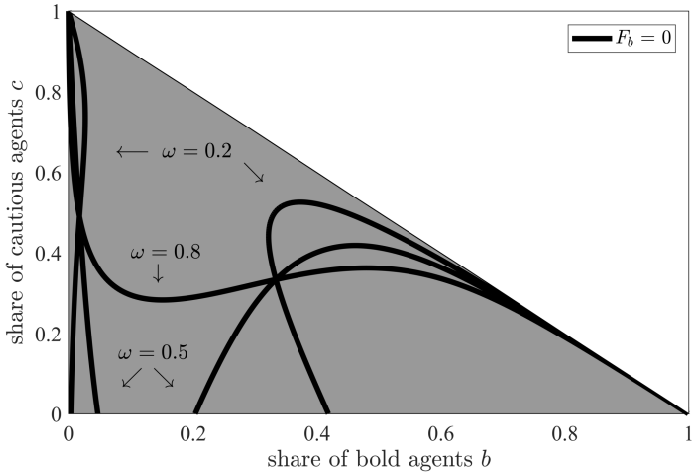

Figure 8: Phase plane representation of $F_b = 0$ for herding intensity $\phi = 3.5$ and weight $\omega = 0.2, 0.5, 0.8$. Two nonlinear isoclines for $\omega = 0.2, 0.5$ and one nonlinear isocline for $\omega = 0.8$ are visible.

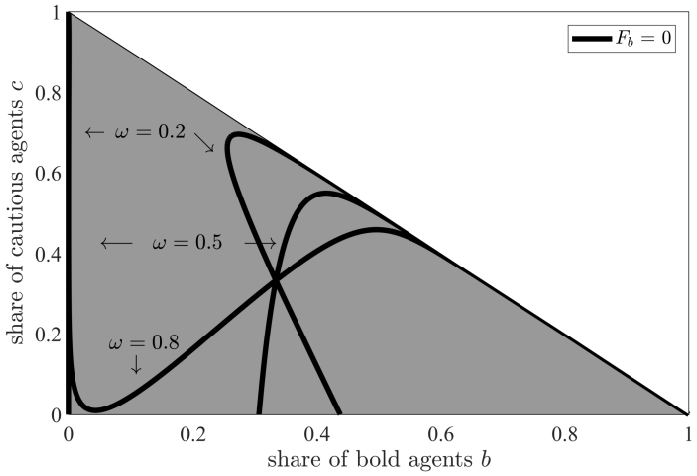

Figure 9: Phase plane representation of $F_b = 0$ for herding intensity $\phi = 10.0$ and weight $\omega = 0.2, 0.5, 0.8$. Two nonlinear isoclines for $\omega = 0.2, 0.5$ and one nonlinear isocline for $\omega = 0.8$ are visible.

are unified. The same observation can be made for the combination $(\phi = 3.5, \omega = 0.2)$, cf. Fig. 8, the combination $(\phi = 10.0, \omega = 0.2)$ and the combination $(\phi = 10.0, \omega = 0.5)$, cf. Fig. 9. Considering the remaining representations there is only one single isocline per herding component and weighting intensity displaying the underlying differential equation $F_b = 0$, i.e. combinations $(\phi = 1.8, \omega = 0.5)$, $(\phi = 1.8, \omega = 0.8)$, $(\phi = 3.5, \omega = 0.5)$, $(\phi = 3.5, \omega = 0.8)$ and $(\phi = 10.0, \omega = 0.8)$. If the herding component ϕ increases all isoclines obtain a distorted shape and adapt to the boundaries of the unit simplex S.

For further phase plane representations of both differential equations $F_b = 0$ and $F_c = 0$, the values chosen for the herding component ϕ agree with the values chosen for the phase plane representations of the single differential equation $F_b = 0$, cf. Fig. 7, Fig. 8 and Fig. 9 .

In Fig. 10 and Fig. 11 the phase plane representation for both types of parabolic isoclines $F_b = 0$ and $F_c = 0$ is displayed for a small weight $\omega = 0.2$ and increasing herding ϕ. If the herding is small, i.e. $\phi = 1.0$, the symmetric equilibrium $(b^s, c^s) = (\frac{1}{3}, \frac{1}{3})$ is the only intersection point and it is stable, see Fig. 10a.

For a moderate herding intensity $\phi = 1.4$ this equilibrium turns into an unstable node and two additional intersection points evolve. The dynamic system exhibits bistability, cf. Fig. 10b. Additionally corresponding vector field dynamics are displayed here. They indicate an equilibrium reflecting a stable neutral majority. It is represented by the coordinates $(b, c) = (0, 0)$ and it is not attainable with this degree of herding for any initial value. Only the extreme attitudes bold b and cautious c, represented by the coordinates in the neighborhood of $(b, c) = (1, 0)$ and $(b, c) = (0, 1)$, are attracting.
For each differential equation $F_b = 0$ and $F_c = 0$ two types of nonlinear isoclines evolve in the phase plane for $\phi = 1.8$, cf. Fig. 11a. The recurring reflected representation of two pairs of isoclines with respect to the symmetry line is evident. Seven points of intersection can be observed, four unstable equilibrium points which are located close to the centroid of the unit simplex S and three stable equilibria located close to the vertices of the simplex.

Figure 11b contains vector field dynamics for $\phi = 2.5$. In this scenario all three attitudes, i.e. bold, cautious and neutral, have the possibility to maintain a stable majority depending on the initial point. However, the stability region including all attracting initial values in the neighborhood of $(b, c) = (0, 0)$, representing a majority consisting of agents with a neutral attitude, is smaller than the other two stability regions.
In Fig. 12 the corresponding phase plane representations for $\omega = 0.5$ and $\omega = 0.8$ are shown, including vector field dynamics which show regions of attraction.[16] The magnitude of herding is chosen such that seven equilibrium points result from intersections and their locations in the unit simplex S are approximately the same compared to the previous case for $\omega = 0.2$. It can be concluded that an increasing weighting factor ω, i.e. the effect of extreme attitudes, $b - c$ and $c - b$, dominates or the influence of the agents having a neutral position diminishes, requires an immense increase in the herding intensity to ensure the same (b, c)-coordinates for the stable equilibria, i.e. $(b, c) = (0, 0)$ for a majority of neutral agents, $(b, c) = (1, 0)$ for a majority of bold agents and $(b, c) = (0, 1)$

[16] See Appendix A.1.2 for additional phase plane diagrams showing the isoclines for $\omega = 0.5$ and $\omega = 0.8$ with smaller values of the herding component ϕ.

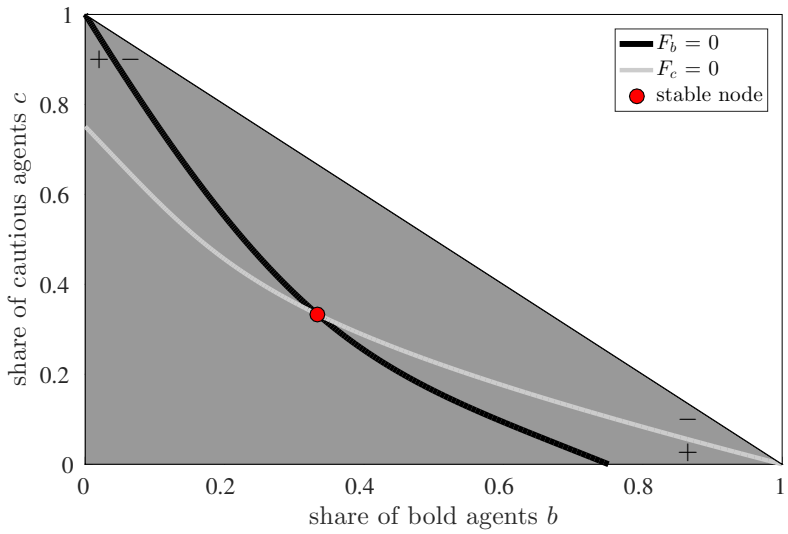

(a) $\phi = 1.0, \omega = 0.2$, one stable equilibrium (red dot).

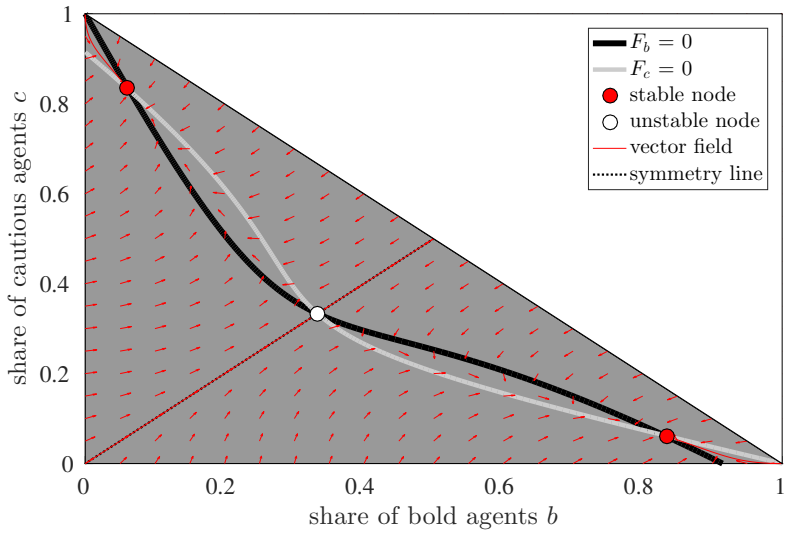

(b) $\phi = 1.4, \omega = 0.2$, two stable equilibria (red dots), one unstable equilibrium (white dot). Vector field dynamics pointing towards two attracting nodes in the vertices of the simplex.

Figure 10: Phase plane representation of $F_b = 0$ (black) and $F_c = 0$ (white) for $\phi = 1.0, 1.4$ and $\omega = 0.2$, including vector field dynamics (red arrows).

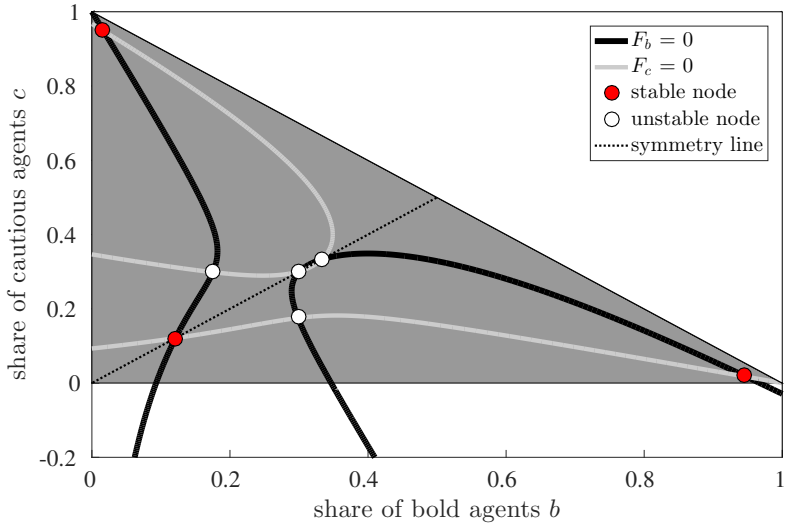

(a) $\phi = 1.8, \omega = 0.2$, three stable equilibria (red dots), four unstable equilibria (white dots).

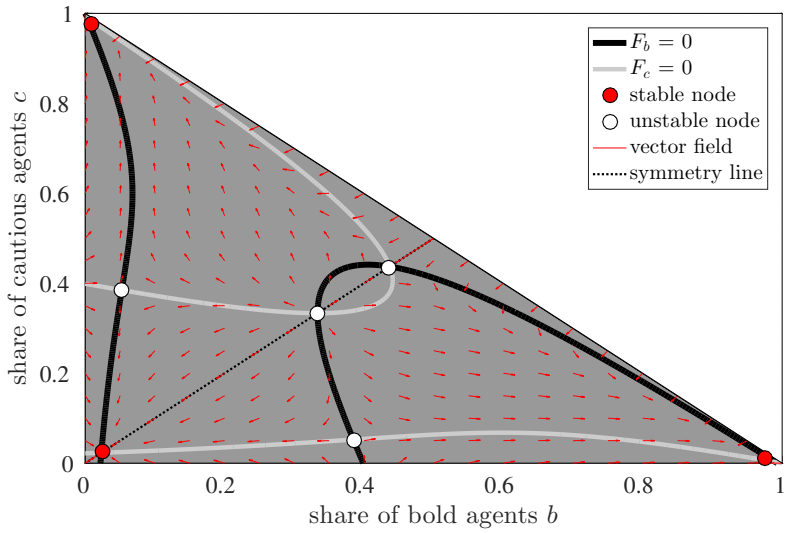

(b) $\phi = 2.5, \omega = 0.2$, three stable equilibria (red dots), four unstable equilibria (white dots). Vector field dynamics pointing towards three attracting nodes in the vertices of the simplex.

Figure 11: Phase plane representation of $F_b = 0$ (black) and $F_c = 0$ (white) for $\phi = 1.8, 2.5$ and $\omega = 0.2$, including vector field dynamics (red arrows).

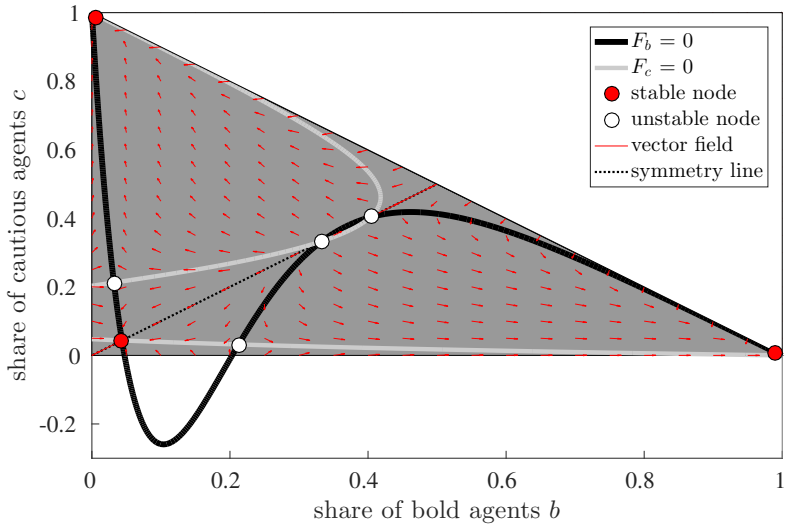

(a) $\phi = 3.5, \omega = 0.5$, three stable equilibria (red dots), four unstable equilibria (white dots). Vector field dynamics pointing towards three attracting nodes in the vertices of the simplex. Axis of ordinates is extended to show the accurate shape of the nonlinear isocline $F_b = 0$.

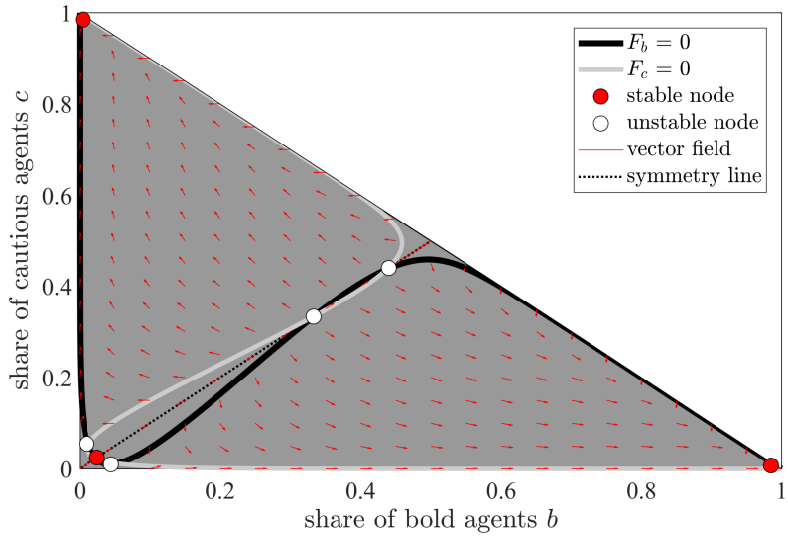

(b) $\phi = 10.0, \omega = 0.8$, three stable equilibria (red dots), four unstable equilibria (white dots). Vector field dynamics pointing towards three attracting nodes in the vertices of the simplex.

Figure 12: Phase plane representation of $F_b = 0$ (black) and $F_c = 0$ (white) for $\omega = 0.5$ and 0.8, including vector field dynamics (red arrows).

	Brute-force	**Newton-Raphson**	**Bisection**
intersection points	502	504	510
computing time	71 s	4282 s	44 s

Table 2: Comparison of computing time of three root detection methods for $\omega = 0.2$. Number of intersection points chosen ≈ 500.

for a majority of cautious agents. This means the herding needs to be exceedingly high in order to ensure the existence of a neutral majority at all. For the weighted feedback scenario multistability of the system is possible as well. It is evident that the symmetric equilibrium (b^s, c^s) prevails for all values of herding ϕ and weight ω.

2.4.2 Bifurcation Analysis for Augmented Feedback

In case of weighed feedback-based herding dynamics it is not possible to consider symmetry arguments in the same way as in the unweighted scenario. Therefore the efficiency and computation time of the three methods used for root detection differ in comparison to the unweighted feedback case.

Considering the same weight ω and the same herding interval for ϕ the Newton-Raphson method needs more than one hour to detect the same amount of intersection points as the brute-force method which needs only more than one minute. However the computation time of the Bisection method adds up to even less than one minute, see Tab. 2.

The bifurcation diagrams and the bifurcation routes for weighted feedback are depicted in Fig. 13, Fig. 14 and Fig. 15. All bifurcation diagrams show one degenerate parabola with an asymmetrical shape of the manifolds. They are located in the left quarter of the diagram and part into two manifolds for a herding intensity $\phi < 1.5$. These two manifolds of each degenerate parabola exhibit the same stability behavior. Furthermore two regular parabolas are depicted in each bifurcation diagram. They are located in the

right half of the diagram and show different degrees of dilation and compression. The stability behavior varies only for two manifolds of one of these regular parabolas in each bifurcation diagram. Additionally the shapes of all parabolas vary with increasing weight component ω.

The (b, c)-coordinates are denoted by (b^j, c^j) where superscript j denotes the specific bifurcation type, i.e. $j \in \{sn,\ t,\ p/p_{\text{sub/sup}}\}$ where sn is the notation for a saddle-node bifurcation, a transcritical bifurcation is denoted by t and $p/p_{\text{sub/sup}}$ represent a pitchfork bifurcation.[17] Indices sub/sup refer to subcritical, respectively supercritical versions of this bifurcation.

Figure 13a illustrates the stability behavior of the equilibria for weight $\omega = 0.2$. For $\phi = 1.228$ two saddle-node bifurcations occur at $(b_1^{sn}, c_1^{sn}) = (0.529, 0.204)$ and $(b_2^{sn}, c_2^{sn}) = (0.204, 0.529)$. Increasing the herding parameter slightly to $\phi = 1.25$ one supercritical pitchfork bifurcation occurs at the symmetric equilibrium $(b^{p_{\text{sub}}}, c^{p_{\text{sub}}}) = (0.333, 0.333)$. An additional supercritical saddle-node bifurcation is observed at $\phi = 1.716$ with $(b_3^{sn}, c_3^{sn}) = (0.2121, 0.2121)$. A further increase of ϕ to 1.724 exhibits one pitchfork saddle-source bifurcation at $(b^p, c^p) = (0.2449, 0.2449)$.[18]
The final bifurcation is transcritical and occurs at the symmetric equilibrium with $(b^t, c^t) = (0.333, 0.333)$ at $\phi = 1.875$. More specifically, it is a transcritical saddle-source bifurcation.[19] The number of equilibria changes from $1-3-5-3-4-5-7-6-7$ with two jumps in the step function for $\phi = 1.875$ from $7-6-7$, cf. Fig. 13b.

The corresponding bifurcation diagram for weight $\omega = 0.5$ is depicted in Fig. 14a. One pitchfork bifurcation occurs for $\phi = 1$ at the symmetric equilibrium $(b^{p_{\text{sup}}}, c^{p_{\text{sup}}}) =$

[17] Transcritical bifurcations can occur in a one-dimensional system constructed from standard neoclassical growth theory where the change in capital intensity depends on per-capita-output, labor growth rate and the savings rate. Pitchfork bifurcations can occur in versions of the Kaldor model where the change in capital stock is assumed to depend on the gross investment and savings. See Lorenz (2012) for more details.

[18] A pitchfork saddle-source bifurcation is defined as a pitchfork bifurcation with one unstable (source) manifold and one saddle manifold, see Appendix B.1.3.2 for the definition of a pitchfork bifurcation.

[19] A transcritical saddle-source bifurcation is defined as a transcritical bifurcation with one unstable (source) manifold and one saddle manifold, see Appendix B.1.3.3 for the definition of a transcritical bifurcation.

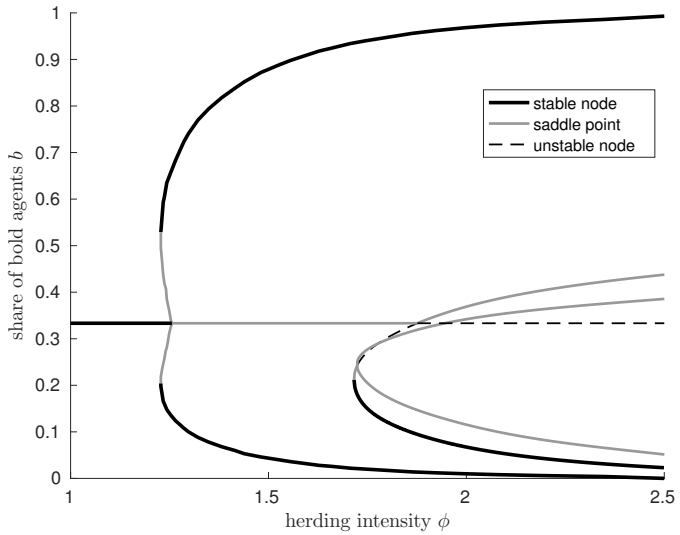

(a) Bifurcation diagram for $\omega = 0.2$ with $\phi \in [1, 2.5]$.

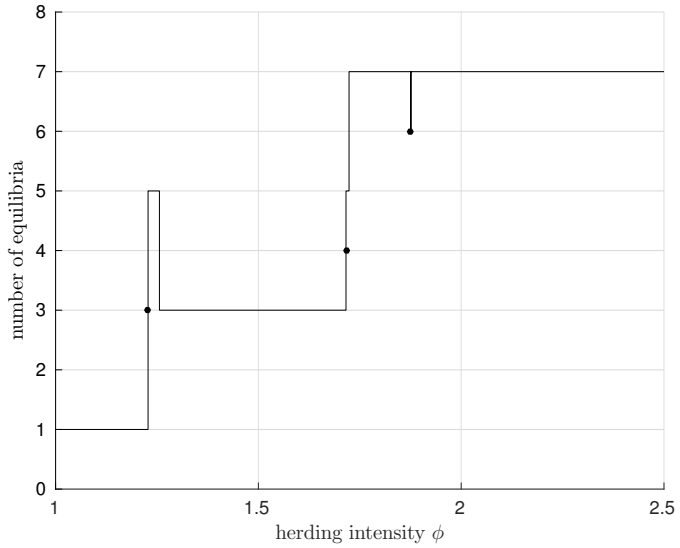

(b) Diagram with number of equilibria for $\omega = 0.2$ and jump at $\phi = 1.875$.

Figure 13: Bifurcation diagram for $\omega = 0.2$ in (a) and illustration showing the development for number of equilibria in (b) with herding intensity $\phi \in [1.0, 2.5]$.

$(0.333, 0.333)$ and it is supercritical.
Furthermore a supercritical saddle-node bifurcation is visible at $\phi = 2.746$ with $(b^{sn}, c^{sn}) = (0.2185, 0.2185)$. Increasing the herding parameter slightly to $\phi = 2.9$, one subcritical pitchfork bifurcation occurs at $(b^{p_{\text{sub}}}, c^{p_{\text{sub}}}) = (0.1131, 0.1131)$. A transcritical saddle-source bifurcation occurs for $\phi = 3.0$ at the symmetric equilibrium $(b^t, c^t) = (0.333, 0.333)$. The number of equilibria evolves non-monotonically from $1-3-4-5-7-6-7$ and at $\phi = 3.0$ the step function jumps from seven to six and back to seven again, cf. Fig. 14b.

Figure 15a illustrates the evolution for weight $\omega = 0.8$. For $\phi = 0.833$ one supercritical pitchfork bifurcation is visible at the symmetric equilibrium $(b^{p_{\text{sup}}}, c^{p_{\text{sup}}}) = (0.333, 0.333)$. A supercritical saddle-node bifurcation occurs for $\phi = 6.866$ with $(b^{sn}, c^{sn}) = (0.2165, 0.2165)$. For $\phi = 7.5$ a transcritical saddle-source bifurcation occurs at the symmetric equilibrium $(b^t, c^t) = (0.333, 0.333)$ and for $\phi = 9.568$ a pitchfork bifurcation occurs at
$(b^{p_{\text{sub}}}, c^{p_{\text{sub}}}) = (0.0284, 0.0284)$ which is supercritical. A non-monotonic sequence of steady-states is created, e.g. from $1-3-4-5-4-5-7$ equilibria. This step function exhibits two jumps for $\phi = 7.5$ from $5-4-5$, cf. Fig. 15b.
The bifurcation diagrams for all weights $\omega = 0.2, 0.5$ and 0.8 depict each at least two stable manifolds for a moderate herding component, i.e. $\phi < 3$. These two manifolds originate from two supercritical saddle-node bifurcations in the case of $\omega = 0.2$ and from one pitchfork bifurcation in the case of $\omega = 0.5$ and 0.8. In all cases these stable manifolds relate to the situation when a majority of bold agents prevails, see upper stable manifold, and a majority of cautious agents prevails, see lower stable manifold.

In order to inspect the possible stable configurations for a majority of neutral agents Fig. 16 needs to be considered. It depicts enlarged bifurcation diagrams for $\omega = 0.2, 0.5$ and 0.8 with a focus on pitchfork bifurcations occurring for smaller fractions of bold agents, i.e. $b^s < 0.333$.

It is evident that with a weighted feedback and a high influence of the extreme attitudes, that is with a higher weight ω, a stable majority of neutral agents is possible,

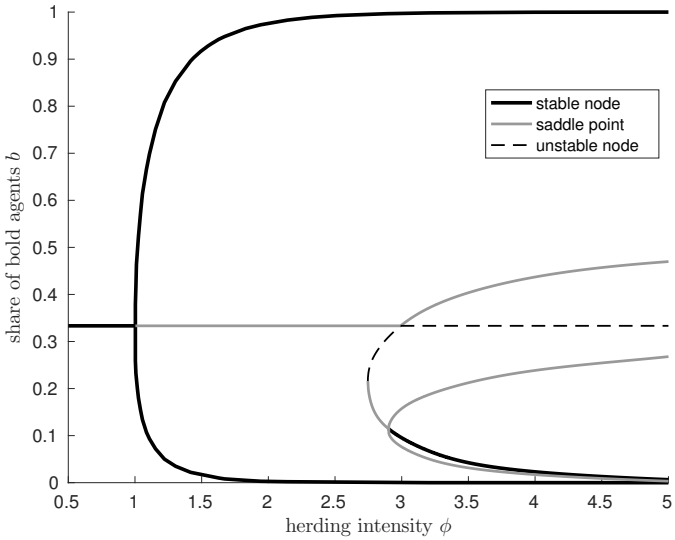

(a) Bifurcation diagram for $\omega = 0.5$ with $\phi \in [0.5, 5.0]$.

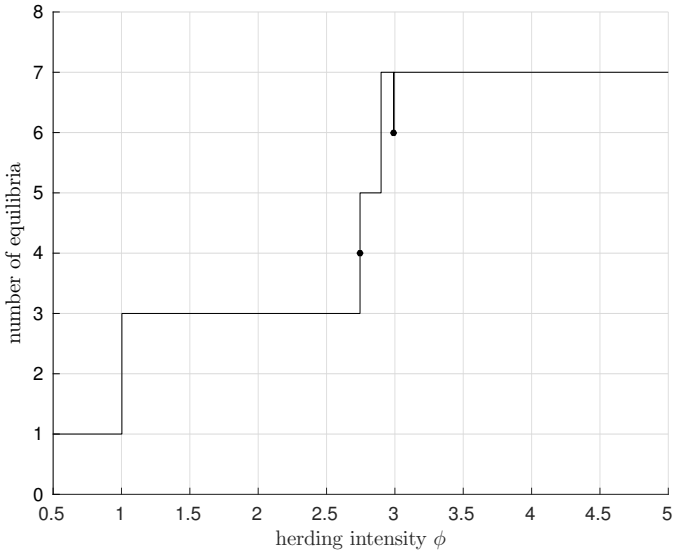

(b) Diagram with number of equilibria for $\omega = 0.5$ and jump at $\phi = 3.0$.

Figure 14: Bifurcation diagram for $\omega = 0.5$ in (a) and illustration showing the development for number of equilibria in (b) with herding intensity $\phi \in [0.5, 5.0]$.

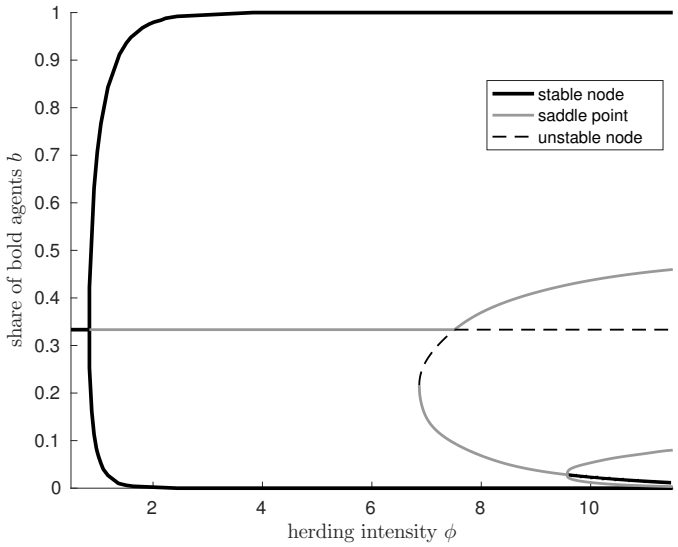

(a) Bifurcation diagram for $\omega = 0.8$ with $\phi \in [0.5, 11.5]$.

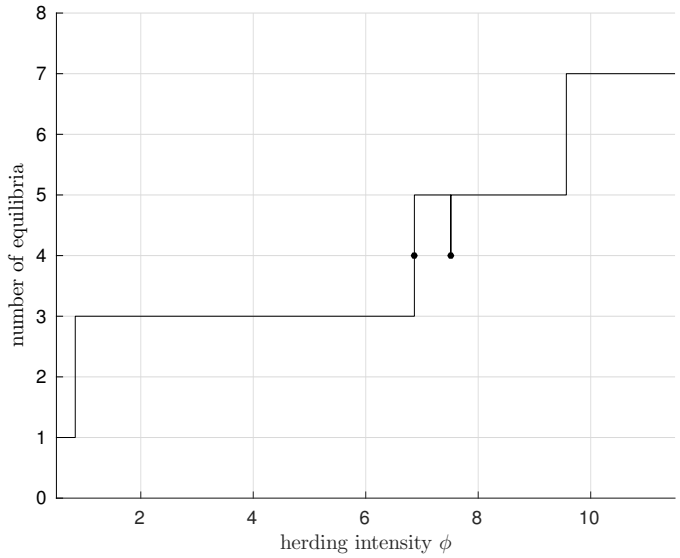

(b) Diagram with number of equilibria for $\omega = 0.8$ and jump at $\phi = 7.5$.

Figure 15: Bifurcation diagram for $\omega = 0.8$ in (a) and illustration showing the development for number of equilibria in (b) with herding intensity $\phi \in [0.5, 11.5]$.

but the occurrence requires a relatively high herding parameter, see stable sections of the manifolds in the bifurcation diagrams in Fig. 16. This result is in line with the fundamental idea that a higher influence of extreme attitudes leads to stable equilibria including extreme attitudes bold b and cautious c only.

Knowledge of these bifurcation diagrams provides key insight how complicated dynamics can arise in a two-dimensional parameter space (ϕ, ω).

2.5 Comparison of Pure Feedback and Augmented Feedback

In Sec. 2.3 the isoclines evolve fixed along the symmetry line in the phase plane. Additionally the equilibrium points are distributed uniformly around the symmetric equilibrium point $(b^s, c^s) = (0.333, 0.333)$, cf. Fig. 4. The corresponding parabolas to these equilibrium points are located symmetrically around the straight line $(\phi, b^s + \epsilon c^s)$ in the bifurcation diagram, see Fig. 6a. This straight line represents the symmetric equilibrium point for all values of herding ϕ.

Due to the second parameter, i.e. the weighting component ω, the shape of the isoclines in the phase plane diagram and correspondingly the setup of the parabolas in the bifurcation diagrams differ remarkably from the representations shown in the previous chapter, especially for a weight $\omega > 0.2$. The symmetric evolution of the isoclines in the phase plane tends to be nonsystematic and the balanced original setup of the parabolas becomes asymmetrical, cf. Fig. 8 and exemplary Fig. 14a.

The stability behavior of the symmetric equilibrium varies from stability for $\phi < 1.5$ to saddle node stability for $\phi = 1.5$ to instability for $\phi > 1.5$. $\phi = 1.5$ can be called a stability threshold value. Once the weighting ω is incorporated the stability threshold value ϕ for the symmetric equilibrium decreases with increasing influence of ω, i.e. the higher the weighted influence of extreme attitudes is the lower the herding has to be to maintain a stable symmetric equilibrium. Additionally the range of the herding component ϕ increases from $\phi = 0.5$ to e.g. $\phi \in [1.25, 1.875]$ for weight $\omega = 0.2$ to ensure saddle node stability of the symmetric equilibrium. The stable equilibrium

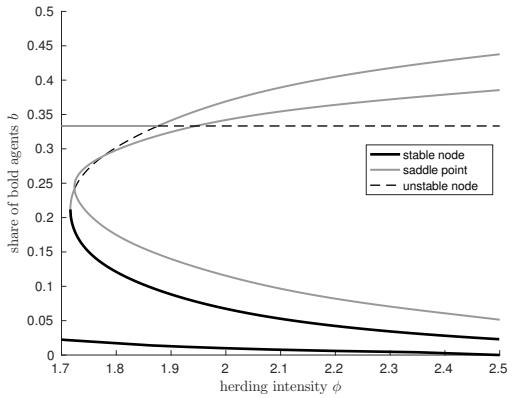

(a) $\omega = 0.2$, $\phi \in [1.7, 2.5]$

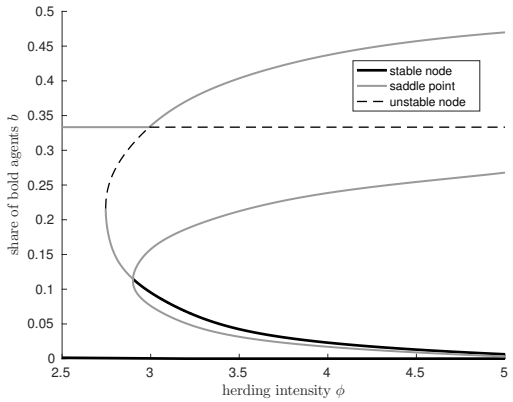

(b) $\omega = 0.5$, $\phi \in [2.5, 5.0]$

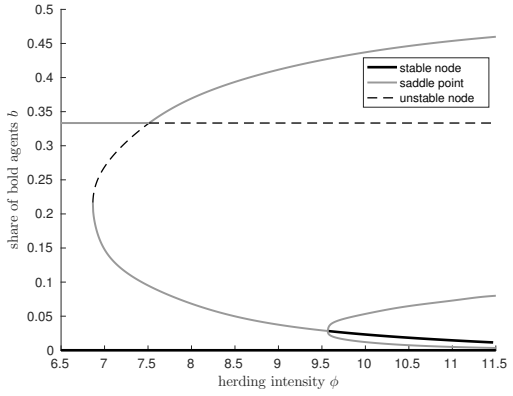

(c) $\omega = 0.8$, $\phi \in [6.5, 11.5]$

Figure 16: Enlarged bifurcation diagrams for $\omega = 0.2, 0.5$ and 0.8 with share of bold agents $b \in [0, 0.5]$.

representing a majority of neutral agents only occurs for higher values of the herding component ϕ, i.e. $\phi > 1.373$ for the pure unweighted feedback scenario compared to $\phi > 1.716$ for the weighted feedback $\omega = 0.2$.

In the pure feedback setup only the stability behavior for the symmetric equilibrium $(b^s, c^s) = (0.333, 0.333)$ alters with increasing herding, i.e. from stable node to unstable node. The remaining six equilibria retain their behavior and remain stable nodes and saddle points.

For all weighting components $\omega = 0.2, 0.5$ and 0.8 the stability behavior of single equilibrium points in the phase plane changes more frequently, see Fig. 16. This augmented dynamical system exhibits a higher number of stability behavior configurations with the same amount of equilibria, i.e. from one symmetric equilibrium to seven equilibria overall.

It is also revealed that for every intersection of two equilibrium points the stability behavior of both equilibria changes after the intersection, i.e. when ϕ increases, except for the two saddle point manifolds of the supercritical saddle-node bifurcations for $\omega = 0.2$ and $\phi = 1.25$.

The alterations in the amount of equilibria are significantly higher compared to the unweighted feedback scenario, cf. Fig. 6b and exemplary Fig. 14b. This is in line with the finding of additional bifurcation values for an increasing herding parameter ϕ.

Both frameworks deal with local bifurcations, i.e. one equilibrium point changes its stability property or additional equilibria emerge. In the pure feedback version the saddle-node bifurcations show that multiple, co-existing stable and unstable equilibrium points can be observed for relatively small values of the herding component ϕ. Therefore a steady state representing a majority of neutral agents is a possible outcome of this dynamical system.

For the augmented feedback version in addition to saddle-node bifurcations, transcritical bifurcations and pitchfork bifurcations show up. The latter bifurcation generates multiple, co-existing stable and unstable equilibrium points as well. In comparison to the reduced setup additional new complex dynamics occur only for higher values of ϕ,

i.e. at least $\phi = 1.716$ for $\omega = 0.2$, $\phi = 2.746$ for $\omega = 0.5$ and $\phi = 7.5$ for $\omega = 0.8$. For transcritical bifurcations the stability behavior changes. A stable neutral majority is a possible outcome of these dynamical systems as well. Note that this outcome becomes less likely for $\omega = 0.8$ due to the strong herding that is required to obtain this stable manifold.

Assuming a financial market setting this result can lead to a period with a market sentiment dominated by bullish traders, bearish traders or neutral traders, i.e. inactive traders. It is possible to analyze these calm periods on financial markets and relate them to return rates, volatility or other key figures. This has been done for the regular sentiment variable defined by the difference of noise traders, i.e. bullish and bearish traders.

Among others, Lux (2012) studies the influence of sentiment on DAX returns. In Fisher and Statman (2000) sentiments of three groups and their indication for changes in the S&P 500 are under review. Four sentiment indicators and their ability to forecast German economic activity are investigated by Hüfner and Schröder (2002). See Lee et al. (2002) for an analysis of the impact of investor sentiment on US stock market volatility.

2.6 Conclusions

This chapter has been concerned with an extended binary choice problem, the three-state choice problem for agents in a large population.

It provided a framework using a novel model of sentiment dynamics with three attitudes, i.e. bold, cautious and neutral. Individual transition probabilities were introduced which lead to changes in the shares of these groups of agents. Note that changes between extreme attitudes, i.e. bold and cautious, were excluded. These transition rates incorporate so-called feedback indices. The main influence within the feedback comes from the sentiment components which are weighted with a herding parameter.

Two versions of feedback components were considered. The first approach used a

sentiment ratio including the neutral attitude. Furthermore we presented an augmented feedback component. In this second approach agents used a linear combination of the traditional sentiment variable, i.e. the difference of the two extreme attitudes, and the sentiment variable including neutrality.

A nonlinear two-dimensional system of ordinary differential equations was obtained in each version. Our goal was to investigate the generic possibility of complicated dynamics, i.e. multiple equilibrium points. The bifurcation analysis exhibited saddle-node, transcritical and pitchfork bifurcations and complex bifurcation routes with multiple equilibria. Agents herd towards an extreme distribution of the attitudes, which persist over time.

The occurrence of these bifurcation types show that the analyzed dynamical systems can generate multiple, co-existing stable and unstable equilibrium points. Additionally, several bifurcation values were obtained which indicate structural instability of the dynamical system for this value. All types of bifurcations are local bifurcations. Therefore only the behavior in the neighborhood of a single bifurcation point is affected.

We incorporated neutral agents in the well-established definition of sentiment variables, i.e. the difference of bold and cautious agents. The analysis of the evolution of neutral agents revealed that for all versions and specifications a neutral majority may prevail depending on the herding. Based in these findings further extensions of both feedback-guided versions of the transitions probability approach of an agent-based model are feasible. One possibility is to include macroeconomic or finance variables, see Franke and Westerhoff (2019), and conduct empirical business cycle research. Westerhoff and Franke (2018) consider two agent-based models for economic policy design. They present a financial market model as well as a goods market model and analyze the effectivity of certain regulatory policies.

3 Discrete Choice Approach

This chapter presents a discrete choice version of a three-state model of sentiment dynamics with attitudes bold, cautious and neutral. The agents' decision to choose a sentiment is independent of the previously adopted attitude. A comparison to the transition probability approach in Chap. 2 is provided.

3.1 Introduction

When we refer to a large population of agents who repeatedly face a binary decision problem, an alternative description of aggregate sentiment dynamics to the presented transition probability approach needs to be considered, namely the discrete choice approach. This approach is broadly known through Brock and Hommes (1997). They consider a cobweb type model where agents can choose between two types of expectations. This model is able to generate complex dynamics depending on the specifications. In Hommes and Ochea (2012) two three-strategy models based on logit dynamics[20] are presented. The occurrence of stable periodic orbits and multiple, interior steady states is shown.[21]

There is literature on aggregated sentiment models which consider both specifications, the transition probability approach and the discrete choice approach. With respect to macroeconomic models, Franke and Westerhoff (2017) contribute a literature survey on *animal spirits*. Furthermore they find that both approaches are closely related and that they are capable of generating cyclical behavior. Franke (2014) inspects the transition probability approach as well as the discrete choice approach in a two-dimensional model of aggregated sentiment dynamics. It is shown that both versions of the two specifications give rise to essentially the same dynamics.

[20] *Logit dynamics* are a version of *Best Reply dynamics* which belong to the class of belief-based dynamics. These dynamics are categorized as pairwise comparison dynamics. Together with imitative dynamics they build the set of evolutionary dynamics.

[21] For further insights on discrete choice theory in evolutionary dynamics see Hommes (2013) and the analysis of *Logit dynamics* in Ochea (2010).

Following the latter contribution we want to show that our version of a discrete choice approach including neutral agents and the pure feedback version of the transition probability approach from Subsec. 2.2 exhibit equivalent dynamics.

This chapter focuses on the qualitative analysis of the resulting nonlinear dynamical system. For literature on different applications including empirical estimation see Franke and Westerhoff (2017).

3.2 Sentiment Dynamics

In contrast to the concept of transition probabilities, as they have been presented in Chap. 2, in the discrete choice setup the agents' decision is independent of the previously adopted attitude. From this follows that in each period all agents become bold (b), cautious (c) or neutral (0) with the same logit choice probabilities π_t^b, π_t^c and π_t^0.
Following Franke (2014) we obtain the following logit choice probabilities

$$\begin{aligned}
\pi_t^b &= \pi_t^b(f_b) = \frac{\exp(\beta f_b)}{\exp(\beta f_b) \; + \; \exp(\beta f_c) \; + \; \exp(\beta f_0)}\,, \\
\pi_t^c &= \pi_t^c(f_c) = \frac{\exp(\beta f_c)}{\exp(\beta f_b) \; + \; \exp(\beta f_c) \; + \; \exp(\beta f_0)}\,, \\
\pi_t^0 &= \pi_t^0(f_0) = \frac{\exp(\beta f_0)}{\exp(\beta f_b) \; + \; \exp(\beta f_c) \; + \; \exp(\beta f_0)}\,.
\end{aligned} \tag{15}$$

Here f_b, f_c and f_0 refer to the feedback indices for the attitudes bold b, cautious c and neutral 0. They are defined as

$$\begin{aligned}
f_b &= \phi \, \frac{n^b}{N} = \phi \, b\,, \\
f_c &= \phi \, \frac{n^c}{N} = \phi \, c\,, \\
f_0 &= \phi \, \frac{1 - n^b - n^b}{N} = \phi \, (1 - b - c)\,.
\end{aligned} \tag{16}$$

The intensity of herding is measured by the positive coefficient ϕ. The parameter β is

known as the intensity of choice. If the feedback indices remain unchanged and β is close to zero these three probabilities are almost identical. For $\beta \to \infty$ the probabilities highly depend on the explicit composition of the feedback indices. If one feedback index dominates the corresponding logit choice probability tends towards one and the remaining probabilities tend towards zero.

In this framework the discrete choice approach with asynchronous updating is introduced. It uses a fixed probability per unit of time μ reflecting that an agent actually reconsiders its attitude. At the macroscopic level it is sufficient to track the population shares of the bold and cautious agents since the fraction of the neutral agents is defined as the residual $1 - b_t - c_t$. Using the probabilities (15), the two differential equations for the evolution of the population shares b and c become[22]

$$\begin{aligned} \dot{b} &= \mu \left[\frac{\exp(\beta f_b)}{\exp(\beta f_b) + \exp(\beta f_c) + \exp(\beta f_0)} - b \right] \\ \dot{c} &= \mu \left[\frac{\exp(\beta f_c)}{\exp(\beta f_b) + \exp(\beta f_c) + \exp(\beta f_0)} - c \right]. \end{aligned} \tag{17}$$

3.2.1 Stability Analysis

Figure 17, Fig. 18 and Fig. 19 depict the phase plane representations for $\mu = 1.0$, $\beta = 1.0$ and increasing herding parameter ϕ.[23] At first view the evolution of the isoclines $F_b = 0$ and $F_c = 0$ is symmetric and they are mirrored at the symmetry line.

For a herding component $\phi < 2.75$ two single nonlinear isoclines are visible. For $\phi = 2.75$ two additional ellipsoidal isoclines arise symmetrically and augment their radii while the herding component ϕ increases. Their peaks stretch in the direction of the upper left, respectively lower right, corner of the phase plane. At some point these isoclines exceed the boundaries of the unit simplex, cf. Fig. 19.

Due to the symmetric structure of the underlying dynamic system the points of inter-

[22] See Appendix B.2.1 for the deterministic adjustment equations leading to this system of ODEs.

[23] See Appendix A.2.1 for phase plane diagrams showing the isoclines for $\mu = 1.0$, $\beta = 1.0$ and $\phi = 0, 1.5$.

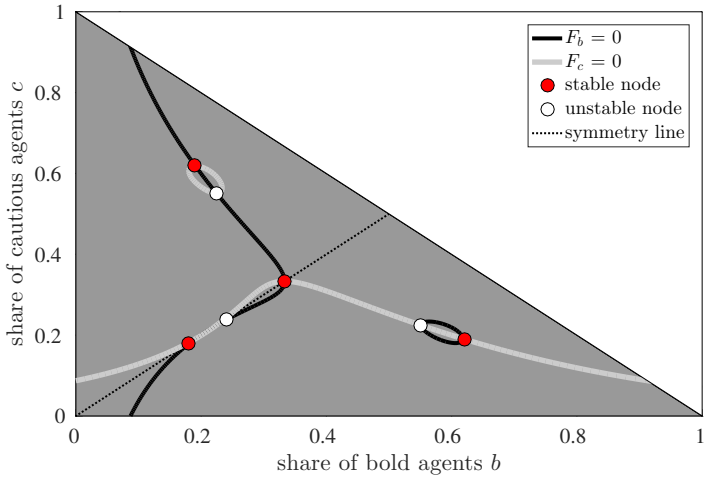

Figure 17: Phase plane representation of $F_b = 0$ (black) and $F_c = 0$ (white) for $\mu = 1.0$, $\beta = 1.0$ and $\phi = 2.75$. Additional ellipsoidal isoclines occur close to the center of the unit simplex. Four stable equilibria (red dots) and three unstable equilibria (white dots) are visible.

section are either arranged on the symmetry line or emerge pairwise in the phase plane and one equilibrium point can be reflected with respect to the symmetry line to obtain the second equilibrium point.

For the given values of μ and β it is possible to obtain the same qualitative behavior of the equilibrium points compared to the transition probability approach with unweighted feedback.

3.2.2 Bifurcation Analysis

Considering a broader range of the herding parameter $\phi \in [2.5, 5.0]$ the bifurcation diagram related to the discrete-choice setup, see Fig. 20, has the exact same qualitative structure as the bifurcation diagram utilizing transition probabilities with an unweighted feedback and $\phi \in [1.3, 2.3]$, cf. Fig. 6a. Both adjusted bifurcation diagrams display the augmented coordinate introduced in Subsec. 2.3.3 with $\epsilon = 0.2$.

Three parabolas are visible. Originally they have been symmetric in the non-adjusted bifurcation diagram. For $\phi = 2.74$ three saddle-node bifurcations occur at $(b_1^{sn}, c_1^{sn}) =$

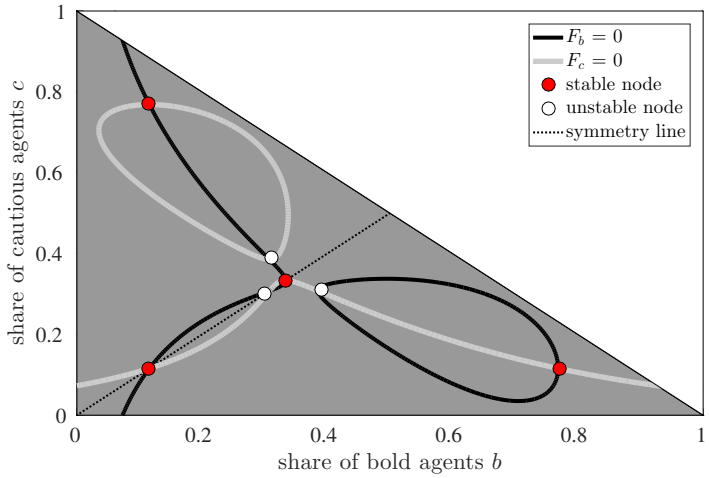

Figure 18: Phase plane representation of $F_b = 0$ (black) and $F_c = 0$ (white) for $\mu = 1.0$, $\beta = 1.0$ and $\phi = 2.9$. Four stable equilibria (red dots) and three unstable equilibria (white dots) are visible.

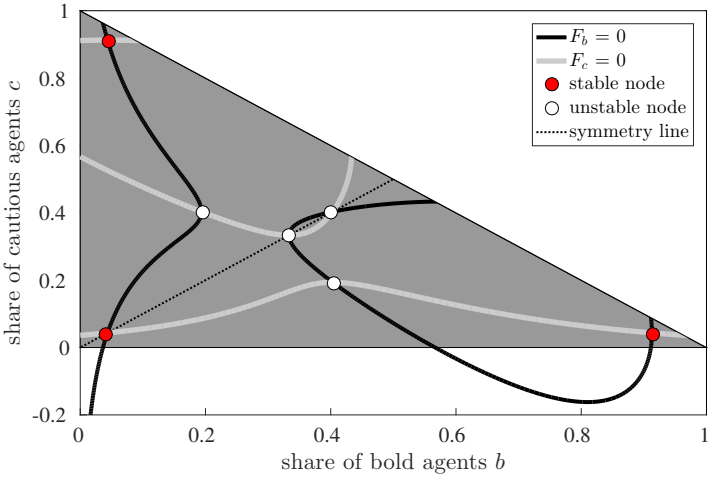

Figure 19: Phase plane representation of $F_b = 0$ (black) and $F_c = 0$ (white) for $\mu = 1.0$, $\beta = 1.0$ and $\phi = 3.5$. Three stable equilibria (red dots) and four unstable equilibria (white dots) are visible. Axis of ordinates is extended to show the accurate shape of the nonlinear isocline $F_b = 0$.

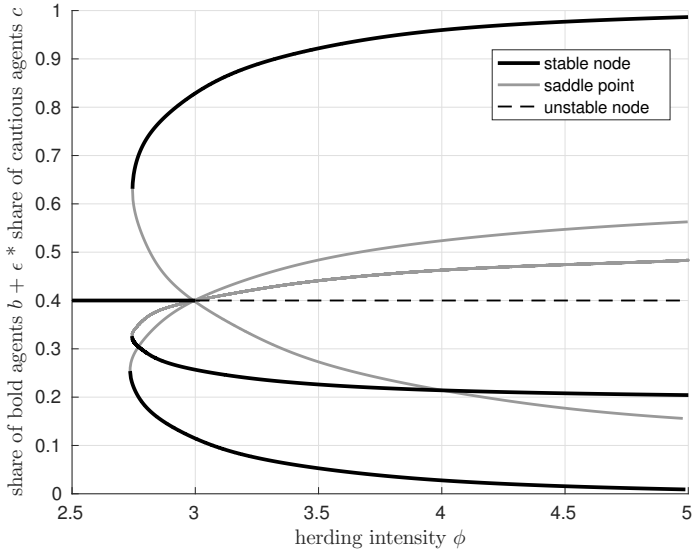

Figure 20: Bifurcation diagram with augmented coordinate $b + \epsilon c$ and $\epsilon = 0.2$, $\mu = 1.0$, $\beta = 1.0$ and $\phi \in [2.5, 5.0]$.

$(0.5702, 0.2145)$, $(b_2^{sn}, c_2^{sn}) = (0.2145, 0.5702)$ and $(b_3^{sn}, c_3^{sn}) = (0.2145, 0.2145)$ where (b^{sn}, c^{sn}) are the (b, c)-coordinates of the supercritical saddle-node bifurcations. These are non-adjusted (b, c)-coordinates which coincide with the symmetric structure of the equilibria distribution in the phase plane representation. An additional hyperbolic fixed point occurs for $\phi = 3$ and three equilibria collide into the symmetric equilibrium which undergoes a bifurcation and becomes unstable.

A non-monotonic sequence of steady-states is created, e.g. from $1 - 4 - 7 - 4 - 7$ equilibria. The step function exhibits two jumps for $\phi = 3$ from 7 to 4 to 7.

This framework deals with saddle-node bifurcations, i.e. local bifurcations. In this discrete choice approach saddle-node bifurcations show that multiple, co-existing stable and unstable equilibrium points can be observed for moderate values of the herding component ϕ. Therefore a steady state representing a majority of neutral agents is a possible outcome of this dynamical system.

3.3 Comparison of Transition Probability Approach and Discrete Choice Approach

Both approaches include an extension of the traditional sentiment dynamics models, namely the neutral sentiment is considered. The main difference in the setup between the discrete choice approach discussed in this chapter and the alternative approach presented in Chap. 2 is the allocation and definition of the underlying probabilities. Additionally there are alterations in the feedback indices.

The transitions probability approach assigns individual probabilities depending on a feedback index which includes a sentiment variable. Based on these specifications not every agent changes its attitude within time period $[t, t+\Delta t]$. In fact only a limited number of agents from each attitude, which arises from random draws with corresponding probabilities, switch their attitude.

In contrast, with logit choice probabilities in the discrete choice approach all agents are assigned the same probabilities in each period independent of their previously adopted attitude. Here the logit choice probabilities are based on feedback indices as well. But in each case they are the product of the shares of the three attitudes and the herding component ϕ. Due to these disparities in the setup of these two approaches the isoclines evolving in the phase plane have different shapes and almost no similarities in the evolution process in the phase plane can be detected. This is true for the pure and augmented feedback version.

First we focus on the comparison of the transition probability approach using pure feedback indices and the discrete choice approach. Even if the shapes of the nonlinear isoclines differ in both approaches they evolve fixed along the symmetry line in the phase plane. Additionally it can be detected that the equilibrium points are distributed uniformly around the symmetric equilibrium point $(b^s, c^s) = (0.333, 0.333)$ for all values of the herding parameter ϕ, cf. exemplary Fig. 4b and Fig. 18. The inspection of the corresponding parabolas to these equilibrium points reveals that they are located symmetrically around the straight line $(\phi, b^s + \epsilon c^s)$ in the bifurcation diagram, see Fig. 20.

This straight line represents the symmetric equilibrium point for all values of herding ϕ. This result corresponds to the bifurcation diagram obtained in the unweighted feedback scenario, cf. Fig. 6a. The very same qualitative behavior and therefore the very same bifurcation types can be seen.[24] This is in line with Franke (2014). The only difference concerns the scaling of the herding intensity ϕ. In the previous version an additional hyperbolic fixed point occurs for $\phi = 1.5$ and three equilibria collide into the symmetric equilibrium which undergoes a bifurcation and becomes unstable. The exact same features occur for the approach presented in this chapter, only for $\phi = 3$. The manifolds in the latter bifurcation diagram are shifted to the right. For the discrete choice approach a higher intensity of herding generates equivalent qualitative behavior. Thus there are no alterations in the amount of equilibria except for the considerd interval of the herding parameter ϕ.

The investigation of the differences of the transition probability approach using augmented feedback indices and the discrete choice approach can be adopted from the results in Subsec. 2.5. Due to the equivalency in qualitative behavior of the transition probability approach using pure feedback indices and the discrete choice approach all statements regarding the comparison with the weighted feedback scenario are valid for this comparison as well.

3.4 Conclusions

We formalized a discrete choice framework using a model of sentiment dynamics with three attitudes, i.e. bold, cautious and neutral.

The first goal of this chapter was to integrate neutral agents into an existing sentiment dynamics model. Therefore the logit choice probabilities for all agents from Franke (2014) have been augmented by the probability to become neutral. These rates incorporate feedback indices which are individual for all three attitudes. The main influence within the feedback comes from the sentiment components which are a weighted

[24] In the classical coordination game under Logit Dynamics analyzed by Hommes and Ochea (2012) the same qualitative behavior can be observed for their payoff parameter $\epsilon = 0$.

with a herding parameter. The particular sentiment is equal to the share of the respective group, e.g. $b = \frac{n^b}{N}$. A nonlinear two-dimensional system of ordinary differential equations was obtained.

The second goal was to investigate the generic possibility of complicated dynamics, i.e. multiple equilibrium points. The bifurcation analysis exhibited saddle-node bifurcations. The occurrence of this bifurcation type showed that the analyzed dynamical system can generate multiple, co-existing stable and unstable equilibrium points.

The analysis of the evolution of neutral agents revealed that a neutral majority may prevail depending on the herding. Based on these findings further macroeconomic extensions of this extended discrete choice approach for three-state dynamics are feasible.

4 A Stochastic Model of Investor Sentiment

We present a bi-variate model of investor sentiment with attitudes bold, cautious and neutral. A bold opinion index and a neutrality index are introduced. Individual transition rates specify changes between all three groups of agents. Bi-weekly survey data on American investor sentiment is used to estimate the model parameters via maximum likelihood estimation.

4.1 Introduction

Various stochastic frameworks of a collective process of opinion formation have been studied. Models mostly focus on binary decision problems of groups of agents. Among those and simpler alternative models, there is a bulk of empirical literature on the parameter estimation of dynamic opinion processes since survey data on sentiment indices are available from many academic and private institutes.

Hengelbrock et al. (2013) measure the predictive power of German and American investor sentiment indicators and test whether the market responds immediately to the release of new sentiment data. For the German market, they use the Sentix value index and find that for some periods German investor sentiment correctly anticipates equity market moves over the next few months. For the American market, they use *American Association of Individual Investors (AAII)* value index and find that American investor sentiment once used to be a contrarian indicator for equity market moves over coming months, but its predictive power has disappeared. Strong evidence that individual investor sentiment is related to increased volatility in special investment funds is provided by Brown (1999). See Verma and Verma (2008) and Verma and Soydemir (2010) for additional studies on AAII data.

Schmeling (2009) applies consumer confidence data from the *Directorate Generale for Economic and Financial Affairs* provided by the European Commission and Brown and Cliff (2004) uses AAII data to investigate the influence of investor sentiment on stock returns. In Lux (2009a), data from *animusX* on short-term and medium-term

sentiment for German investors are considered. Evidence for strong social interaction in short-term sentiment and moderate social influences in medium-run sentiment was found.

Sentiment data usually contain information on the share of neutral agents. However, in the literature these data are often neglected or divided and allocated equally to optimistic and pessimistic sentiment. Sentiment variables in the dynamic adjustment processes are often defined in such a way that neutrality is a possible state, i.e. sentiment variable x with domain $x \in [-1, 1]$ and $x = 0$ represents a state with an average neutral majority.[25] However, the transition rates do not explicitly reflect the additional behavioral specifics of neutral agents. In fact neutrality is understood as an intermediate state.

We close this gap by incorporating neutrality in a separate sentiment index. Therefore three types of attitudes are considered, i.e. bold, cautious and neutral. Transition rates for a dynamical process are formulated for all configurations of possible changes. These transition probabilities include a bold opinion index and a neutrality index accordingly. The probability fluxes for every configuration of sentiment change are summarized. The resulting model of investor sentiment is estimated via maximum likelihood estimation and AAII sentiment data to check if the incorporated neutrality index is able add explanatory power. The sensitivity analysis tests the robustness of this benchmark model by gradually restricting the influencing model parameters and compare the performance of the models. The most significant models are used for an out-of-sample forecast in order to evaluate the models' overall significance.

[25] In Boudin and Salvarani (2009) methods from statistical mechanics are utilized for an opinion formation model. See Toscani (2006), Düring et al. (2009) and Lux (2012) for further models of opinion formation. Düring et al. (2018) study a rating model for a large number of players motivated by the well-known Elo rating system. Their 'sentiment' variable is defined by the difference in strength of the two players.

4.2 Investor Sentiment Data

Since 1987 the *American Association of Individual Investors (AAII)* Investor Sentiment Survey collects weekly data from members regarding their vote on the direction of the U.S. stock market over the next six months. The survey measures the percentage of individual investors who obtain a bullish, bearish and neutral attitude on the stock market. A vote for an upward, respectively downward movement of the stock market is considered bullish, respectively bearish. A neutral attitude is assumed if the member expects that stock prices will not change over the next six months. *AAII* states the survey is able to work as a prompt to determine whether a buying, selling or rebalancing opportunity exists. Since 2013 around 300 members take the survey online on an average week. *AAII* having 160.000 members, the response rate is less than $0.2\,\%$. Additionally, data on the weekly high, low and close values of the S&P 500 are provided.

4.2.1 Time Series Analysis

Figure 21 shows the bi-weekly time series of the S&P 500 index and the quarterly moving average from 1999 until 2018. This period comprises the development and burst of the *Dot-com Bubble* from 1999 until end of 2002 as well as the *Global Financial Crisis* starting in 2007 and its aftermath. The bi-weekly time series of the S&P 500 return rates and the quarterly moving average are depicted in Fig. 22.
Figure 23, Fig. 24 and Fig. 25 show bi-weekly time series of the *AAII* Investor Sentiment Survey data from 1999 until 2018. The panels depict bullish, bearish and neutral sentiment shares and their corresponding mean values and quarterly moving average curves. It is worthwhile to consider these two types of time series, i.e. stock indices and sentiment shares, and correlate these data.

The attitude of individual investors swings from bullish to bearish. These swings reflect attitudes toward the direction of the stock market, the state of the economy and other macroeconomic factors impacting individual investors short-term outlook for stock prices, e.g. the period from November 2007 through February 2009, when bearish sen-

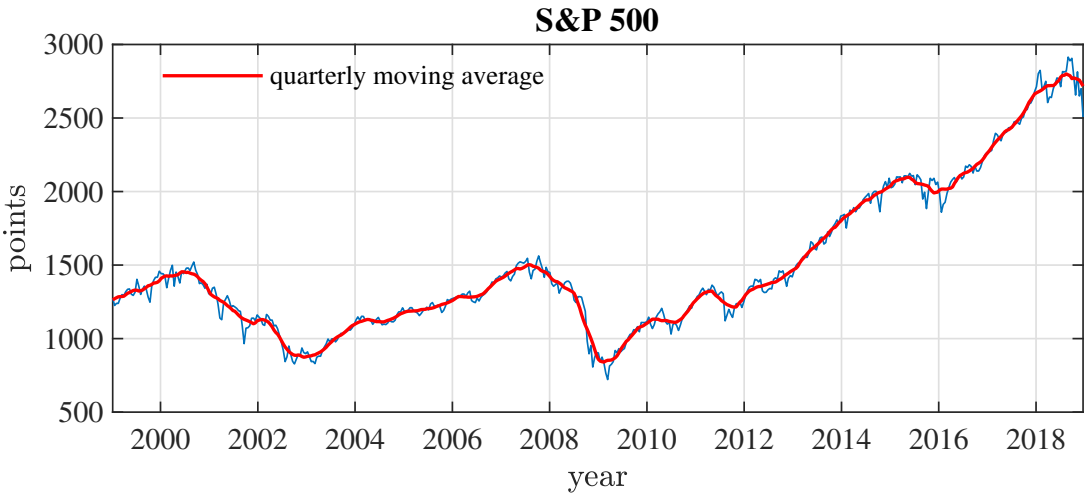

Figure 21: Bi-weekly time series of S&P 500 points (blue line). Quarterly moving average curve highlights trend (red line).

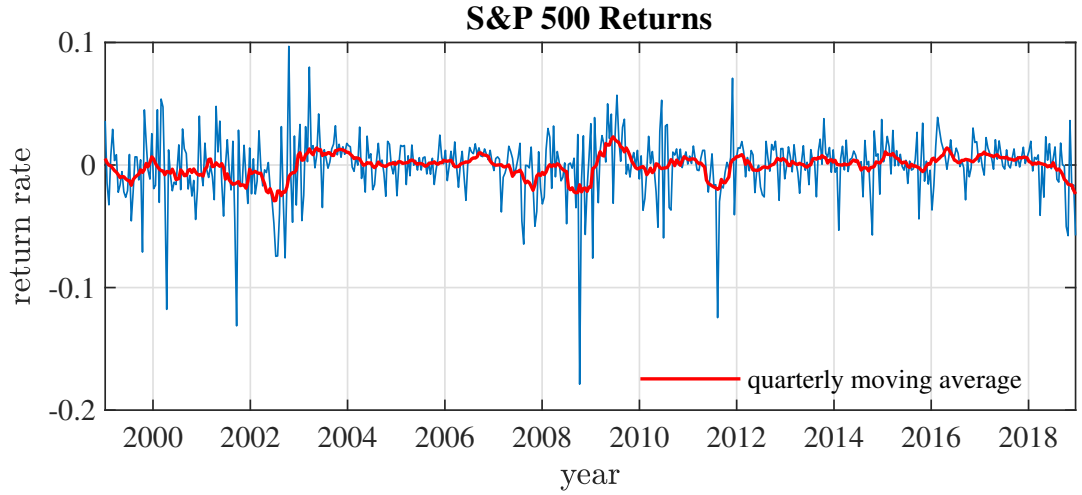

Figure 22: Bi-weekly time series of S&P 500 return rates (blue line). Quarterly moving average curve highlights trend (red line).

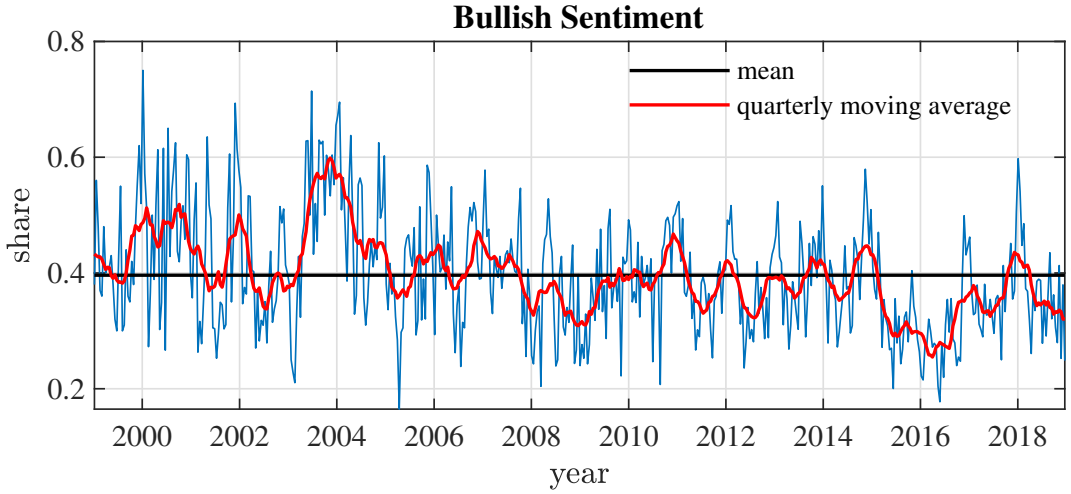

Figure 23: Bi-weekly time series of *AAII* Bullish Sentiment Survey data. Quarterly moving average curve highlights trend (red line). Mean value is equal to 0.39 (black line).

timent dominated and reached the record high share of 0.7 on March 5, 2009. Neutral sentiment reached its record low share of 0.08 on October 9, 2008. The record high for bullish sentiment is 0.75, set on January 6, 2000. Bearish and neutral sentiment have a historical average share of 0.31 over the life of the survey. Bullish sentiment has a historical average share of 0.39.

It can be observed that historically high levels of neutral sentiment have been followed by an above-average market performance of the S&P 500 over the preceding 26- and 52-week periods, i.e. a median 26-week rise in the S&P 500 of $8.6\,\%$ with a median return of $5.2\,\%$ for the same period, respectively a median 52-week rise of $17.7\,\%$ with a median return of $10.7\,\%$ for the same period.

High levels of neutral sentiment indicate that investors remain stock holders even if they are not as active on the market as investors with bullish sentiment. Therefore the share of the neutral sentiment is trendsetting for the direction of the index. This is not true for the *Dot-com Boom* as well as for the *Global Financial Crisis*. In this case the neutral sentiment serves as an indicator for a reverse trend of the market performance.

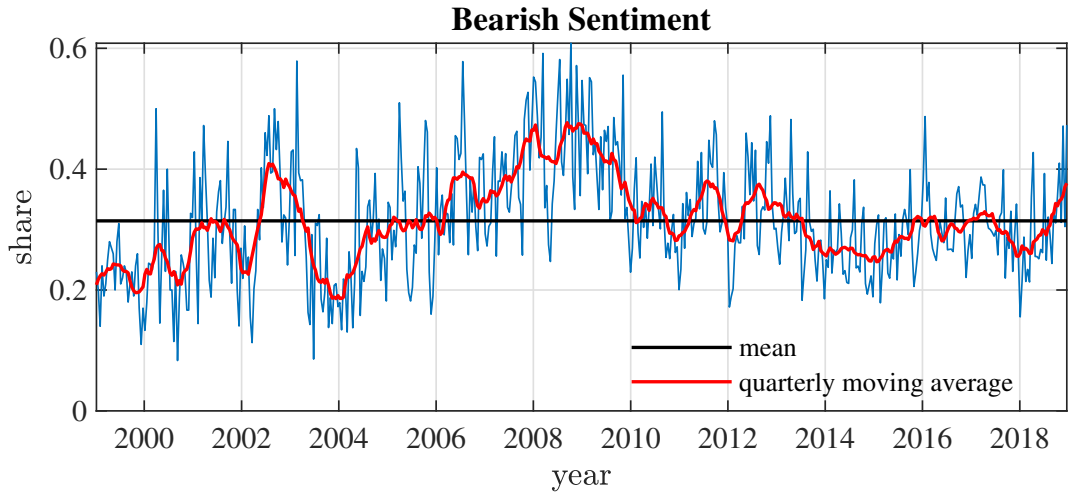

Figure 24: Bi-weekly time series of *AAII* Bearish Sentiment Survey data. Quarterly moving average curve highlights trend (red line). Mean value is equal to 0.31 (black line).

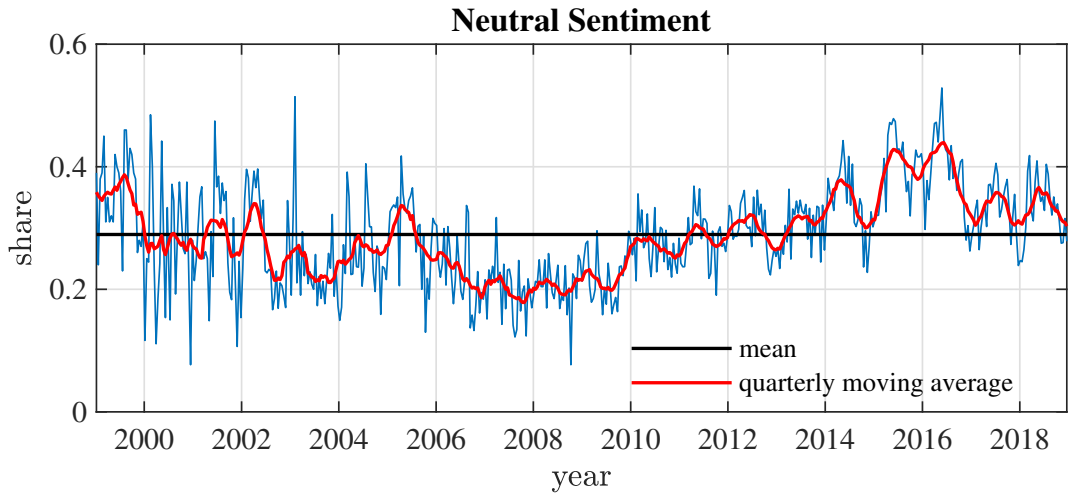

Figure 25: Bi-weekly time series of *AAII* Neutral Sentiment Survey data. Quarterly moving average highlights trend (red line). Mean value is equal to 0.31 (black line).

During the period of the *Dot-com Boom* the share of neutral sentiment decreases significantly while the share of bullish sentiment increases drastically. An increase of the share of bearish sentiment can be observed only after the burst of the *Dot-com Bubble* which is quite intuitive. The shares of bullish and neutral sentiment drop during the *Global Financial Crisis* while the share of bearish sentiment rises drastically due to increasing insecurity. Investors are highly risk-averse and do not want to hold stocks, they are active on the market.

In Fig. 26 the annualized and averaged standard deviations for all three types of sentiment are depicted. Additionally Tab. 3 provides summary statistics. It can be seen that the share of neutral sentiment exhibits less pronounced peaks and less fluctuations compared to the shares of bullish and bearish sentiment, i.e. total standard deviation of neutral sentiment of 0.08 to approximately 0.1 for bullish and bearish sentiment.

Investors with a neutral position have the expectation of no movements on the market. They still own stocks, but the neutral attitude is more considered an investment strategy.

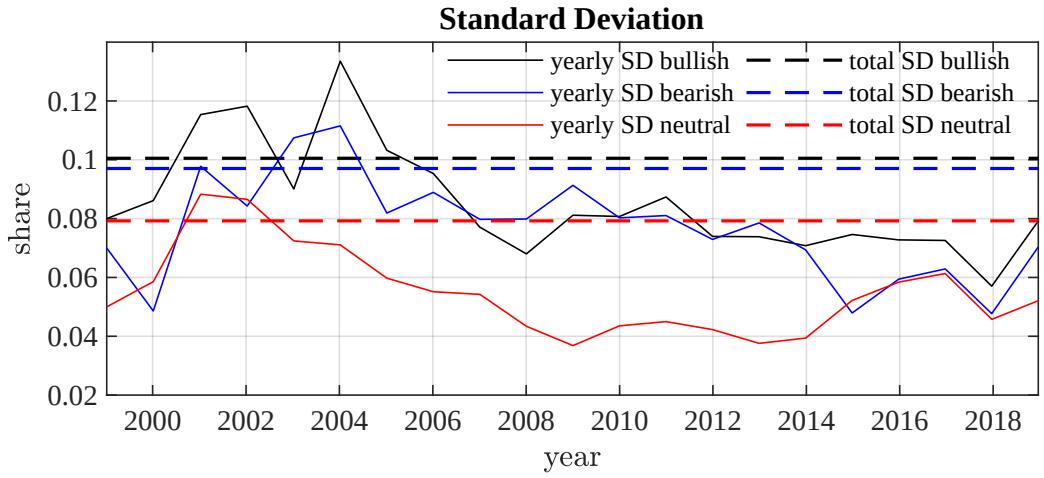

Figure 26: Yearly standard deviation of bullish, bearish and neutral sentiment (black, blue and red solid lines). Total standard deviation of bullish, bearish and neutral sentiment (black, blue and red dashed lines).

	Bullish sentiment	Bearish sentiment	Neutral sentiment
Maximum	0.75	0.7027	0.5286
Minimum	0.1648	0.0667	0.0769
Mean	0.3961	0.3144	0.2894
Standard deviation	0.1005	0.097	0.0792
Variance	0.0101	0.0094	0.0063

Table 3: Summary statistics for sentiment data from 1999 to 2018.

4.2.2 Correlation Analysis

Figure 27 displays the correlation matrix with regard to all observed key figures. The histograms of the variables appear along the matrix diagonal while the scatter plots of variable pairs appear on the off-diagonal. The slope of the least-squares fit in each scatter plot is equal to the displayed correlation coefficient.

The correlation coefficients and corresponding p-values are displayed in Tab. 4. Bullish and bearish sentiment have a strong negative linear relationship, see correlation coefficient equal to -0.68. A moderate negative correlation of -0.44 can be seen for neutral and bullish sentiment whereas a weak to moderate negative relationship with coefficient -0.36 can be seen for neutral and bearish sentiment. The S&P 500 index and bullish sentiment, as well as the index, respectively the S&P 500 return rates and bearish sentiment exhibit only weak negative linear correlations, i.e. -0.21, -0.16, respectively -0.25. No correlation is detected for the relationship of the S&P 500 return rates with the S&P 500 index as well as neutral sentiment, cf. coefficients 0.05, 0.02. S&P 500 return rates and bullish sentiment have only a weak positive linear relationship, see correlation coefficient equal to 0.22. A moderate positive correlation of 0.46 can be seen for neutral sentiment and the S&P 500 index. This is in line with statements

concerning neutral sentiment in Subsec. 4.2.1.

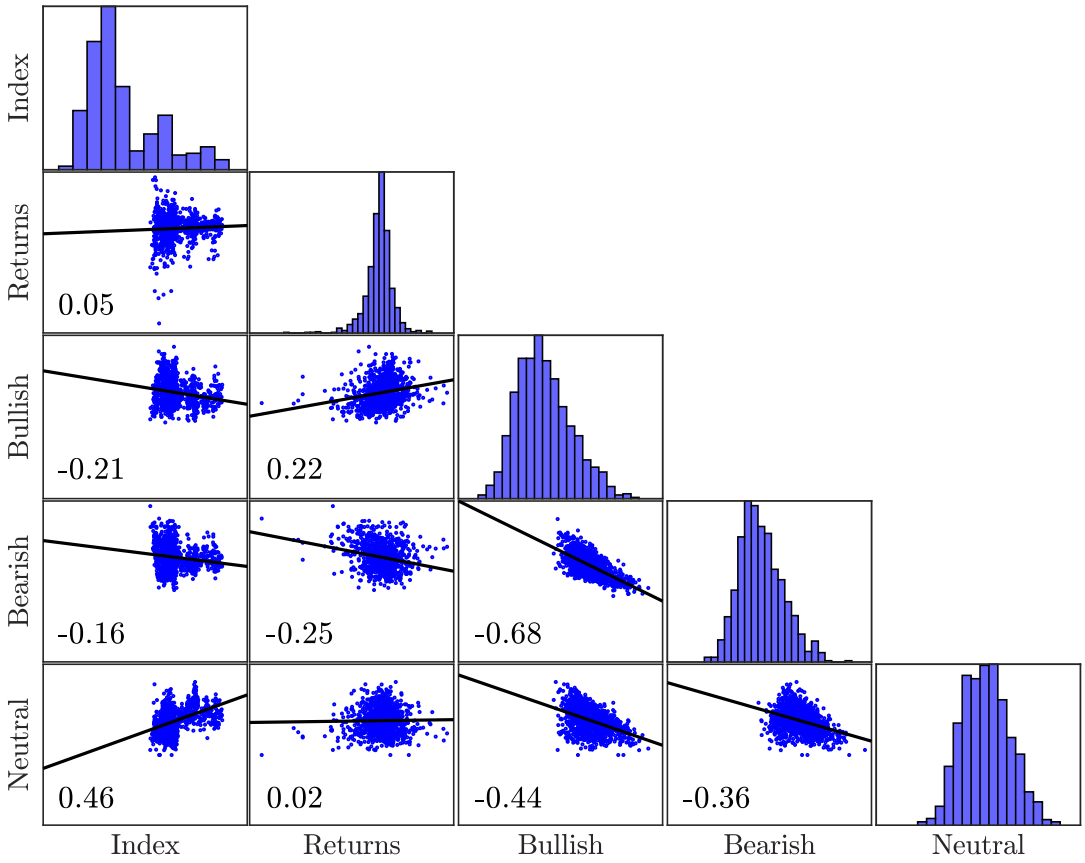

Figure 27: Correlation matrix with histograms of the variables on the diagonal. Off-diagonal elements are scatter plots including reference lines (black) with slopes equal to the displayed correlation coefficients.

It can be determined that the S&P 500 return rates have no significant relationship with any other observed key figure. However weak to moderate correlations between neutral sentiment and bullish, respectively bearish sentiment, as well as S&P 500 index are apparent. This is one additional reason to investigate neutral sentiment more in detail and incorporate this attitude into a model of investor sentiment.

	Index	Returns	Bullish	Bearish
Returns	0.05 (0.10)	-	$*$	$*$
Bullish	-0.21 (0.00)	0.22 (0.00)	-	$*$
Bearish	-0.16 (0.00)	-0.25 (0.00)	-0.68 (0.00)	-
Neutral	0.46 (0.00)	0.02 (0.57)	-0.44 (0.00)	-0.36 (0.00)

Table 4: Correlation coefficients of pairs of all variables and their corresponding p-values.

4.3 Sentiment Dynamics

The following group dynamics are based on the stochastic framework in Weidlich and Haag (1983) and Lux (1995). The original setup includes two types of opinions agents can adopt, e.g. optimistic/bullish and pessimistic/bearish investors or buyers and sellers. In this chapter this configuration is extended by neutral agents.[26] Considering financial markets a neutral sentiment is assumed if investors hold stocks.

In this model single agents can be characterized as having one of three attitudes: bold (b), cautious (c) or neutral (0). Let n_b, n_c and n_0 be the number of bold, cautious and neutral agents. For the overall number N of agents this identity holds:

$$n_b + n_c + n_0 = N.$$

We define the following opinion indices based on the number of bold and neutral agents

$$\begin{aligned} x &:= \frac{n_b}{N}, \; x \in [0,1], \\ y &:= \frac{n_0}{N}, \; y \in [0,1]. \end{aligned} \tag{18}$$

[26] Lux (1995) explicitly does not allow for neutral agents.

Let x be the bold opinion index and y is a neutrality index.[27] The ratio of cautious agents is expressed in terms of the residual

$$1 - x - y := \frac{n_c}{N}.$$

Agents transition between sentiments over time. These changes occur according to individual transition rates per unit time $p_{ij}(n, m)$ with $i, j \in \{b, c, 0\}$.

The individual probabilities assume an exponential form and specify changes from sentiment j to sentiment i:

$$\begin{aligned}
p_{bc}(n_b, n_0) &= \nu_0 \, \exp(U_{11}) \, , \, U_{11} = +\alpha_0 + \, \alpha_1 \, n_b + \alpha_2 \, n_0, \\
p_{cb}(n_b, n_0) &= \nu_0 \, \exp(U_{12}) \, , \, U_{12} = -\alpha_0 - \, \alpha_1 \, n_b + \alpha_2 \, n_0, \\
p_{b0}(n_b, n_0) &= \nu_1 \, \exp(U_{21}) \, , \, U_{21} = +\beta_0 + \, \beta_1 \, n_b - \beta_2 \, n_0, \\
p_{0b}(n_b, n_0) &= \nu_1 \, \exp(-U_{21}) \, , \\
p_{c0}(n_b, n_0) &= \nu_1 \, \exp(U_{22}) \, , \, U_{22} = +\beta_0 - \, \beta_1 \, n_b - \beta_2 \, n_0, \\
p_{0c}(n_b, n_0) &= \nu_1 \, \exp(-U_{22}) \, .
\end{aligned}$$

In comparison to the model assumptions in Chap. 2 direct switches from one extreme sentiment to the other, i.e. bold, respectively cautious, are incorporated. This allows for additional dynamics and might capture extraordinary events and periods. Note that the focus of this formalization is primary on an advanced characterization of individual behavior. Therefore the parameters for the dynamic part of the stochastic model are chosen carefully.

The parameters are established in a two-tier structure. The first group of parameters relates to the transitions between extreme sentiments bold and cautious only while the second group relates to transitions to and from neutral sentiment.

[27] In Lux (2012) the index is formalized in such a way that neutrality is not excluded. It is not captured in a separate opinion index but rather embedded in the opinion index as balanced state ($x = 0$) between an optimistic ($x = 1$) and pessimistic majority ($x = -1$).

ν_0 and ν_1 are parameters related to the individual speed of adjustment of pairs of agents from different sentiments. They measure the frequency of opinion reevaluation for bold, neutral and cautious sentiment. The 'long distance' speed of adjustment parameter is denoted by ν_0. It determines the frequency of changes from bold to cautious sentiment and vice versa. ν_1 is considered a parameter capturing the 'short distance' speed of adjustment. It determines the frequency of transitions from bold to neutral sentiment, from neutral to cautious sentiment and vice versa. This parameter considers the neutral attitude as intermediate state.

The functions or forcing terms U_{kl}, $k, l \in \{1, 2\}$, include all determinants which have an influence on the decision of agents to transition between sentiments.

The parameters α_0 and β_0 formalize the bias agents have towards one opinion, i.e. bold b or cautious c. α_0 represents a bias for the transition between the extreme sentiments bold and cautious only. It is assumed that this bias is reversed regarding the direction of the transition between these two sentiments. The remaining transition rates relate to switches which include the neutral sentiment and have incorporated a bias β_0. Therefore a separate bias for neutrality is not necessary. This bias is supposed to be identical towards bold and cautious sentiment, cf. p_{b0} and p_{c0}, and reversed regarding the direction of the transition between two sentiments, cf. p_{b0} and p_{0b}.

The coefficients α_1 and β_1 measure the influence of the fraction of bold agents n_b while the coefficients α_2 and β_2 measure the influence of the fraction of neutral agents n_0. It is assumed that α_1 is opposed and α_2 is identical regarding the direction of the transition between the two affected sentiments bold and cautious. The latter shows that neutral sentiment has the same weighting in transition rates that do not include this very sentiment. The parameter β_1 is supposed to be reversed regarding the direction of the transition between two sentiments, e.g. p_{b0} and p_{0b}, as well as regarding transitions to and from neutral sentiment, e.g. p_{b0} and p_{c0}. β_2 is assumed to be identical regarding transitions from and to neutral sentiment, e.g. p_{0b} and p_{0c}, while it is supposed to be reversed regarding the direction of the transition between two sentiments, e.g. p_{c0} and p_{0c}.

The aggregated and scaled transition rates per unit time $N w_{ij}(x,y) = n_j\, p_{ij}(n_b, n_0)$ are given by:

$$\begin{aligned}
w_{bc}(x,y) &= \nu_0\,(1-x-y)\,\exp(+\alpha_0 + \alpha_1\,x + \alpha_2\,y)\,,\\
w_{cb}(x,y) &= \nu_0\,x\,\exp(-\alpha_0 - \alpha_1\,x + \alpha_2\,y)\,,\\
w_{b0}(x,y) &= \nu_1\,y\,\exp(+\beta_0 + \beta_1\,x - \beta_2\,y)\,,\\
w_{0b}(x,y) &= \nu_1\,x\,\exp(-\beta_0 - \beta_1\,x + \beta_2\,y)\,,\\
w_{c0}(x,y) &= \nu_1\,y\,\exp(+\beta_0 - \beta_1\,x - \beta_2\,y)\,,\\
w_{0c}(x,y) &= \nu_1\,(1-x-y)\,\exp(-\beta_0 + \beta_1\,x + \beta_2\,y)\,.
\end{aligned} \tag{19}$$

In this continuous-time framework the probability distribution over the sentiment-configuration of all agents N is of interest. Therefore the probability that at time t the configuration (x,y) prevails, i.e. $p\,(x,y;t)$, needs to be obtained. The equation of motion for $p\,(x,y;t)$ is given by the following *Master equation*[28]:

$$\begin{aligned}
\frac{\partial p\,(x,y;t)}{\partial t} &= p\,(x, y-\tfrac{1}{N})\,w_{0c}\,(xN, yN-1) - p\,(x,y)\,w_{0c}\,(xN,yN)\\
&\quad + p\,(x, y+\tfrac{1}{N})\,w_{c0}\,(xN, yN+1) - p\,(x,y)\,w_{c0}\,(xN,yN)\\
&\quad + p\,(x+\tfrac{1}{N}, y-\tfrac{1}{N})\,w_{0b}\,(xN+1, yN-1) - p\,(x,y)\,w_{0b}\,(xN,yN)\\
&\quad + p\,(x-\tfrac{1}{N}, y+\tfrac{1}{N})\,w_{b0}\,(xN-1, yN+1) - p\,(x,y)\,w_{b0}\,(xN,yN)\\
&\quad + p\,(x-\tfrac{1}{N}, y)\,w_{bc}\,(xN-1, yN) - p\,(x,y)\,w_{bc}\,(xN,yN)\\
&\quad + p\,(x+\tfrac{1}{N}, y)\,w_{cb}\,(xN+1, yN) - p\,(x,y)\,w_{cb}\,(xN,yN)
\end{aligned}$$

[28] See Weidlich and Braun (1992) for a nonlinear model describing macroeconomic dynamics. They use a probabilistic approach which leads to a Master equation.

$$
\begin{aligned}
= \; & p\left(x, y-\tfrac{1}{N}\right) w_{0c}\left(xN, yN-1\right) \\
& + p\left(x, y+\tfrac{1}{N}\right) w_{c0}\left(xN, yN+1\right) \\
& + p\left(x+\tfrac{1}{N}, y-\tfrac{1}{N}\right) w_{0b}\left(xN+1, yN-1\right) \\
& + p\left(x-\tfrac{1}{N}, y+\tfrac{1}{N}\right) w_{b0}\left(xN-1, yN+1\right) \\
& + p\left(x-\tfrac{1}{N}, y\right) w_{bc}\left(xN-1, yN\right) \\
& + p\left(x+\tfrac{1}{N}, y\right) w_{cb}\left(xN+1, yN\right) \\
& - p\left(x, y\right) \cdot \big[w_{bc}\left(xN, yN\right) + w_{cb}\left(xN, yN\right) + w_{0c}\left(xN, yN\right) \\
& \qquad + w_{c0}\left(xN, yN\right) + w_{0b}\left(xN, yN\right) + w_{b0}\left(xN, yN\right) \big].
\end{aligned}
\tag{20}
$$

The positive expressions in (20) describe the probability flux into the configuration (x, y) from configurations in the neighborhood, e.g. a neutral agent changes the attitude to cautious, i.e. $(x, y + \frac{1}{N})$. The negative expressions describe the probability flux from the configuration (x, y) into configurations in the neighborhood.

We use a Taylor series expansion[29] and insert transition rates (19) in order to formulate a two-dimensional *Fokker-Planck* equation[30] for the density $p(x, y; t)$,

$$
\frac{\partial p}{\partial t}(x, y; t) = -\sum_{i=1}^{2} \frac{\partial}{\partial i}(A_i(x, y)p(x, y; t)) + \frac{1}{2}\sum_{i,j=1}^{2} \frac{\partial^2}{\partial i \partial j}(B_{ij}(x, y)p(x, y; t)) \,, \tag{21}
$$

with a two-dimensional drift vector $A(x, y)$ and an associated 2×2 diffusion matrix $B(x, y)$. They are given by

$$
A\left(x, y\right) = \begin{pmatrix} A_1\left(x, y\right) \\ A_2\left(x, y\right) \end{pmatrix} = \begin{pmatrix} -w_{bc}\left(x, y\right) + w_{cb}\left(x, y\right) - w_{b0}\left(x, y\right) + w_{0b}\left(x, y\right) \\ -w_{0c}\left(x, y\right) + w_{c0}\left(x, y\right) - w_{0b}\left(x, y\right) + w_{b0}\left(x, y\right) \end{pmatrix} ,
$$

[29] See Appendix B.3.1 for the derivation.

[30] See Curado and Nobre (2003) for the derivation of a nonlinear Fokker-Planck equation as an approximation to the Master equation. See Risken (1989) for general information on Fokker-Planck equations.

and

$$B(x,y) = \frac{1}{N}\begin{pmatrix} B_{11}(x,y) & B_{12}(x,y) \\ B_{21}(x,y) & B_{22}(x,y) \end{pmatrix},$$

$$B_{11}(x,y) = w_{bc}(x,y) + w_{cb}(x,y) + w_{b0}(x,y) + w_{0b}(x,y)$$

$$B_{22}(x,y) = w_{0c}(x,y) + w_{c0}(x,y) + w_{b0}(x,y) + w_{0b}(x,y)$$

$$B_{12}(x,y) = B_{21}(x,y) = -2(w_{0c}(x,y) + w_{c0}(x,y) + w_{0b}(x,y) + w_{b0}(x,y)).$$

The obtained Fokker-Planck equation describes the time evolution of the probability density function $p(x,y;t)$ of the underlying stochastic system.

4.4 Empirical Application

The model parameters of the Fokker-Planck equation are estimated via maximum likelihood estimation. The empirical results based on American investor sentiment data are presented.

4.4.1 Estimation Methodology

The large parameter set θ of our stochastic system, i.e. $\theta = (\nu_0, \nu_1, \alpha_0, \alpha_1, \alpha_2, \beta_0, \beta_1, \beta_2)$, needs to be estimated, this will be done via maximum likelihood estimation. Thus, the solution of the Fokker-Planck equation (21) is required. Fokker-Planck equations provide the exact law of motion for the transient density of a diffusion process with drift and diffusion terms but for agent-based models, only an approximate law of motion for the transient density $p(x,y;t)$ is provided.[31] Closed-form solutions of Fokker-Planck equations exist for basic systems only.[32] The presented bi-variate nonlinear stochastic model is too advanced to analytically derive its transient density. Therefore, the param-

[31] See Lux (2009b) for details on the methodology for estimating the parameters of a dynamic opinion process.

[32] Polyanin and Zaitsev (2004) provide exact solutions to more than 1600 nonlinear equations and nonlinear partial differential equations.

eter estimation is dependent on the numerical solution of the Fokker-Planck equation. The following log likelihood function $\mathcal{L}$ is used for maximization:

$$\log \mathcal{L}(\theta) = \log p(x, y; 0|\theta) + \sum_{t=0}^{T-1} \log p(x, y; t|\theta) \,. \tag{22}$$

Due to the properties of Fokker-Planck equations, i.e. they are a precise description for diffusion processes, only an estimation of the diffusion approximation of our underlying investor sentiment model is possible. Therefore the corresponding maximum likelihood estimation is essentially not exact.[33]

For partial differential equations, like the Fokker-Planck equation, several numerical integration schemes are available.

Following Lux (2012) the *Peaceman-Rachford* algorithm is selected.[34] This algorithm belongs to the class of alternative direction (ADI) schemes.

4.4.2 Sensitivity Analysis

The survey data considered starts in January 1999 and ends in December 2018. Based on the response rate provided by *AAII* the number of agents $N = 300$ is fixed. The data format matches the definitions of the bold opinion index and the neutrality index, i.e. the shares of bullish respectively neutral investors correspond to x respectively y.

See Model I in Tab. 5 for the parameter estimates $\theta = (\nu_0, \nu_1, \alpha_0, \alpha_1, \alpha_2, \beta_0, \beta_1, \beta_2)$, the standard errors in brackets and the corresponding goodness-of-fit measures, i.e. log-likelihood values ($\mathrm{Log\ L}$), Akaike information criterion (AIC) values and Bayesian information criterion (BIC) values, for the original unrestricted bi-variate stochastic mod-

[33] Numerical approximations of the Fokker-Planck equation for maximum likelihood estimation of bi-variate and even tri-variate models can be found in Lux (2013).

[34] See Lux (2013) and Peaceman and Rachford (1955) for discretization schemes. The latter present their alternating-direction implicit method in detail for the numerical solution of parabolic differential equations. For further information on alternative finite difference schemes and ADI schemes for partial differential equations in higher dimensions see Strikwerda (2004), Thomas (1995) and Morton and Mayers (2005). A finite difference scheme for the numerical solution of a two dimensional Fokker-Planck equation and one application is analyzed in detail in Zorzano et al. (1999).

els of investor sentiment.

For the speed of adjustment parameters we obtain $\nu_0 < \nu_1$. Interactions involving neutral agents have a higher intensity. It is plausible that the speed of adjustment for interactions between bold and cautious agents is smaller since these are extreme attitudes and under regular market conditions their interaction frequency is reduced. Primarily bold and cautious agents interact with neutral agents, this is reflected by parameter ν_1 with a higher value.

A neutral bias α_0 for cautious/bold sentiment and a negative bias β_0 can be observed. $\beta_0 < 0$ indicates a bias towards neutrality. For switches between extreme attitudes we find positive values for α_1 and α_2, while $\alpha_1 > \alpha_2$. The influence from the bold sentiment itself, i.e. α_1, is relatively high. There is a smaller reinforcement from neutral sentiment α_2. For changes from neutral to bold and from cautious to neutral we find a negative reinforcement from bold sentiment β_1 while $\beta_2 > 0 > \beta_1$. Changes from bold and cautious to neutral therefore include a strong positive reinforcement from neutral sentiment β_2. All parameters except for $\alpha_0 = 0$ are significant.

In Fig. 28 the probability distribution of the unrestricted estimated stochastic opinion dynamics is provided. Since an analytical solution is not available for our nonlinear bi-variate Fokker-Planck equation (21), we have integrated the transitional density until it converged to a stationary distribution. We find a unimodal distribution with probability mass concentrated closely around the calculated mean for both axes, i.e. the share of bold agents and the share of neutral agents, cf. Tab. 3.[35]

Additionally a sensitivity analysis is performed. Several restricted versions of the original general bi-variate stochastic model have been estimated, i.e. Model II to Model X with parameter estimates and goodness-of-fit measures in Tab. 5, Tab. 6 and Tab. 7. For Model II $\alpha_2 = 0$ is assumed, indicating that neutral sentiment has no influence on transitions between bold and cautious sentiment. For the sake of completeness we assume $\beta_2 = 0$ for the second specific model, i.e. no influence from neutral agents on

[35] See Appendix A.3.1 for two-dimensional probability distributions for the share of neutral agents n_0 and the share of bold agents n_b for the period from 1999 to 2018.

	Model I	Model II	Model III	Model IV
		Parameter estimates		
ν_0	2.8243 (0.0002)	3.0 (0.0643)	2.8432 (0.0002)	2.5899 (0.0002)
ν_1	4.0 (0.0)	3.9416 (0.0101)	4.0911 (0.0043)	3.9072 (0.0009)
α_0	0.0 (0.0024)	0.0691 (0.0266)	-0.0956 (0.0959)	-0.4279 (0.001)
α_1	0.6741 (0.002)	0.6646 (0.0226)	0.6296 (0.0005)	0.3125 (0.0)
α_2	0.1624 (0.0)	-	0.17 (0.0002)	-
β_0	-0.5112 (0.0437)	-0.5313 (0.0818)	-0.3805 (0.3384)	-0.6192 (0.5968)
β_1	-0.228 (0.0628)	-0.2292 (0.0661)	-0.7487 (0.3152)	-0.329 (0.0804)
β_2	1.2367 (0.0109)	1.234 (0.0119)	-	-
		Goodness-of-fit measures		
Log L	-424.0169	-444.7883	-1334.1644	-1350.0777
AIC	862.0338	903.5766	2682.3288	2712.1554
BIC	882.1065	923.6493	2702.5015	2729.3606

Table 5: Parameter estimates $\theta = (\nu_0, \nu_1, \alpha_0, \alpha_1, \alpha_2, \beta_0, \beta_1, \beta_2)$, corresponding standard errors in brackets and goodness-of-fit measures for the unrestricted bi-variate stochastic model of investor sentiment (Model I) and three restricted models regarding the neutrality index (Model II - Model IV).

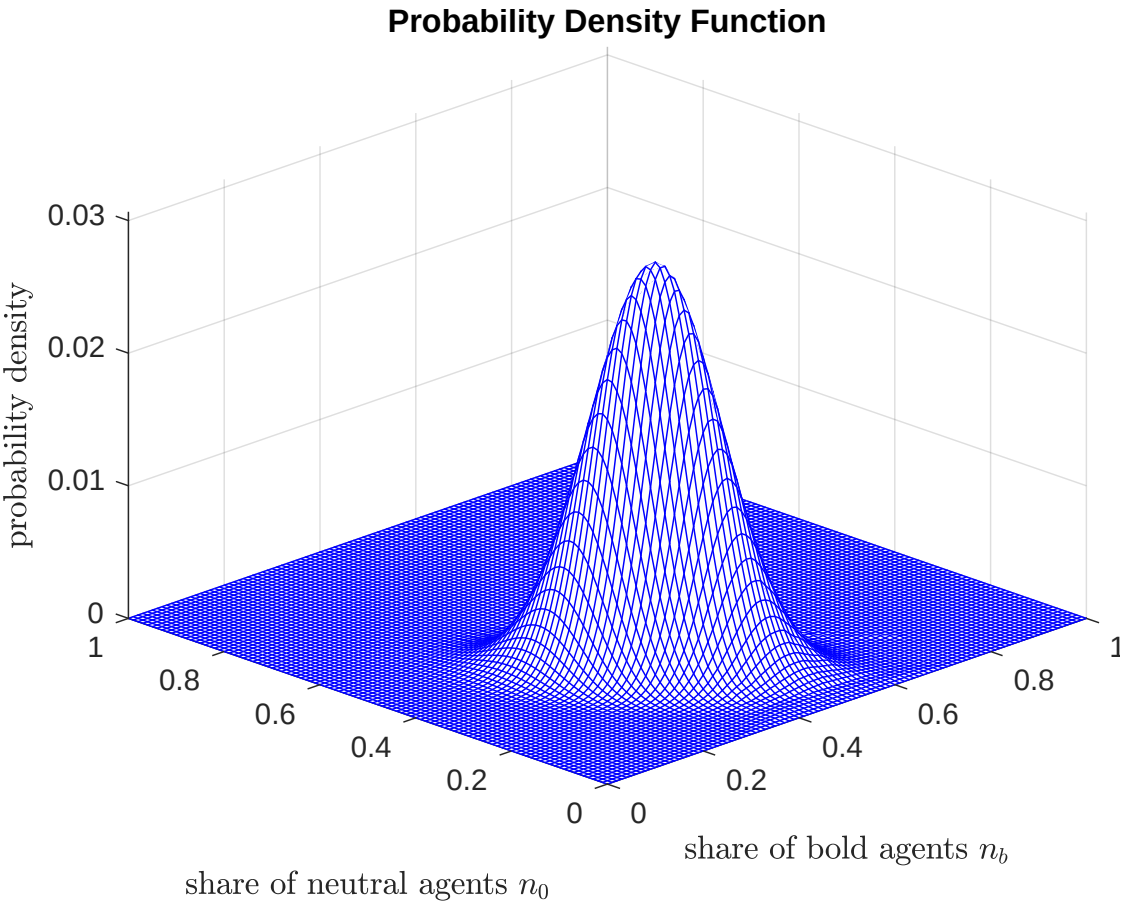

Figure 28: Three-dimensional probability distribution for the period from 1999 to 2018.

changes involving the neutral attitude. Model IV combines $\alpha_2 = 0$ and $\beta_2 = 0$, so there is no reinforcement from neutral sentiment on any transition rate at all. This leads to a uni-variate stochastic model.

For Model II to Model IV we obtain $\nu_0 < \nu_1$ for the speed of adjustment parameters. The direction of the bias towards bold sentiment α_0 is ambiguous for these restricted versions. For $\beta_2 = 0$ in Model III and Model IV a bias towards the cautious sentiment can be observed, i.e. $\alpha_0 < 0$, but this parameter shows statistical significance only for Model IV. $\beta_0 < 0$ indicates a rather high bias towards neutrality. For transitions between extreme attitudes we find positive values for α_1 in all models and $\alpha_2 > 0$ in Model III, while $\alpha_1 > \alpha_2$. There is only a smaller reinforcement from neutral sentiment α_2 on these two transition rates. Considering changes for neutral agents we find a moderate negative reinforcement from bold sentiment for all restricted models. We find $\beta_2 > 0 > \beta_1$ for Model II and β_2 has a relative high value. All of the parameters of Model II are statistically significant while for Model III α_0 and β_0 are insignificant. For Model IV significance is seen for all parameters except for β_0.

The log-likelihood values of Model I and Model II have almost the same magnitude, i.e. from -424 for Model I and -445 for Model II. The values for AIC information criterion and the BIC information criterion show a similar range. For Model III and Model IV log-likelihood values around -1334 and -1350 are detected.

The likelihood ratio tests speak in favor of Model I for all three restricted models. The p-values for Model II, Model III and Model IV are equal to zero. A nominal significance level of 0.05 is chosen for the hypothesis tests. The test rejection decisions indicate rejection of the restricted models in favor of the unrestricted model.

From these results we conclude that the transition rates describing changes between the extreme attitudes heavily depend on the bold opinion index and less on the neutrality index, see Model II. Transition rates describing changes between one of the extreme attitudes and the neutral attitude however are strongly dependent on the neutrality index, see smaller log-likelihood values of Model III and Model IV with $\beta_2 = 0$.

The restricted Model V to Model VII, with parameter estimates, standard errors in

brackets and goodness-of-fit measures in Tab. 6, successively drop the influence of the bold opinion index, i.e. $\alpha_1 = 0$, $\beta_1 = 0$ and $\alpha_1 = \beta_1 = 0$.

For all models the speed of adjustment frequency ν_0 is smaller than ν_1. For Model V, Model VI and Model VII we see similar parameter estimates for β_0 and β_2 regarding transition probabilities involving the neutral state. A negative bias α_0 can be observed for bold sentiment, except for Model VII, while $\beta_0 < 0$ indicates a bias towards neutrality for these restricted models. The influence of neutral sentiment on the interaction between extreme attitudes, i.e. α_2, is positive and of smaller size. The influence of bold sentiment on the interaction between extreme attitudes and the neutral attitude for Model V, i.e. β_1, is negative while the influence of neutral sentiment on the interaction between extreme attitudes and the neutral attitude β_2 is positive and of similar larger size for all three restricted models.

The goodness-of-fit tests indicate a slight superiority of the model with no influence of bold sentiment on the interaction between extreme attitudes, i.e. Model V. The corresponding values are close to the goodness-of-fit measures of the original model. The log-likelihood values of Model VI and Model VII are smaller than the value for Model V, i.e. from -790 for Model VI, -1045 for Model VII and -444 for Model V. Only the parameter β_0 is statistically insignificant for Model V. All parameters are significant in case of Model VI, respectively Model VII, except for α_2, respectively α_0.

p-values are equal to 0, which indicate that there is strong evidence suggesting that the unrestricted model fits the data better than the restricted model. Therefore the likelihood ratio tests speak again in favor of Model I for all three unrestricted models.

The last set of restricted stochastic models of investor sentiment analyzes the relevance of the initial bias parameters α_0 and β_0, cf. Tab. 7 for the corresponding parameter estimates, standard errors in brackets and goodness-of-fit measures.

For Model VIII the goodness-of-fit measures show values slightly below (for the log-likelihood) and slightly above (for the AIC criterion and the BIC criterion) the values obtained for the original unrestricted bi-variate stochastic models of investor sentiment. For Model IX and Model X the goodness-of-fit measures differ and are inferior, cf. the

	Model V	Model VI	Model VII
Parameter estimates			
ν_0	2.8775 (0.0001)	2.7777 (0.6179)	2.8243 (0.0388)
ν_1	3.9993 (0.0002)	3.9073 (0.339)	4.0 (0.0883)
α_0	-0.0318 (0.0024)	-0.0952 (0.0047)	0.0 (0.1357)
α_1	-	0.5783 (0.2059)	-
α_2	0.1637 (0.0)	0.2357 (0.2596)	1.624 (0.0722)
β_0	-0.5259 (0.5222)	-0.4797 (0.0707)	-0.5112 (0.2013)
β_1	-0.2374 (0.0039)	-	-
β_2	1.2426 (0.0558)	1.0013 (0.1013)	1.2367 (0.478)
Goodness-of-fit measures			
Log L	-443.6639	-789.9619	-1045.0996
AIC	901.3278	1593.9238	2102.1992
BIC	921.4005	1613.9965	2119.4044

Table 6: Parameter estimates, corresponding standard errors in brackets and goodness-of-fit measures for three restricted uni- and bi-variate stochastic models of investor sentiment regarding the bold opinion index x.

	Model VIII	Model IX	Model X
Parameter estimates			
ν_0	2.8243 (0.083)	3.0554 (0.2396)	3.0049 (0.0072)
ν_1	4.0 (0.0001)	3.3981 (0.1084)	3.8205 (0.1578)
α_0	-	-0.2145 (0.9511)	-
α_1	0.6741 (0.0194)	0.2954 (0.0159)	1.0968 (0.0054)
α_2	0.1624 (0.0068)	-0.0192 (0.8689)	0.0007 (0.009)
β_0	-0.5112 (0.0177)	-	-
β_1	-0.228 (0.1846)	0.1681 (0.1786)	-1.4882 (0.1753)
β_2	1.2368 (0.4599)	0.7485 (0.0346)	0.045 (0.0015)
Goodness-of-fit measures			
Log L	-427.4224	-1385.4631	-1411.5114
AIC	870.8448	2784.9262	2835.0228
BIC	893.7851	2804.9989	2852.228

Table 7: Parameter estimates, corresponding standard errors in brackets and goodness-of-fit measures for three restricted bi-variate stochastic models of investor sentiment regarding the initial bias parameters α_0 and β_0.

log-likelihood values of Model IX, i.e. -1385, and Model X, i.e. -1412.

The speed of adjustment frequency ν_0 is smaller than ν_1 for all three restricted models and these parameters are statistically significant for all three restricted models. Model VIII with $\alpha_0 = 0$ shows results for the parameter estimates close to the estimates of the original unrestricted Model I.

The parameters α_1 and β_2 are positive for all three versions. The values for α_1 indicate that there is strong reinforcement of bold sentiment on the transition rates governing the changes between extreme attitudes. For Model IX, with $\beta_0 = 0$, α_0, α_2 and β_1 are statistically insignificant. Here it is assumed that there is no initial bias towards any attitude in the transition probabilities involving neutral agents. All parameters of Model X with $\alpha_0 = \beta_0 = 0$ show statistical significance.

These findings do not speak in favor of restricted model which neglect the initial bias regarding neutrality, i.e. β_0. They further suggest an initial bias regarding the extreme attitudes, α_0, is not essential for this setup of these sentiment dynamics.

The test rejection decisions indicate that the restricted models should be rejected in favor of the alternative, unrestricted model. While for the restricted Model VIII a test statistic p-value of $p = 0.0091$ is obtained the p-values for Model IX and Model X are equal to zero and therefore suggest that there is strong evidence for the rejections.

We can conclude that the bias regarding changes between the neutral sentiment and the extreme attitudes, i.e. β_0, definitely has a strong impact on the changes in attitude for bold, cautious and neutral agents. Model VIII, among the restricted models, has the best fit compared to Model I.

These results strongly indicate that multi-collinearity cannot be excluded. There seem to be dependencies between parameters while the bias for transition between the extreme sentiments bold and cautious, i.e. α_0, seems negligible. For the transition probabilities describing the changes between bold an cautious agents the share of neutral agents might not be as relevant as the share of extreme attitudes since these types of agents focus on themselves. However the analysis shows that the transition rates for bold and neutral agents, respectively for cautious and neutral agents, heavily rely on the

bold opinion index and the neutrality index.[36]

4.4.3 Out-of-sample Forecast

A further analysis of the unrestricted stochastic benchmark model, i.e. Model I, includes an out-of-sample forecast. Therefore the model has been estimated for the period from 1999 to 2013. The resulting parameters have been used to forecast investor sentiment for all three sentiment types, i.e. bullish, bearish and neutral, from 2014 until 2018. The applied forecast method uses estimation parameters obtained in subsection 4.4.2 to determine the share of agents with bullish, bearish and neutral sentiment for the next period, i.e. for one week. The forecast starts with the last observed values of bold, cautious and neutral sentiment from 2013, i.e. $(b_T, c_T, 0_T)$. Via transition rates (19) changes between the sentiments are initiated with a forecast horizon of one week to obtain the forecasts for period $T+1$, i.e. $(\hat{b}_{T+1}, \hat{c}_{T+1}, \hat{0}_{T+1})$. In each of the following forecast rounds the underlying *AAII* data serves as the initial value. Therefore to obtain the forecast values for $T+2$, i.e. $(\hat{b}_{T+2}, \hat{c}_{T+2}, \hat{0}_{T+2})$, the last observed values of bold, cautious and neutral sentiment serve as initial values, i.e. *AAII* data in $T+1$, which is the first week in 2014 and so on.

Figure 29, Fig. 30 and Fig.31 show the weekly time series of the *AAII* Investor Sentiment Survey data from 2013. The panels depict bullish, bearish and neutral sentiment shares and their corresponding forecasts for the period from 2014 until 2018.

The graphical analysis yields that the bullish sentiment forecast, the bearish sentiment forecast as well as the neutral sentiment forecast are very close to the original data for all periods.

The magnitude of the share fits the data quite well as well as the direction of the trend. For the bullish sentiment forecast a slight underestimation for several forecast periods can be detected while the opposite is true for the neutral sentiment forecast. The bearish sentiment forecast shows some periods in which the share is overestimated but

[36]These findings are supported by two additional restricted models, see Tab. 9 in Appendix B.3.2. Model XI considers $\alpha_0 = 0$ and $\alpha_1 = 0$ while Model XII assumes $\alpha_0 = \alpha_2 = 0$.

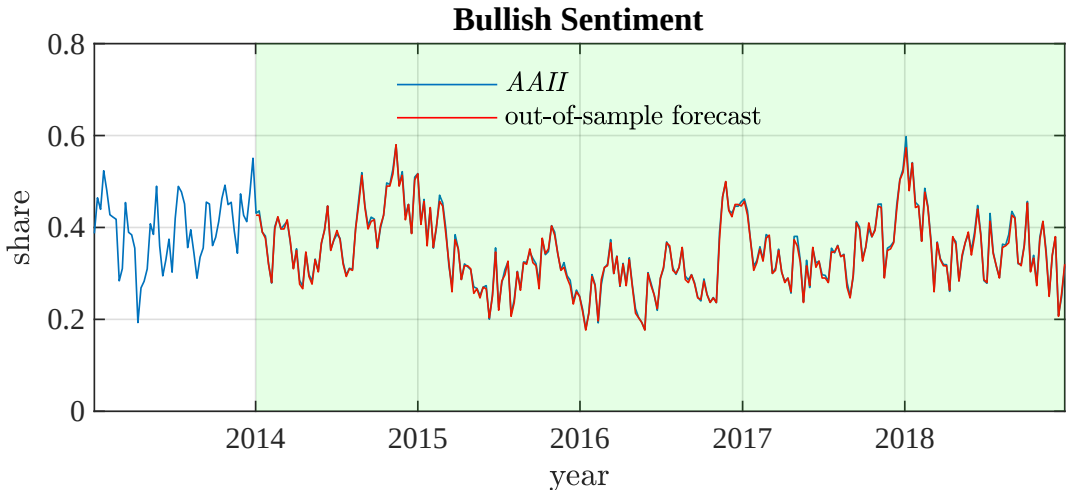

Figure 29: Time series of *AAII* Bullish Sentiment Survey data with forecast from 2014 to 2018 (red line) for parameter estimates from Model I.

also periods in which the share is slightly underestimated.[37]

In Tab. 8 the corresponding values of the root-mean-square errors (RMSE) are given for Model I to Model X and a naïve forecast. This forecast method provides a benchmark against the investigated more sophisticated unrestricted and restricted models. The naïve forecast uses past data only, e.g. the forecast for bold sentiment with a forecast horizon of m weeks $\hat{b}_{T+m}$ is given by the last observed value b_T, i.e. $\hat{b}_{T+1} = b_T$ with $m = 1$. Additionally the standard deviations for the period from 2014 to 2018 of the original *AAII* Sentiment Survey data are given.

The magnitude of the RMS errors for all estimated models, restricted and unrestricted, and all sentiment types are below the errors of the naïve forecast. The RMS errors for the restricted Model IX are approximately twice the size of the errors of the unrestricted Model I. The RMS errors of the remaining restricted models lie in-between these two limits. It is noticeable that the RMS errors of neutral sentiment are the highest among all sentiments for all estimated models while bullish sentiment has the largest

[37] See Appendix A.3.2 for the time series of *AAII* Sentiment Survey data with forecasts from 2014 to 2018 for parameter estimates from Model II to Model X.

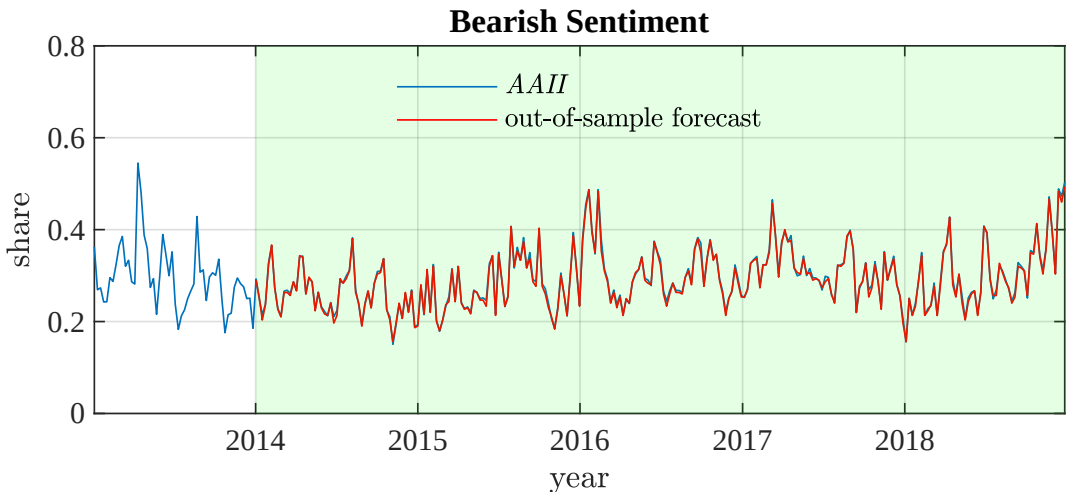

Figure 30: Time series of *AAII* Bearish Sentiment Survey data with forecast from 2014 to 2018 (red line) for parameter estimates from Model I.

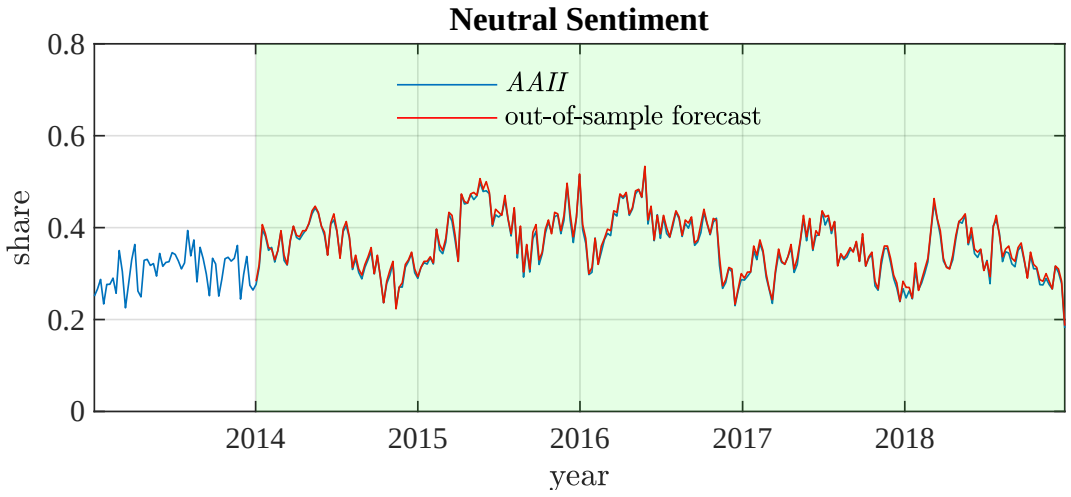

Figure 31: Time series of *AAII* Neutral Sentiment Survey data with forecast from 2014 to 2018 (red line) for parameter estimates from Model I.

	Bullish sentiment	Bearish sentiment	Neutral sentiment
Naïve forecast	0.2177	0.1249	0.1138
Model I	0.0059	0.0054	0.0061
Model II	0.0054	0.0055	0.0076
Model III	0.0094	0.0094	0.0123
Model IV	0.0102	0.0075	0.0108
Model V	0.0066	0.0055	0.0077
Model VI	0.0072	0.0064	0.0088
Model VII	0.0094	0.0078	0.0131
Model VIII	0.0064	0.0051	0.0081
Model IX	0.0105	0.01	0.0136
Model X	0.0101	0.0086	0.0125
Standard deviation	0.0781	0.0618	0.0636

Table 8: Root-mean-square errors for *AAII* Sentiment Survey data and forecast data from 2014 to 2018 for Model I - Model X in comparison to root-mean-square errors for naïve forecast data in brackets. Additionally the standard deviations for *AAII* Sentiment Survey data from 2014 to 2018 are provided.

error regarding the naïve forecast and the standard deviation. This indicates that bullish sentiment is prone to larger fluctuations when the underlying data is considered but the estimated unrestricted and restricted models do not capture this feature. They rather overestimate the fluctuations of neutral sentiment. This is due to the incorporation of a neutrality index in the model set up itself and the strong influence of this state variable on the dynamics of the system.

Overall, the quality of the forecast of Model I is considerable. Furthermore it can be concluded that Model I which incorporates the neutrality index in the transitions between extreme attitudes has lower RMS errors for all three types of sentiment compared to Model IV which drops this index as an influence. Therefore the neutrality index adds additional explanatory power to this stochastic model, at least if we consider the sentiment data from *AAII*.

4.5 Conclusions

There is evidence in the literature on the influence of sentiment on returns or volatility on financial markets, cf. Schmeling (2009) and Lux (2009a). The sentiments defined in these models focus on the difference between the two extreme attitudes. The neutral sentiment is neglected for the most part. As a first step towards a more detailed description of behavioral models of opinion formation the sentiment variables should be reconsidered regarding neutrality.

The main objective of this chapter was a realistic modeling of the dynamic components, i.e. transition rates, of the stochastic framework. Changes between all three attitudes were modeled. A parameter estimation was supposed to test the explanatory power of the novel model including neutrality as a separate sentiment component.

Survey data on three sentiments of American investors were used to estimate the parameters of a stochastic model of opinion formation. The maximum likelihood framework for parameter estimation in bi-variate agent-based models by Lux (2012) was adjusted to the underlying setup.

The sensitivity analysis showed that three restricted models indicate a similar fit to the data but the unrestricted model still performs best. All of these specific models concern the parameters regarding transitions between extreme attitudes. One of these restricted models neglects the initial bias, one drops the influence of bold sentiment and one ignores the neutrality index for transitions between extreme attitudes. This might indicate that a more differentiated and less symmetric approach regarding changes between bullish and bearish sentiment should be analyzed.

There are two explanations for this result. First, the model itself exhibits a realistic description of the underlying group dynamics, including the separate treatment of the neutral agents, but the data considered cannot completely reflect the complex social interaction components. The second reason is that the model is overparameterized and strong dependencies between several parameters cannot be disentangled within this setup.

If we consider the forecast results of the unrestricted benchmark model the included neutrality index is very influential. The forecasting performance of the original model is remarkable in terms of bullish, bearish and neutral sentiment.

We believe these results are important since they provide an indication of the necessary degree of complexity of behavioral models in different scenarios. Overall, it can be concluded that the neutrality index adds additional explanatory power to this stochastic model, at least if we consider the sentiment data from *AAII*.

5 Concluding Remarks

The main objective of this thesis was a detailed modeling of the dynamic components, i.e. transition rates, in a stochastic framework. In addition to bold sentiment and cautious sentiment neutral sentiment was incorporated.

The first model obtained the transition probability approach and changes in the shares of these groups of agents are caused by individual transition probabilities. Changes between extreme attitudes, i.e. bold and cautious, were excluded. The dynamics are initiated by feedback indices which are mainly influenced by herding. Two versions of feedback components were considered. The first approach used a sentiment ratio including the neutral attitude. In the second approach agents used a linear combination of the traditional sentiment variable, i.e. the difference of the two extreme attitudes, and the sentiment variable including neutrality. A nonlinear two-dimensional system of ordinary differential equations was obtained. The occurrence of several bifurcation types and complex bifurcation routes showed that the analyzed dynamical systems can generate multiple, co-existing stable and unstable equilibrium points. The analysis of the evolution of neutral agents reveals that for all versions and specifications a neutral majority may prevail depending on the herding.

Another version of a sentiment dynamics model was formalized via the discrete choice framework using three attitudes. Here the agents' decision is independent of the previously adopted attitude. Logit choice probabilities for all agents have been obtained. These probabilities incorporate feedback indices which are individual for all three attitudes. The main influence within the feedback comes from a herding parameter. We obtained a nonlinear two-dimensional system of ordinary differential equations. A neutral majority may persist over time. This outcome is highly depended on the herding intensity.

Based on these findings, when utilizing the transition probability approach for two model versions as well as the discrete choice approach, further macroeconomic extensions for three-state sentiment dynamics models are feasible.

The last chapter dealt with an investor sentiment model which considers a bold opinion index and a neutrality index. It includes the specification of individual transition rates for the changes between all three groups of agents. The probability fluxes for the configurations of sentiment change were summarized. Survey data on American investor sentiment was used to estimate the model parameters via maximum likelihood. The explanatory power of the additional neutrality index was under investigation. Therefore a sensitivity analysis was performed. Nine additional restricted model versions were estimated and their performances and the significance of the parameter estimations were compared. The original benchmark model is not outperformed by any restricted sentiment model in the sensitivity analysis. But not all the estimated model parameters were statistically significant. These findings might indicate overparameterization within the model setup and multi-collinearity even if the model exhibits a realistic description of the underlying group dynamics, including the separate treatment of the neutral agents.

All estimated models were used for an out-of-sample forecast in order to evaluate the models' overall significance. The results exhibit that the forecasting performance of the original model is remarkable in terms of all three sentiments.

The findings in these different versions of stochastic modeling frameworks are important since they provide an indication of the necessary degree of complexity of behavioral models in different scenarios. It can be concluded that the neutrality index adds additional explanatory power to a stochastic investor sentiment model.

Bibliography

Akerlof, G. and Shiller, R. (2009). *Animal Spirits: How Human Psychology Drives the Economy, and Why It Matters for Global Capitalism*. Princeton University Press.

Akhtar, S. M., Faff, R. W., Oliver, B. R., and Subrahmanyam, A. (2011). Decomposing the effect of consumer sentiment news - evidence from us stock and stock index futures markets. *24th Australasian Finance and Banking Conference 2011 Paper*.

Alfarano, S. and Lux, T. (2005). A noise trader model as a generator of apparent financial power laws and long memory. Economics Working Papers 2005, 13, Kiel University.

Barberis, N., Shleifer, A., and Vishny, R. (1998). A model of investor sentiment. *Journal of Financial Economics*, 49(3):307 – 343.

Boudin, L. and Salvarani, F. (2009). A kinetic approach to the study of opinion formation. *ESAIM: Mathematical Modelling and Numerical Analysis*, 43(3):507–522.

Brock, W. and Hommes, C. (1997). A rational route to randomness. *Econometrica*, 65(5):1059–1095.

Brown, G. W. (1999). Volatility, sentiment, and noise traders. *Financial Analysts Journal*, 55(2):82–90.

Brown, G. W. and Cliff, M. T. (2004). Investor sentiment and the near-term stock market. *Journal of Empirical Finance*, 11(1):1 – 27.

Cooper, J. (2001). *A MATLAB Companion for Multivariable Calculus*. Harcourt/Academic Press.

Curado, E. M. F. and Nobre, F. D. (2003). Derivation of nonlinear fokker-planck equations by means of approximations to the master equation. *Phys. Rev. E*, 67:021107.

Dmitriev, A., Dmitriev, V., Sagaydak, O., and Tsukanova, O. (2017). The application of stochastic bifurcation theory to the early detection of economic bubbles. *Procedia Computer Science*, 122:354 – 361. 5th International Conference on Information Technology and Quantitative Management, ITQM 2017.

Düring, B., Markowich, P., Pietschmann, J.-F., and Wolfram, M.-T. (2009). Boltzmann and fokker-planck equations modelling opinion formation in the presence of strong leaders. *Proceedings of the Royal Society A: Mathematical, Physical and Engineering Science*, 465(2112):3687–3708.

Düring, B., Torregrossa, M., and Wolfram, M.-T. (2018). Boltzmann and fokker–planck equations modelling the elo rating system with learning effects. *Journal of Nonlinear Science*.

Entorf, H., Gross, A., and Steiner, C. (2012). Business cycle forecasts and their implications for high frequency stock market returns. *Journal of Forecasting*.

Fisher, K. L. and Statman, M. (2000). Investor sentiment and stock returns. *Financial Analysts Journal*, 56(2):16–23.

Foster, J. and Flieth, B. (2002). Interactive expectations. *Journal of Evolutionary Economics*, 12(4):375–395.

Franke, R. (2007). Estimation of a microfounded herding model on german survey expecations. Working paper, Kiel University.

Franke, R. (2012). Microfounded animal spirits in the new macroeconomic consensus. *Studies in Nonlinear Dynamics & Econometrics*, 16(4):1–41.

Franke, R. (2014). Aggregate sentiment dynamics: A canonical modelling approach and its pleasant nonlinearities. *Structural Change and Economic Dynamics*, 31(C):64–72.

Franke, R. (2018). A microfoundation of harrodian instability, entailing also some scope for stability. Working paper, Kiel University.

Franke, R. and Westerhoff, F. (2017). Taking stock: A rigorous modelling of animal spirits in macroeconomics. *Journal of Economic Surveys*, 31(5):1152–1182.

Franke, R. and Westerhoff, F. (2019). Different compositions of aggregate sentiment and their impact on macroeconomic stability. *Economic Modelling*, 76:117 – 127.

Gomes, O. and Sprott, J. C. (2017). Sentiment-driven limit cycles and chaos. *Journal of Evolutionary Economics*, 27(4):729–760.

Heiden, S., Klein, C., and Zwergel, B. (2013). Beyond fundamentals: Investor sentiment and exchange rate forecasting. *European Financial Management*, 19(3):558–578.

Hengelbrock, J., Theissen, E., and Westheide, C. (2013). Market response to investor sentiment. *Journal of Business Finance & Accounting*, 40(7-8):901–917.

Hohnisch, M., Pittnauer, S., Solomon, S., and Dietrich, S. (2005). Socioeconomic interaction and swings in business confidence indicators. *Physica A: Statistical Mechanics and its Applications*, 345(3):646 – 656.

Hommes, C. (2013). *Behavioral Rationality and Heterogeneous Expectations in Complex Economic Systems*. Cambridge University Press.

Hommes, C. H. and Ochea, M. I. (2012). Multiple equilibria and limit cycles in evolutionary games with logit dynamics. *Games and Economic Behavior*, 74(1):434–441.

Hüfner, F. and Schröder, M. (2002). Forecasting economic activity in germany - how useful are sentiment indicators? ZEW Discussion Papers 02-56, ZEW - Center for European Economic Research.

Jordan, D. and Smith, P. (2007a). *Nonlinear Ordinary Differential Equations: An Introduction for Scientists and Engineers*. Oxford Texts in Applied and Engineering Mathematics. OUP Oxford.

Jordan, D. and Smith, P. (2007b). *Nonlinear Ordinary Differential Equations: Problems and Solutions*. Oxford Texts in Applied and Engineering Mathematics. OUP Oxford.

Khalil, H. (2002). *Nonlinear Systems*. Pearson Education. Prentice Hall.

Kuznetsov, I. A. (2004). *Elements of Applied Bifurcation Theory*. Applied mathematical sciences. Springer-Verlag, New York, 3rd edition.

Lahl, D. and Hüfner, F. P. (2003). What determines the zew indicator? ZEW Discussion Papers 03-48, ZEW - Center for European Economic Research.

Lee, W. Y., Jiang, C. X., and Indro, D. C. (2002). Stock market volatility, excess returns, and the role of investor sentiment. *Journal of Banking & Finance*, 26(12):2277 – 2299.

Lorenz, H. (2012). *Nonlinear Dynamical Economics and Chaotic Motion*. Springer Berlin Heidelberg, 2nd edition.

Lux, T. (1995). Herd behaviour, bubbles and crashes. *Economic Journal*, 105(431):881–96.

Lux, T. (2009a). Mass psychology in action: Identification of social interaction effects in the german stock market. Kiel Working Papers 1514, Kiel Institute for the World Economy.

Lux, T. (2009b). Rational forecasts or social opinion dynamics? identification of interaction effects in a business climate survey. *Journal of Economic Behavior & Organization*, 72(2):638 – 655.

Lux, T. (2010). Sentiment dynamics and stock returns: the case of the german stock market. *Empirical Economics*, 41(3):663679.

Lux, T. (2012). Estimation of an agent-based model of investor sentiment formation in financial markets. *Journal of Economic Dynamics and Control*, 36(8):1284 – 1302. Quantifying and Understanding Dysfunctions in Financial Markets.

Lux, T. (2013). Inference for systems of stochastic differential equations from discretely sampled data: a numerical maximum likelihood approach. *Annals of Finance*, 9(2):217–248.

Lux, T. and Marchesi, M. (1999). Scaling and criticality in a stochastic multi-agent model of a financial market. *Nature*, 397(6719):498–500.

Lynch, S. (2004). *Dynamical Systems with Applications using MATLAB®*. Birkhäuser Boston.

Medio, A. (1992). *Chaotic Dynamics: Theory and Applications to Economics*. Cambridge Univ. Press, Cambridge.

Medio, A. and Lines, M. (2003). *Nonlinear Dynamics: A Primer*. Cambridge University Press.

Menkhoff, L., Schmeling, M., and Schmidt, U. (2010). Are all professional investors sophisticated? *German Economic Review*, 11(4):418–440.

Morton, K. W. and Mayers, D. F. (2005). *Numerical Solution of Partial Differential Equations: An Introduction*. Cambridge University Press, New York, NY, USA, 2nd edition.

Ochea, M. (2010). *Essays on nonlinear evolutionary game dynamics*. PhD thesis, Amsterdam School of Economics Research Institute (ASE-RI).

Peaceman, D. and Rachford, Jr., H. (1955). The numerical solution of parabolic and elliptic differential equations. *Journal of the Society for Industrial and Applied Mathematics*, 3(1):28–41.

Polyanin, A. and Zaitsev, V. (2004). *Handbook of Nonlinear Partial Differential Equations*. CRC Press.

Press, W. H., Teukolsky, S. A., Vetterling, W. T., and Flannery, B. P. (2007). *Numerical Recipes: The Art of Scientific Computing*. Cambridge University Press, New York, NY, USA, 3rd edition.

Risken, H. (1989). *The Fokker-Planck Equation: Methods of Solution and Applications*. Springer, 2nd edition.

Schmeling, M. (2007). Institutional and individual sentiment: Smart money and noise trader risk? *International Journal of Forecasting*, 23(1):127 – 145.

Schmeling, M. (2009). Investor sentiment and stock returns: Some international evidence. *Journal of Empirical Finance*, 16(3):394 – 408.

Seydel, R. (1988). *From Equilibrium to Chaos: Practical Bifurcation and Stability Analysis*. Elsevier.

Shone, R. (2002). *Economic Dynamics: Phase Diagrams and Their Economic Application*. Economic Dynamics: Phase Diagrams and Their Economic Application. Cambridge University Press, 2nd edition.

Stanoyevitch, A. (2005). *Introduction to Numerical Ordinary and Partial Differential Equations Using MATLAB*. Wiley-Interscience, New York, NY, USA.

Strikwerda, J. C. (2004). *Finite Difference Schemes and Partial Differential Equations*. Other Titles in Applied Mathematics. Society for Industrial and Applied Mathematics (SIAM).

Strogatz, S. (1994). *Nonlinear Dynamics and Chaos: With Applications to Physics, Biology, Chemistry, and Engineering*. Advanced book program. Westview Press.

Thomas, J. (1995). *Numerical Partial Differential Equations: Finite Difference Methods*. Texts in Applied Mathematics. Springer-Verlag, New York.

Toscani, G. (2006). Kinetic models of opinion formation. *Communications in Mathematical Sciences*, 4(3):481–496.

Verma, R. and Soydemir, G. (2010). The impact of u.s. individual and institutional investor sentiment on foreign stock markets. *Journal of Behavioral Finance*, 7(3):128–144.

Verma, R. and Verma, P. (2008). Are survey forecasts of individual and institutional investor sentiments rational? *International Review of Financial Analysis*, 17(5):1139 – 1155.

Weidlich, W. and Braun, M. (1992). The master equation approach to nonlinear economics. *Journal of Evolutionary Economics*, 2(3):233–265.

Weidlich, W. and Haag, G. (1983). *Concepts and Models of a Quantitative Sociology; The Dynamics of Interacting Populations*. Springer-Verlag.

Westerhoff, F. and Franke, R. (2018). *Agent-based models for economic policy design: Two illustrative examples*. The Oxford Handbook of Computational Economics and Finance, Oxford University Press, Oxford. 520-558.

Wiggins, S. (2003). *Introduction to Applied Nonlinear Dynamical Systems and Chaos*. Texts in Applied Mathematics. Springer New York.

Zhang, W. (2005). *Differential Equations, Bifurcations, and Chaos in Economics*, volume 68 of *Series on advances in mathematics for applied sciences*. World Scientific.

Zorzano, M., Mais, H., and Vazquez, L. (1999). Numerical solution of two dimensional fokker-planck equations. *Applied Mathematics and Computation*, 98(2):109 – 117.

Zwillinger, D. (1989). *Handbook of Differential Equations*. Academic Press, Boston, MA.

A Graphical Appendix

A.1 Transition Probability Approach

A.1.1 Pure Sentiment Dynamics

Figure 32 depicts a three-dimensional representation of the adjusted bifurcation diagram from subsection 2.3.3, cf. Fig. 6a. Through rotation about the straight line of symmetric equilibria all parabolas can be converted into one another. This symmetric composition accounts for the need of an augmented component in the adjusted bifurcation diagram which combines the two phase plane components b and c.

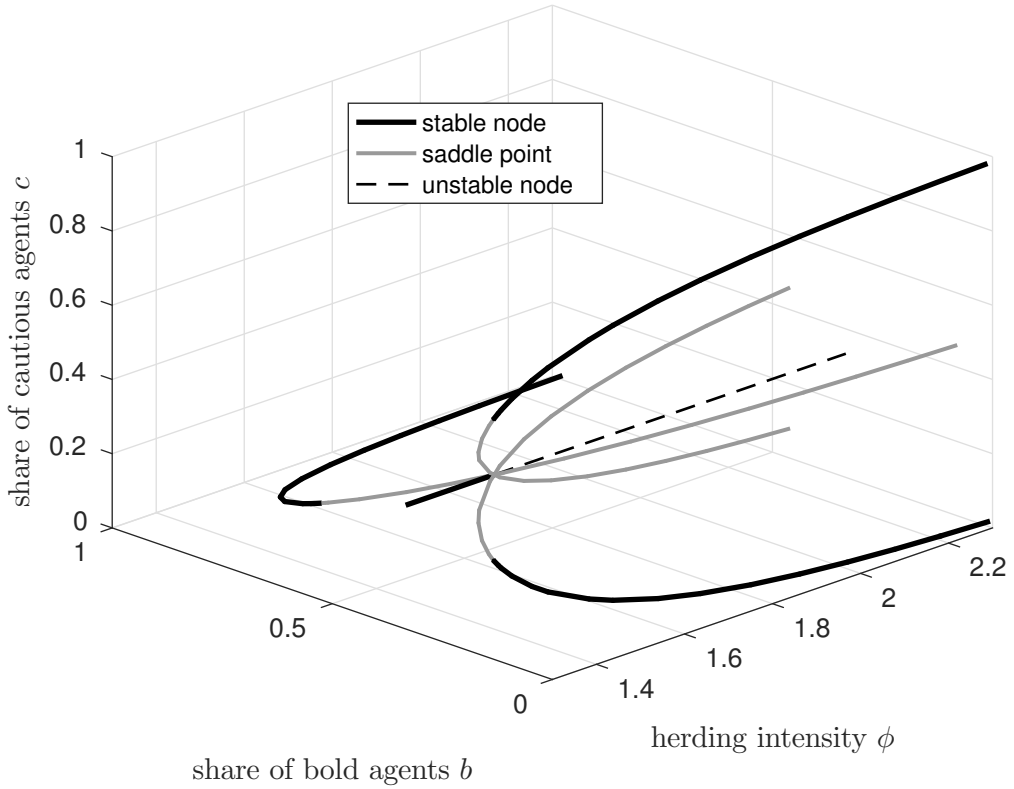

Figure 32: Non-adjusted three-dimensional bifurcation diagram with herding intensity $\phi \in [1.3, 2.3]$.

A.1.2 Augmented Feedback

In Fig. 33, Fig. 34 and Fig. 35 additional phase plane representations for both types of parabolic isoclines $F_b = 0$ and $F_c = 0$ are displayed for a moderate weighting component $\omega = 0.5$ and increasing herding ϕ.

If the herding is small, i.e. $\phi = 0.5$, the isoclines are almost linear and the symmetric equilibrium $(b^s, c^s) = (\frac{1}{3}, \frac{1}{3})$ is a stable point of intersection, see Fig. 33. Once the herding intensity increases more intersection points, respectively equilibria, are generated. Analogous statements hold for the weight $\omega = 0.8$, see Fig. 36, 37 and 38.

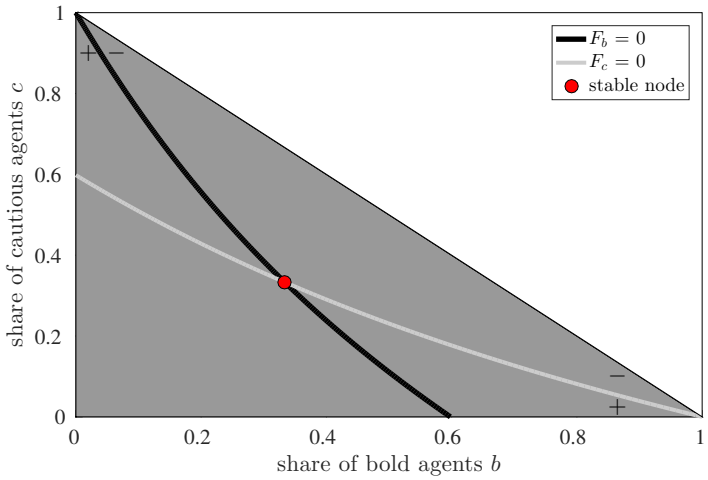

Figure 33: Phase plane representation of $F_b = 0$ (black) and $F_c = 0$ (white) for $\phi = 0.5, \omega = 0.5$. One stable equilibrium (red dot) is visible. $+/-$ indicate $F_b \gtrless 0$, resp. $F_c \gtrless 0$.

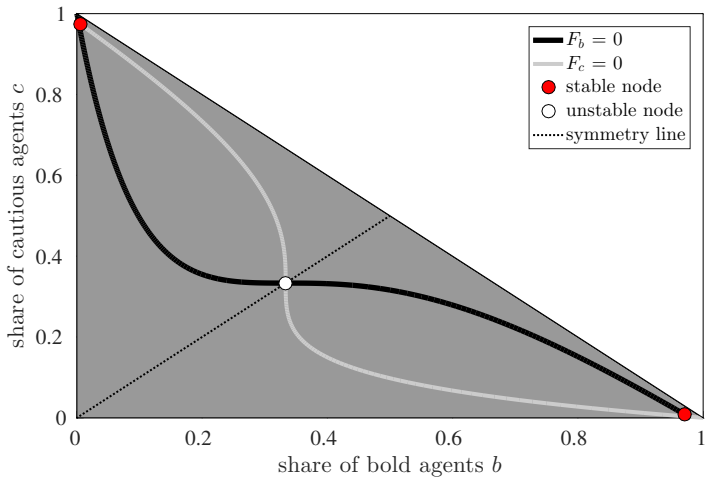

Figure 34: Phase plane representation of $F_b = 0$ (black) and $F_c = 0$ (white) for $\phi = 2.0, \omega = 0.5$. Two stable equilibria (red dots) and one unstable equilibrium (white dot) are visible.

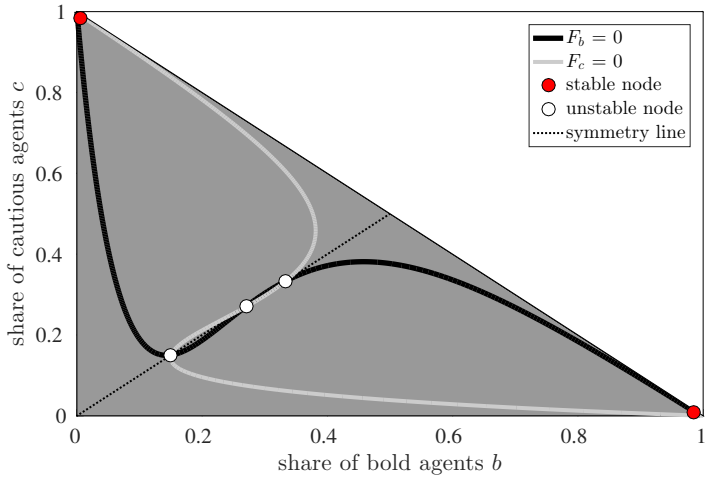

Figure 35: Phase plane representation of $F_b = 0$ (black) and $F_c = 0$ (white) for $\phi = 2.8, \omega = 0.5$. Two stable equilibria (red dots) and three unstable equilibria (white dots) are visible.

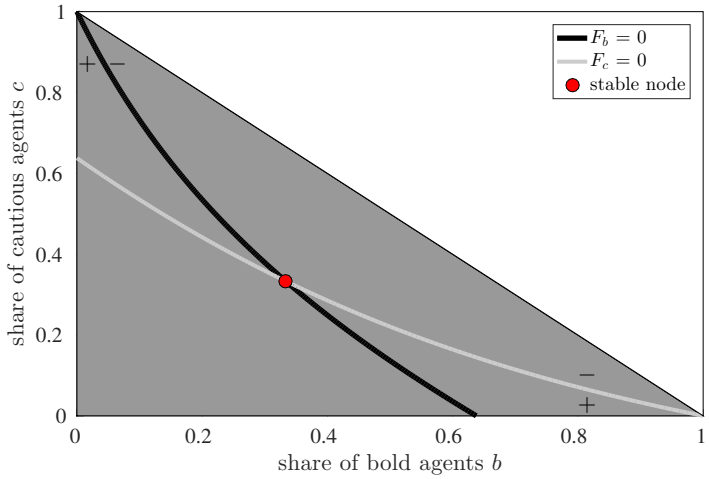

Figure 36: Phase plane representation of $F_b = 0$ (black) and $F_c = 0$ (white) for $\phi = 0.5, \omega = 0.8$. One stable equilibrium (red dot) is visible. $+/-$ indicate $F_b \gtrless 0$, resp. $F_c \gtrless 0$.

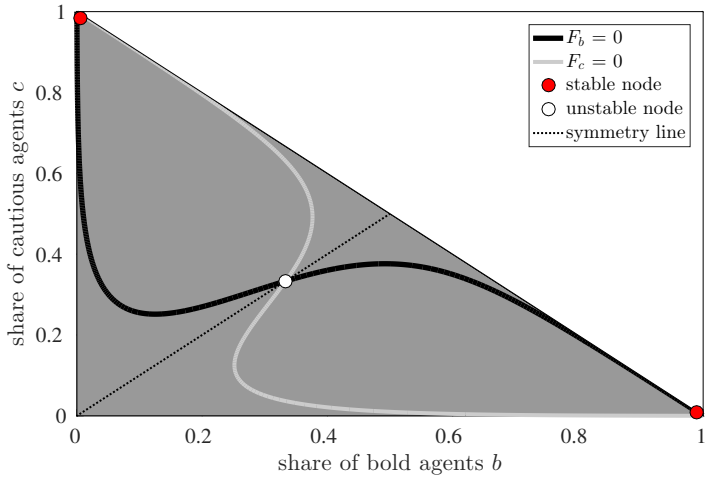

Figure 37: Phase plane representation of $F_b = 0$ (black) and $F_c = 0$ (white) for $\phi = 4.0, \omega = 0.8$. Two stable equilibria (red dots) and one unstable equilibrium (white dot) are visible.

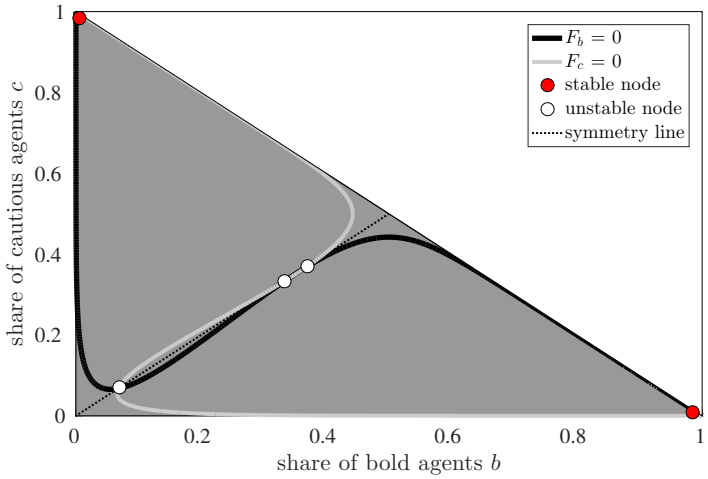

Figure 38: Phase plane representation of $F_b = 0$ (black) and $F_c = 0$ (white) for $\phi = 8.0, \omega = 0.8$. Two stable equilibria (red dots) and three unstable equilibria (white dots) are visible.

A.2 Discrete Choice Approach

A.2.1 Sentiment Dynamics and Discrete-Choice Approach

In Fig. 39 and Fig. 40 additional phase plane representations for both types of parabolic isoclines $F_b = 0$ and $F_c = 0$ are displayed for $\mu = 1.0$, $\beta = 1.0$ and small values of the herding component ϕ.

If there is no herding, i.e. $\phi = 0$, the isoclines are linear and the symmetric equilibrium $(b^s, c^s) = (\frac{1}{3}, \frac{1}{3})$ is a stable point of intersection, see Fig. 39. Once the herding intensity increases slightly, i.e. $\phi = 1.5$ the isoclines become nonlinear but the symmetric equilibrium $(b^s, c^s) = (\frac{1}{3}, \frac{1}{3})$ remains stable, see Fig. 40.

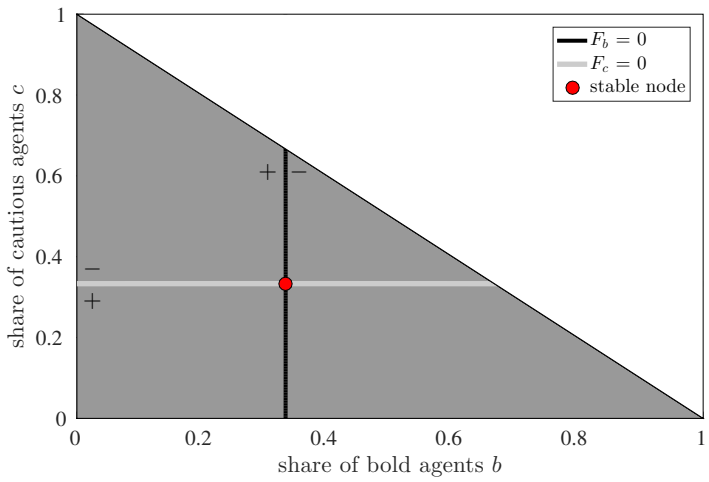

Figure 39: Phase plane representation of $F_b = 0$ (black) and $F_c = 0$ (white) for $\mu = 1.0$, $\beta = 1.0$ and $\phi = 0$. One stable equilibrium (red dot) is visible. $+/-$ indicate $F_b \gtrless 0$, resp. $F_c \gtrless 0$.

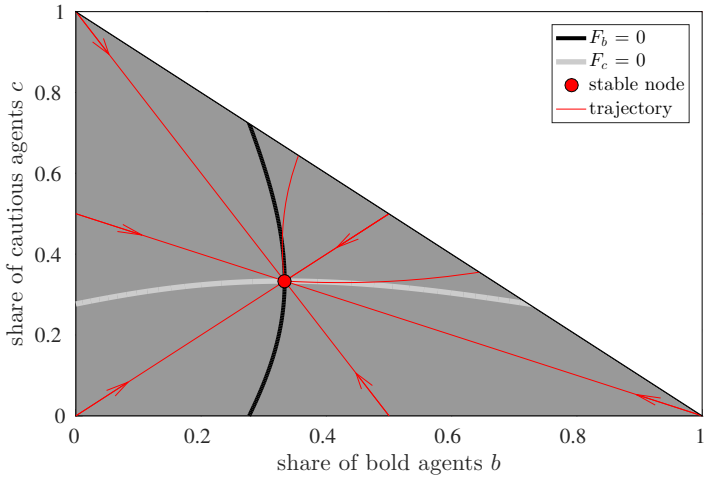

Figure 40: Phase plane representation of $F_b = 0$ (black) and $F_c = 0$ (white) for $\mu = 1.0$, $\beta = 1.0$ and $\phi = 1.5$. Trajectory dynamics (red) with one stable equilibrium (red dot) is visible. $+/-$ indicate $F_b \gtrless 0$, resp. $F_c \gtrless 0$.

A.3 A Stochastic Model of Investor Sentiment

A.3.1 Sensitivity Analysis

In Fig. 41 and Fig. 42 the two-dimensional probability distributions for the share of neutral agents n_0 and the share of bold agents n_b for the period from 1999 to 2018 can be seen.

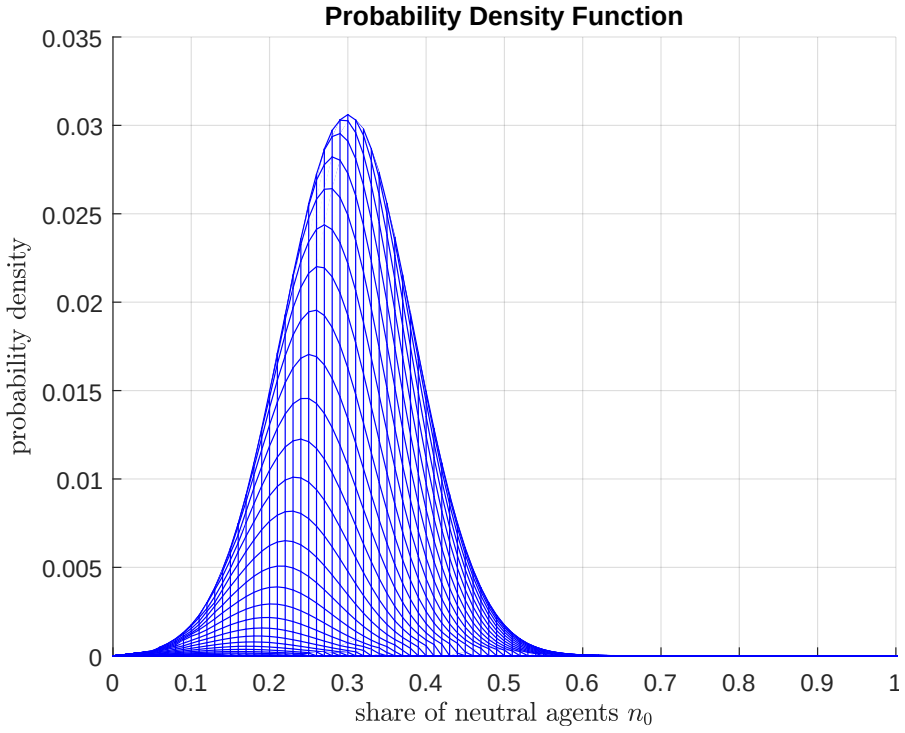

Figure 41: Two-dimensional probability distribution for the share of neutral agents n_0 for the period from 1999 to 2018.

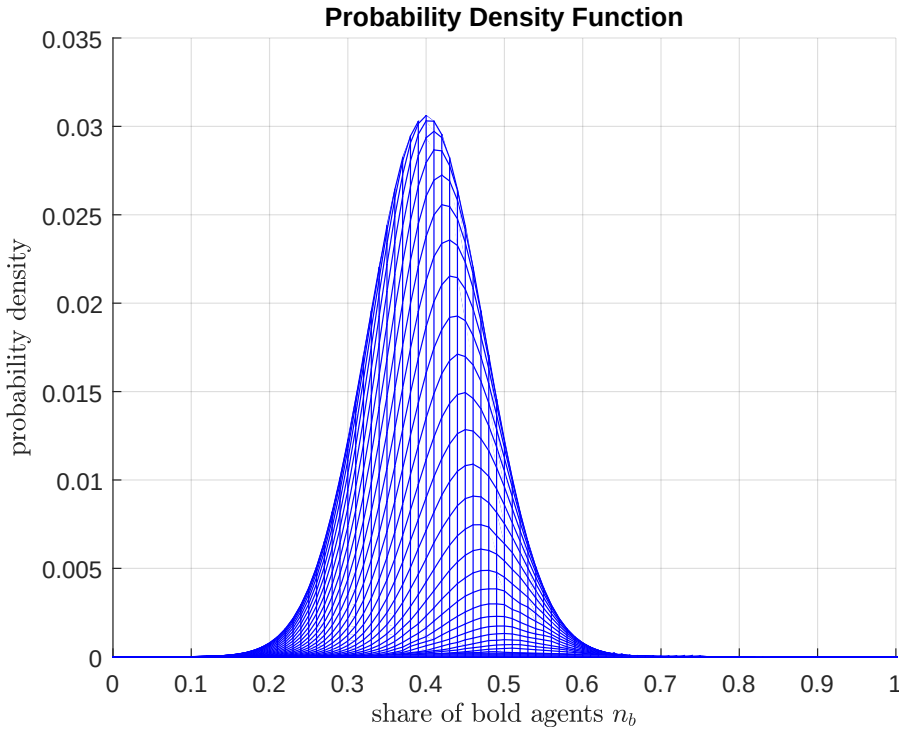

Figure 42: Two-dimensional probability distribution for the share of bold agents n_b for the period from 1999 to 2018.

A.3.2 Out-of-sample Forecast

Figure 43, Fig. 44 and Fig. 45 show the weekly time series of the *AAII* Investor Sentiment Survey data from 1999 until 2013. The panels depict bullish, bearish and neutral sentiment shares and their corresponding forecasts for the period from 2014 until 2018 for Model II.

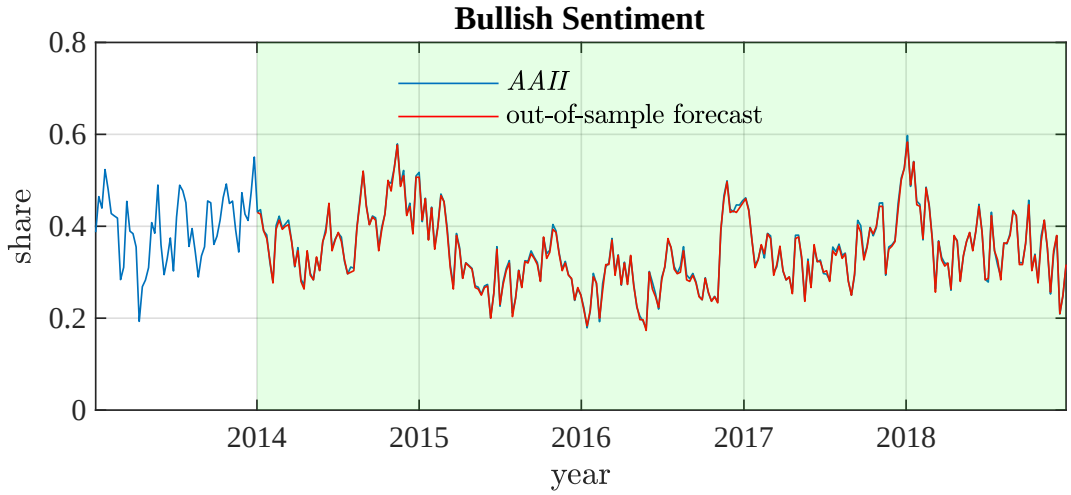

Figure 43: Time series of *AAII* Bullish Sentiment Survey data with forecast from 2014 to 2018 (red line) for parameter estimates from Model II.

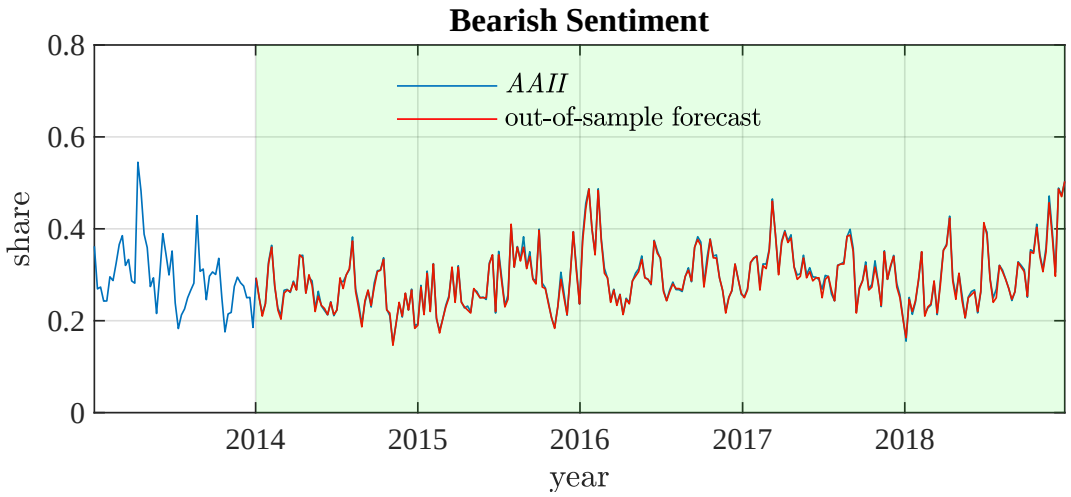

Figure 44: Time series of *AAII* Bearish Sentiment Survey data with forecast from 2014 to 2018 (red line) for parameter estimates from Model II.

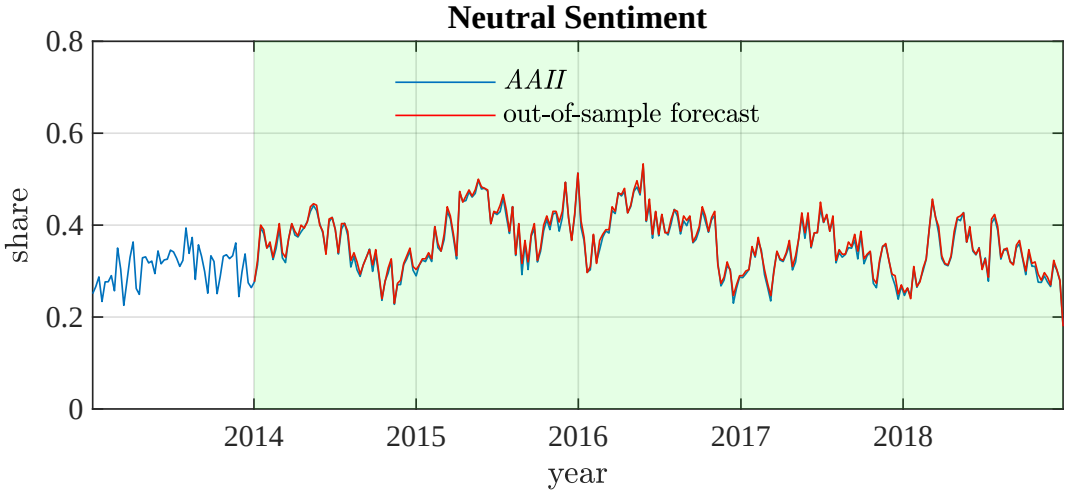

Figure 45: Time series of *AAII* Neutral Sentiment Survey data with forecast from 2014 to 2018 (red line) for parameter estimates from Model II.

Figure 46, Fig. 47 and Fig. 48 show the weekly time series of the *AAII* Investor Sentiment Survey data from 1999 until 2013. The panels depict bullish, bearish and neutral sentiment shares and their corresponding forecasts for the period from 2014 until 2018 for Model III.

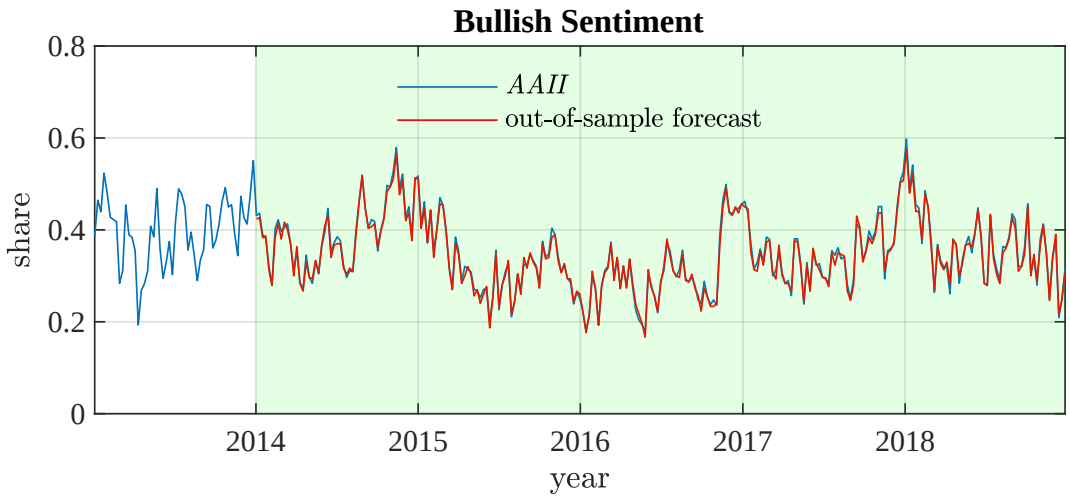

Figure 46: Time series of *AAII* Bullish Sentiment Survey data with forecast from 2014 to 2018 (red line) for parameter estimates from Model III.

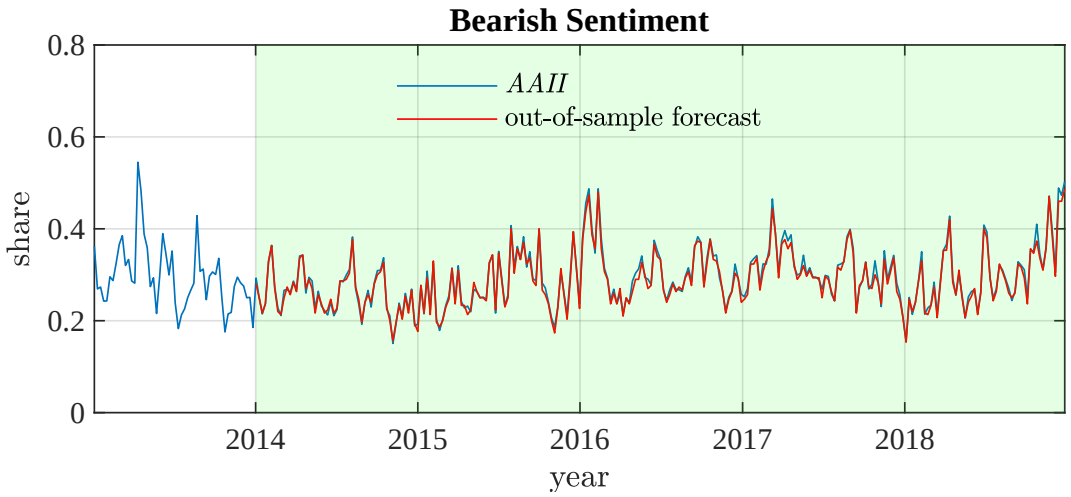

Figure 47: Time series of *AAII* Bearish Sentiment Survey data with forecast from 2014 to 2018 (red line) for parameter estimates from Model III.

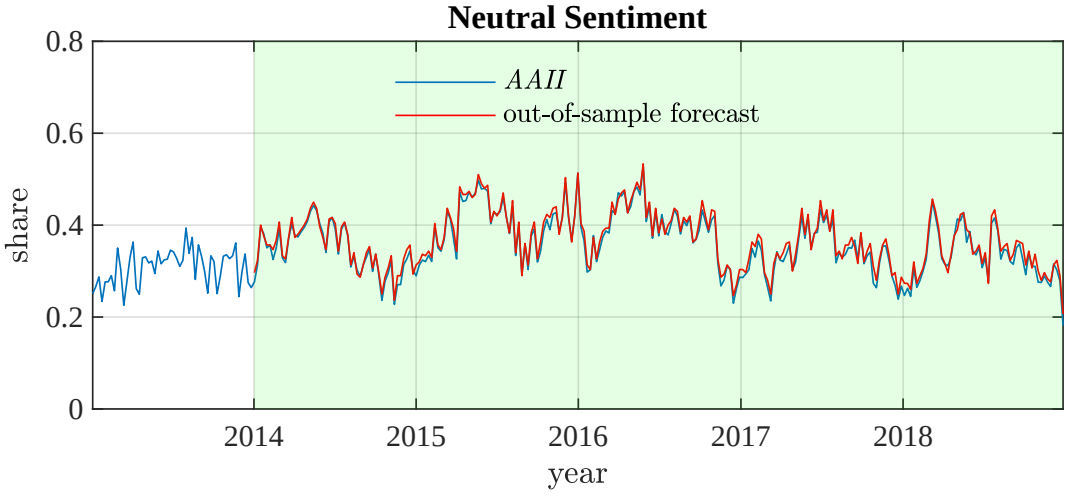

Figure 48: Time series of *AAII* Neutral Sentiment Survey data with forecast from 2014 to 2018 (red line) for parameter estimates from Model III.

In Fig. 49, Fig. 50 and Fig. 51 the weekly time series of the *AAII* Investor Sentiment Survey data from 1999 until 2013 can be seen. The panels depict bullish, bearish and neutral sentiment shares and their corresponding forecasts for the period from 2014 until 2018 for Model IV.

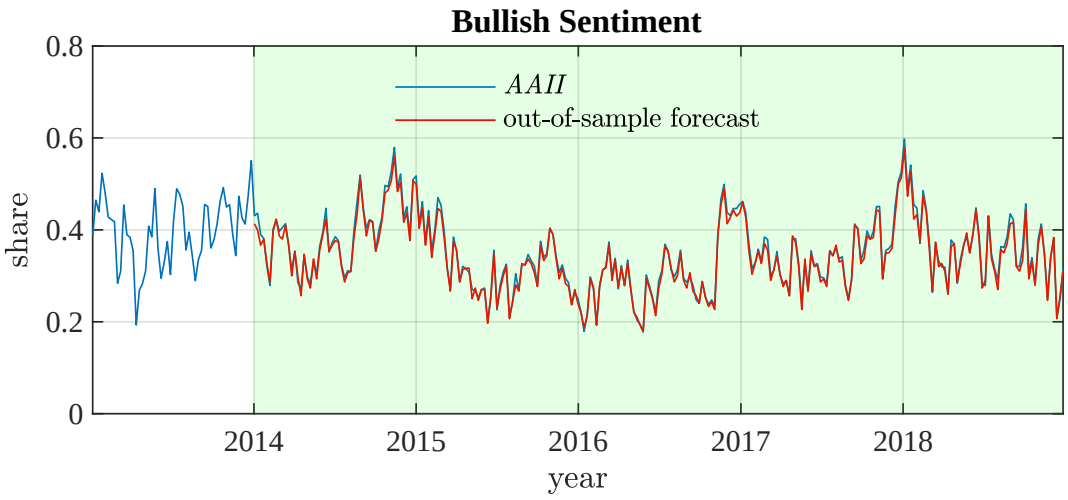

Figure 49: Time series of *AAII* Bullish Sentiment Survey data with forecast from 2014 to 2018 (red line) for parameter estimates from Model IV.

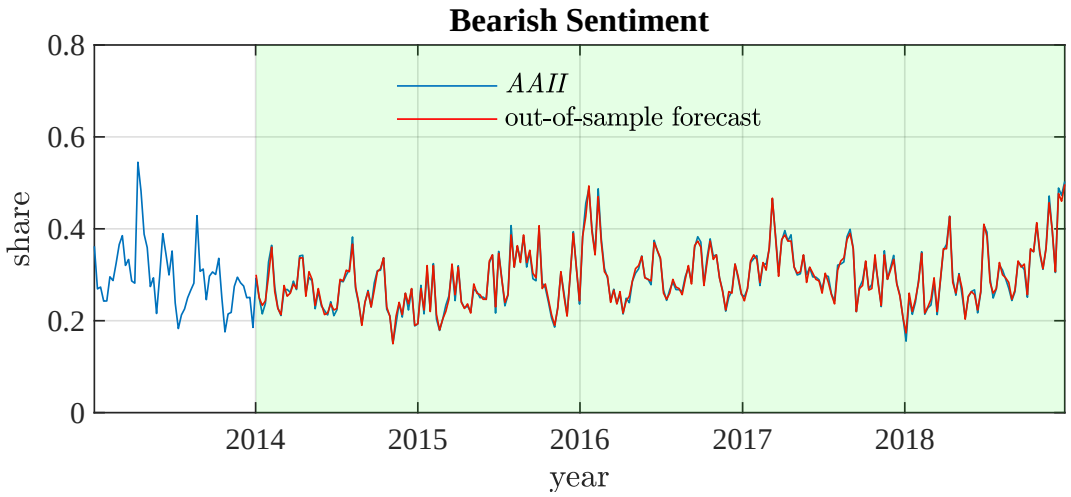

Figure 50: Time series of *AAII* Bearish Sentiment Survey data with forecast from 2014 to 2018 (red line) for parameter estimates from Model IV.

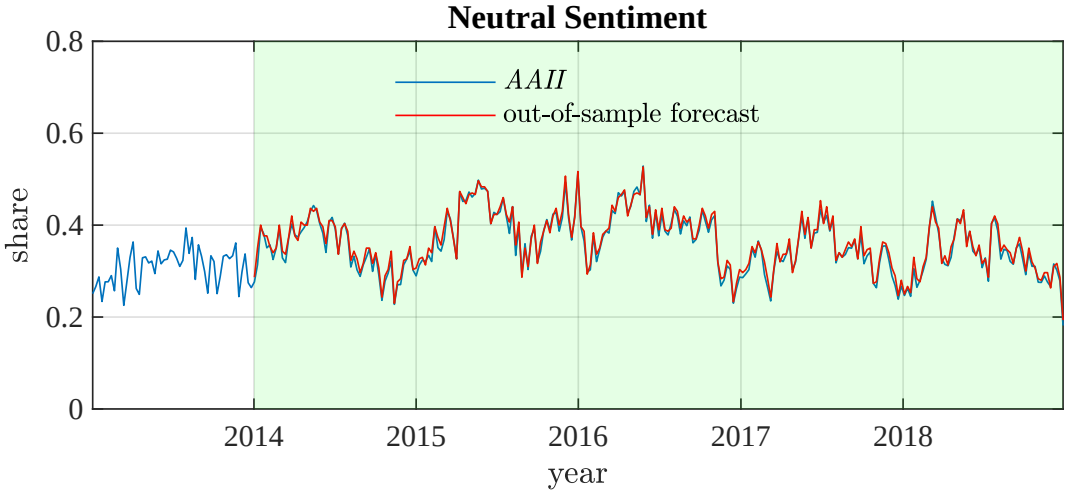

Figure 51: Time series of *AAII* Neutral Sentiment Survey data with forecast from 2014 to 2018 (red line) for parameter estimates from Model IV.

In Fig. 52, Fig. 53 and Fig. 54 the weekly time series of the *AAII* Investor Sentiment Survey data from 1999 until 2013 can be seen. The panels depict bullish, bearish and neutral sentiment shares and their corresponding forecasts for the period from 2014 until 2018 for Model V.

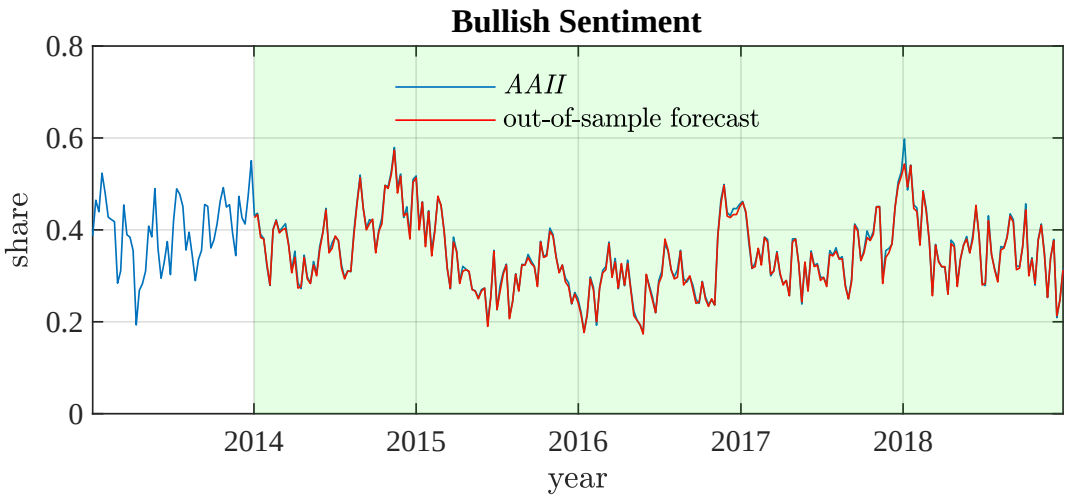

Figure 52: Time series of *AAII* Bullish Sentiment Survey data with forecast from 2014 to 2018 (red line) for parameter estimates from Model V.

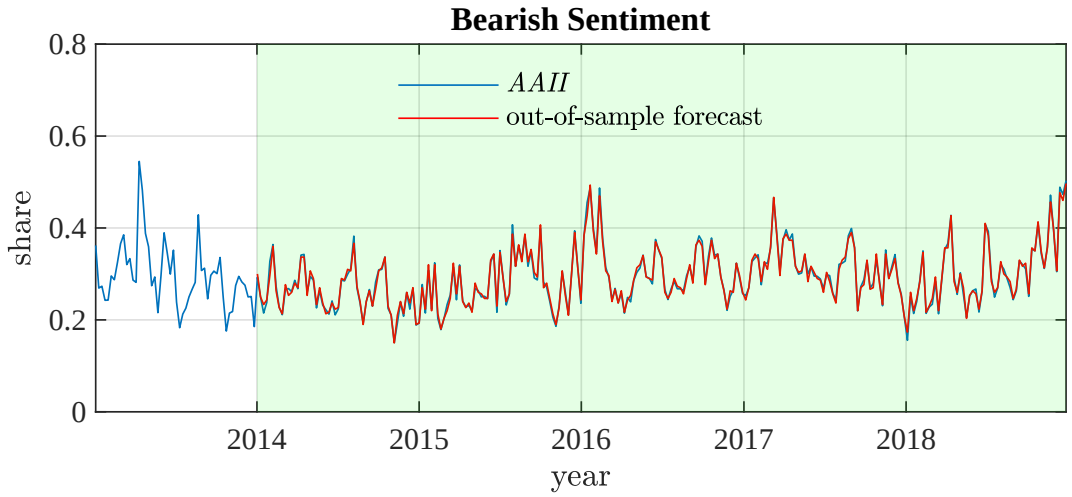

Figure 53: Time series of *AAII* Bearish Sentiment Survey data with forecast from 2014 to 2018 (red line) for parameter estimates from Model V.

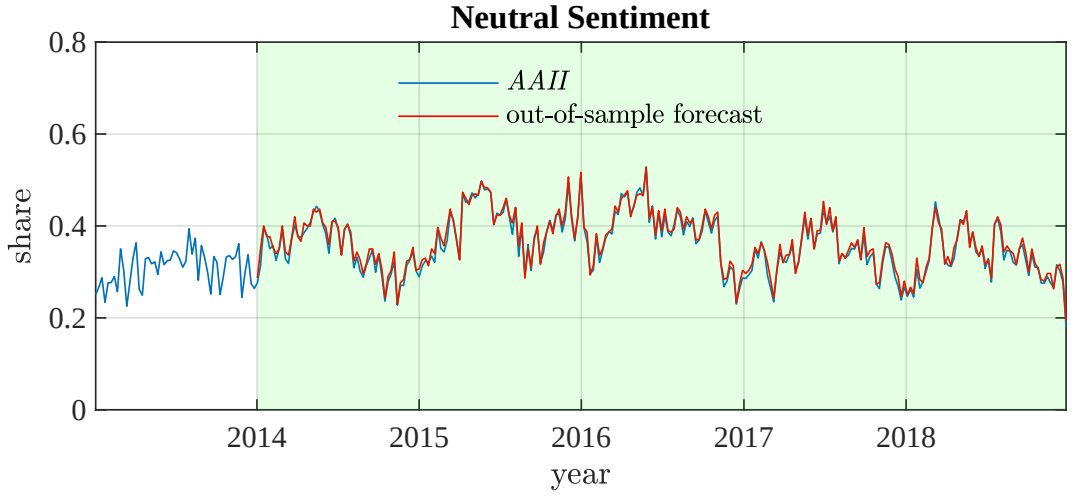

Figure 54: Time series of *AAII* Neutral Sentiment Survey data with forecast from 2014 to 2018 (red line) for parameter estimates from Model V.

Figure 55, Fig. 56 and Fig. 57 show the weekly time series of the *AAII* Investor Sentiment Survey data from 1999 until 2013. The panels depict bullish, bearish and neutral sentiment shares and their corresponding forecasts for the period from 2014 until 2018 for Model VI.

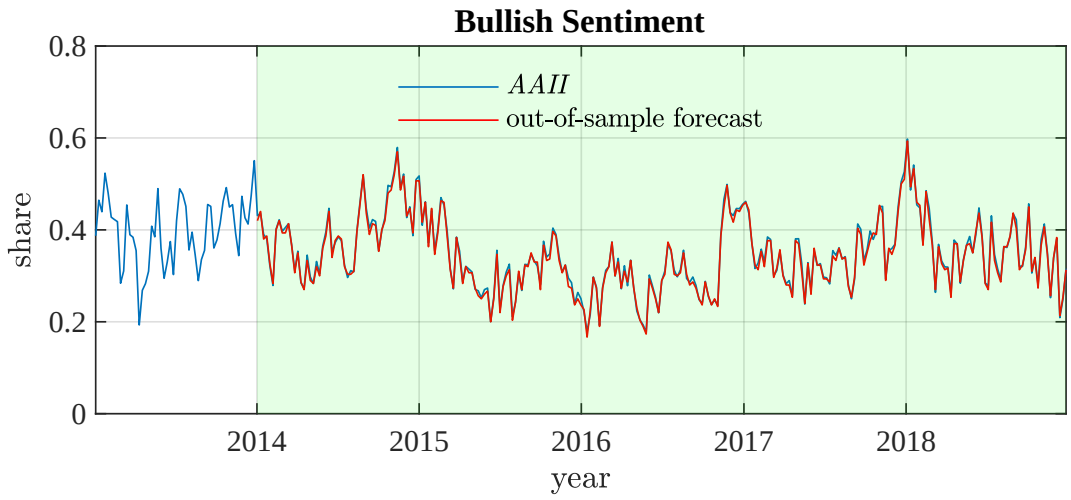

Figure 55: Time series of *AAII* Bullish Sentiment Survey data with forecast from 2014 to 2018 (red line) for parameter estimates from Model VI.

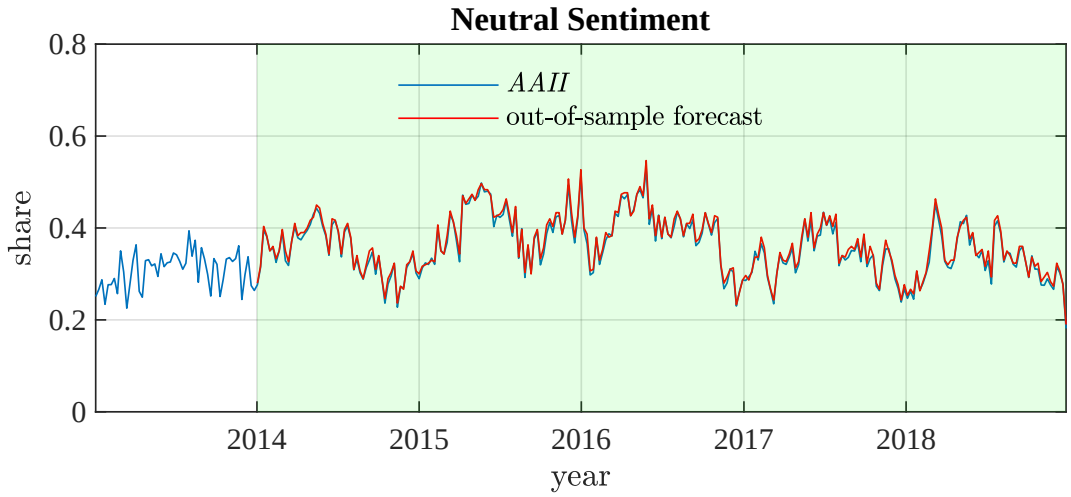

Figure 56: Time series of *AAII* Bearish Sentiment Survey data with forecast from 2014 to 2018 (red line) for parameter estimates from Model VI.

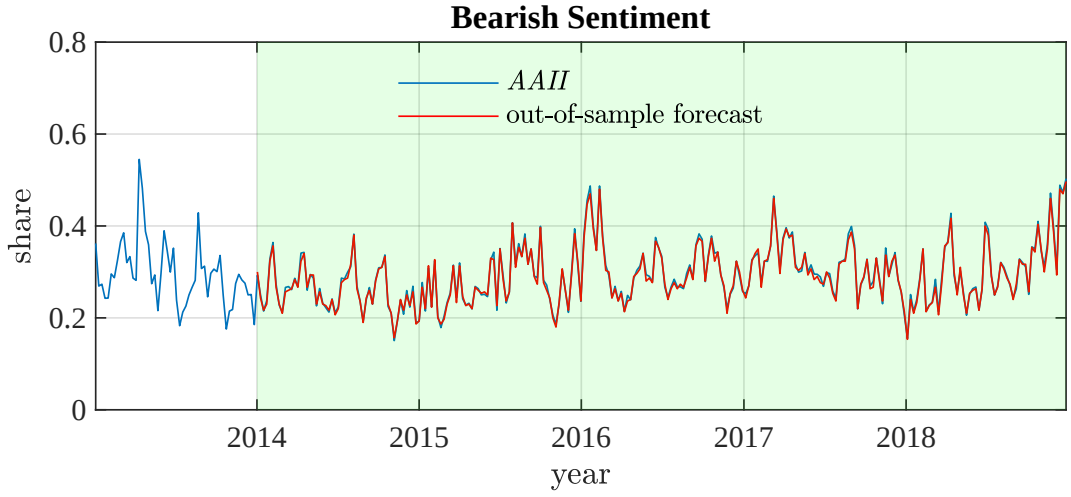

Figure 57: Time series of *AAII* Neutral Sentiment Survey data with forecast from 2014 to 2018 (red line) for parameter estimates from Model VI.

Figure 58, Fig. 59 and Fig. 60 show the weekly time series of the *AAII* Investor Sentiment Survey data from 1999 until 2013. The panels depict bullish, bearish and neutral sentiment shares and their corresponding forecasts for the period from 2014 until 2018 for Model VII.

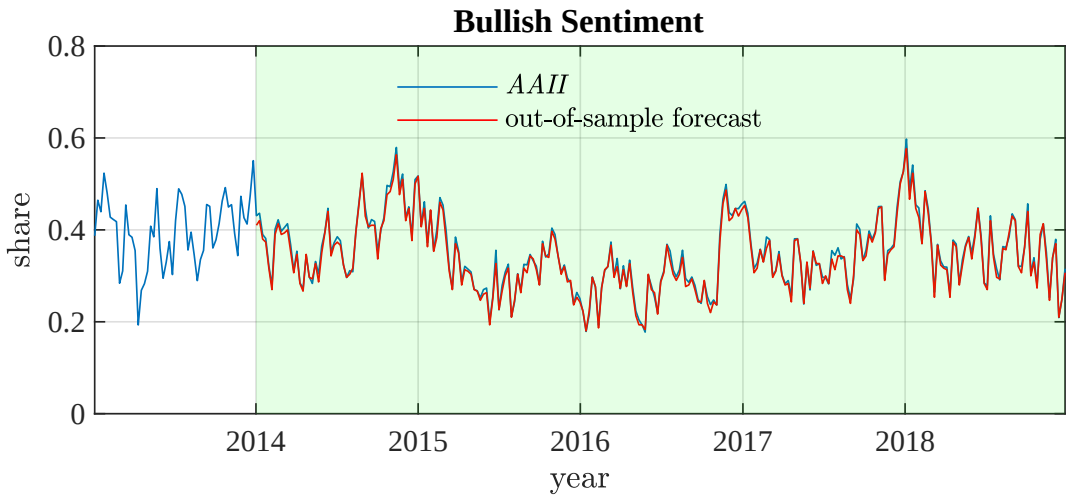

Figure 58: Time series of *AAII* Bullish Sentiment Survey data with forecast from 2014 to 2018 (red line) for parameter estimates from Model VII.

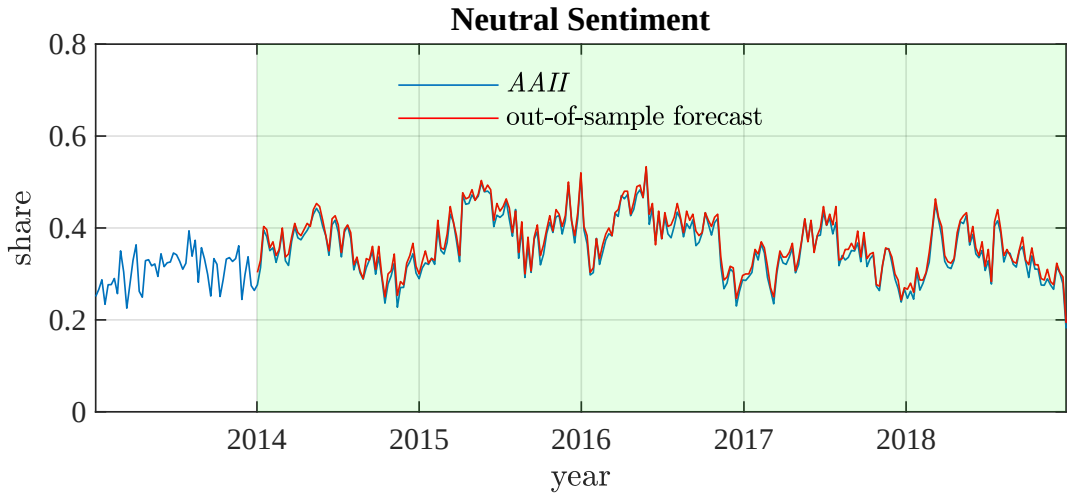

Figure 59: Time series of *AAII* Bearish Sentiment Survey data with forecast from 2014 to 2018 (red line) for parameter estimates from Model VII.

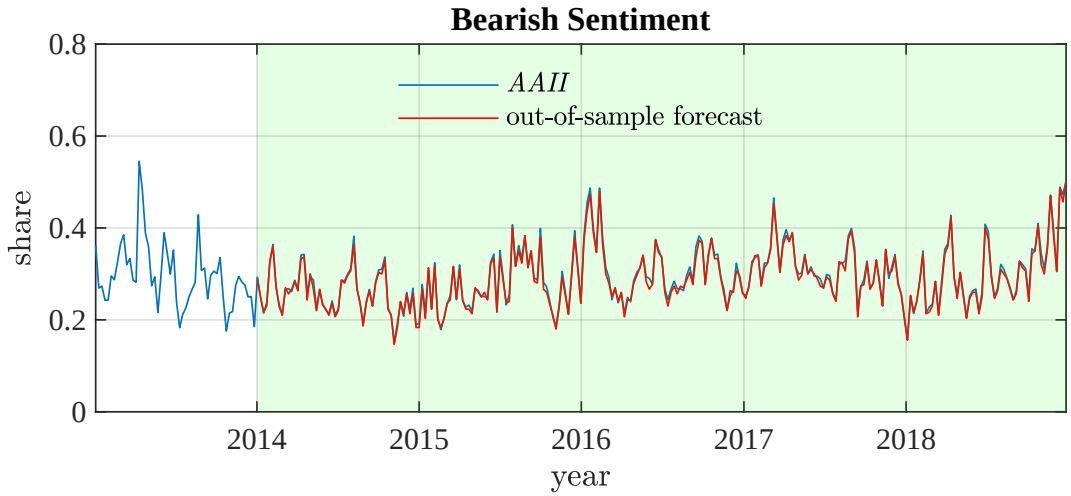

Figure 60: Time series of *AAII* Neutral Sentiment Survey data with forecast from 2014 to 2018 (red line) for parameter estimates from Model VII.

Figure 61, Fig. 62 and Fig. 63 show the weekly time series of the *AAII* Investor Sentiment Survey data from 1999 until 2013. The panels depict bullish, bearish and neutral sentiment shares and their corresponding forecasts for the period from 2014 until 2018 for Model VIII.

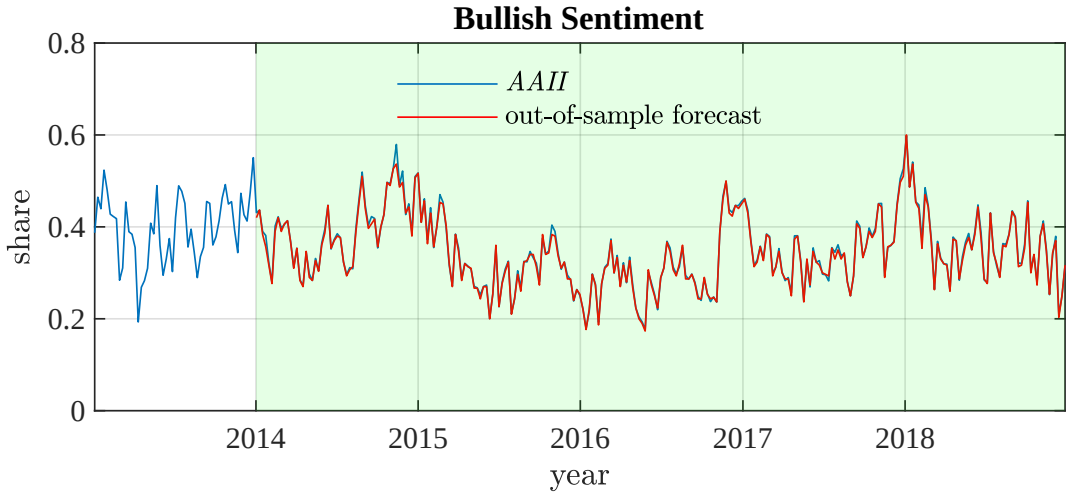

Figure 61: Time series of *AAII* Bullish Sentiment Survey data with forecast from 2014 to 2018 (red line) for parameter estimates from Model VIII.

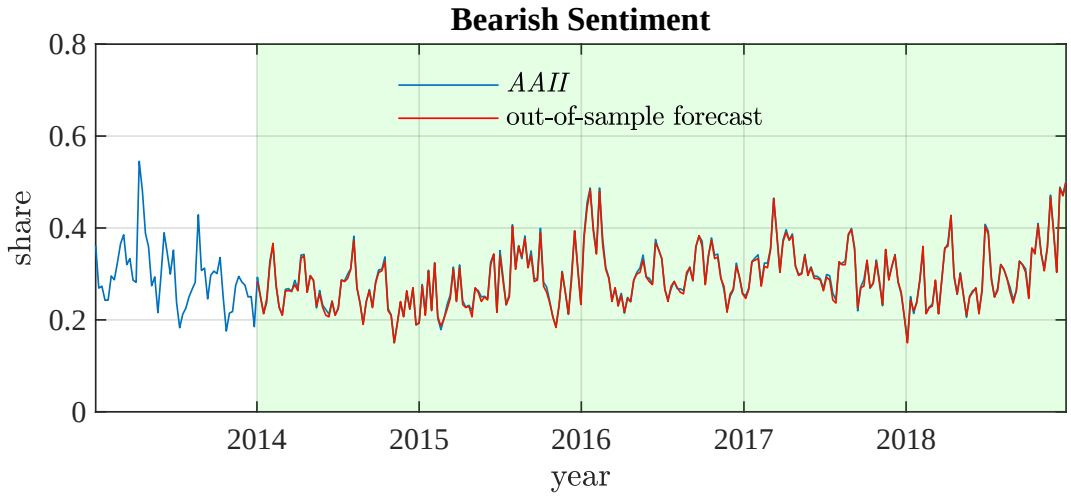

Figure 62: Time series of *AAII* Bearish Sentiment Survey data with forecast from 2014 to 2018 (red line) for parameter estimates from Model VIII.

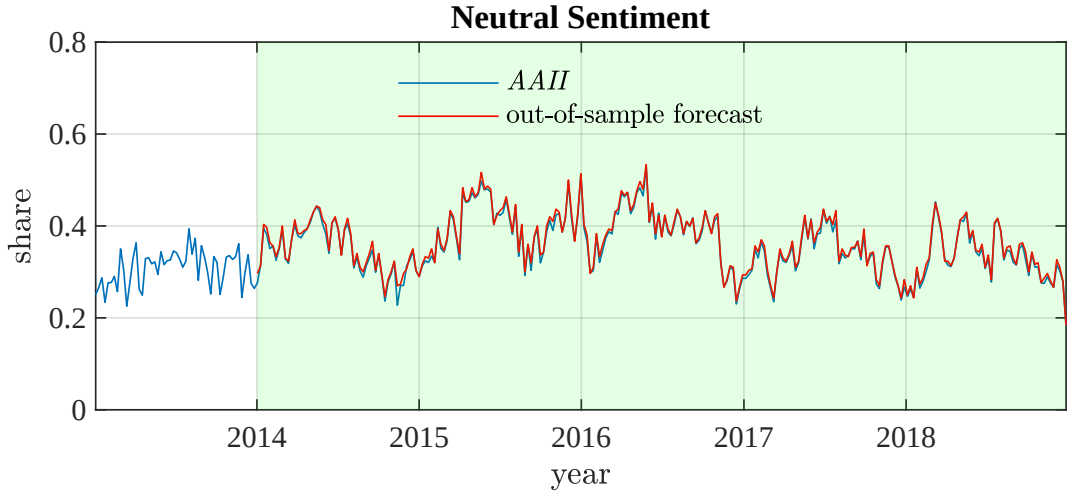

Figure 63: Time series of *AAII* Neutral Sentiment Survey data with forecast from 2014 to 2018 (red line) for parameter estimates from Model VIII.

In Fig. 64, Fig. 65 and Fig. 66 the weekly time series of the *AAII* Investor Sentiment Survey data from 1999 until 2013 can be seen. The panels depict bullish, bearish and neutral sentiment shares and their corresponding forecasts for the period from 2014 until 2018 for Model IX.

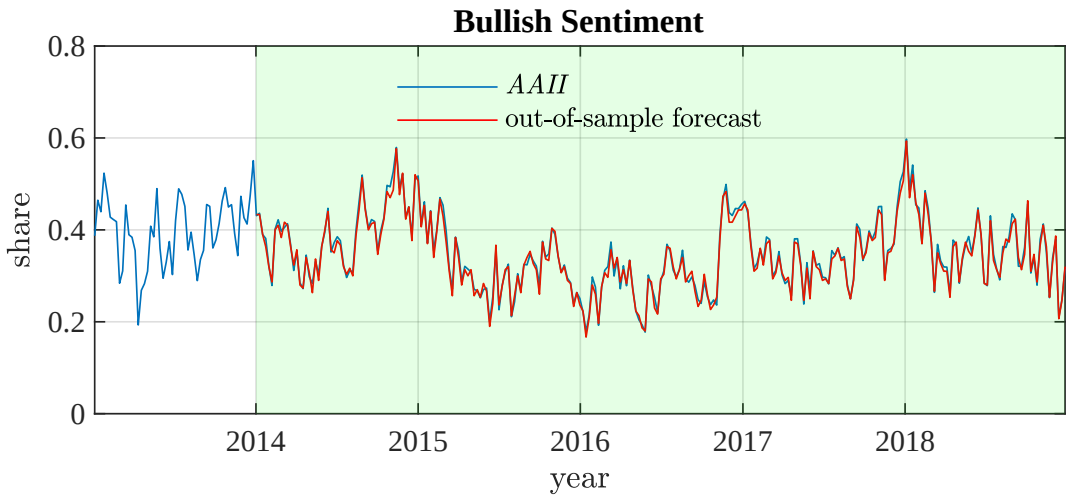

Figure 64: Time series of *AAII* Bullish Sentiment Survey data with forecast from 2014 to 2018 (red line) for parameter estimates from Model IX.

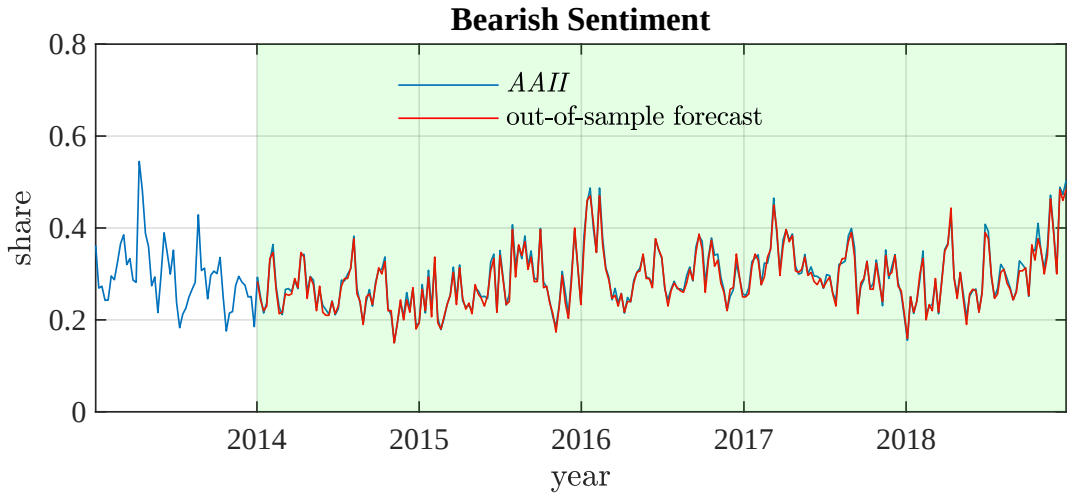

Figure 65: Time series of *AAII* Bearish Sentiment Survey data with forecast from 2014 to 2018 (red line) for parameter estimates from Model IX.

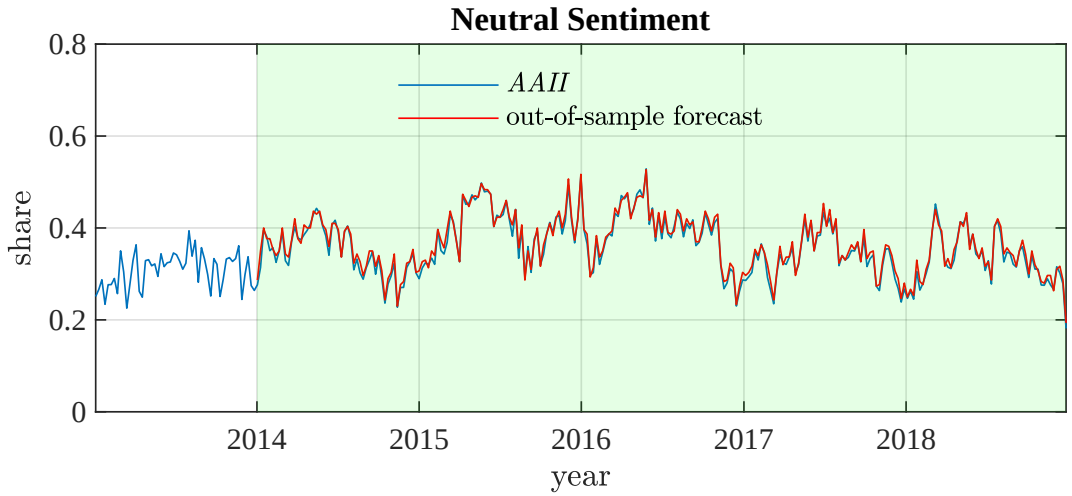

Figure 66: Time series of *AAII* Neutral Sentiment Survey data with forecast from 2014 to 2018 (red line) for parameter estimates from Model IX.

In Fig. 67, Fig. 68 and Fig. 69 the weekly time series of the *AAII* Investor Sentiment Survey data from 1999 until 2013 can be seen. The panels depict bullish, bearish and neutral sentiment shares and their corresponding forecasts for the period from 2014 until 2018 for Model X.

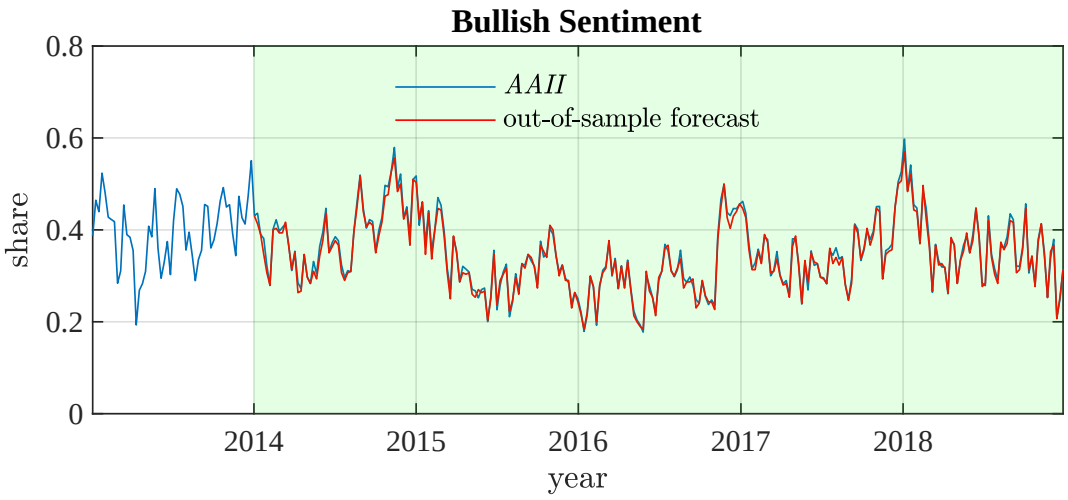

Figure 67: Time series of *AAII* Bullish Sentiment Survey data with forecast from 2014 to 2018 (red line) for parameter estimates from Model X.

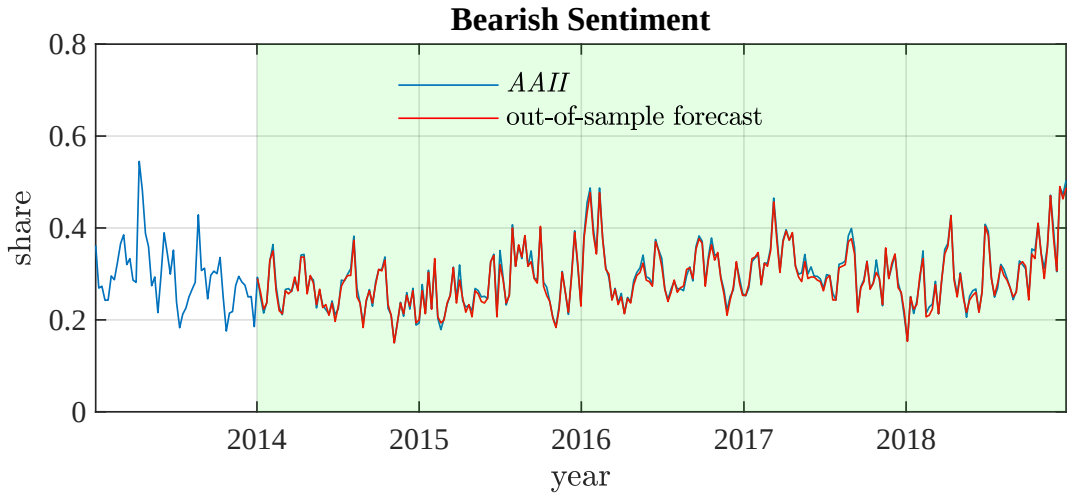

Figure 68: Time series of *AAII* Bearish Sentiment Survey data with forecast from 2014 to 2018 (red line) for parameter estimates from Model X.

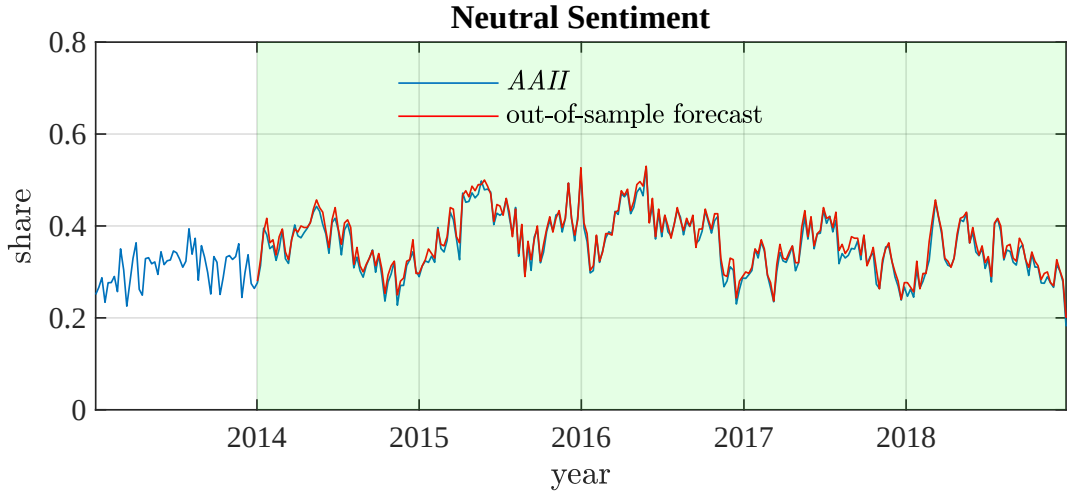

Figure 69: Time series of *AAII* Neutral Sentiment Survey data with forecast from 2014 to 2018 (red line) for parameter estimates from Model X.

B Mathematical Appendix

B.1 Transition Probability Approach

In this section mathematical derivations of equations, proofs and additional theoretical fundamentals are provided for the transition probability approach with unweighted and weighted feedback.

B.1.1 Derivations

B.1.1.1 Derivation of System of ODEs (8)

For $\nu = 1$ the following relationships for hyperbolic functions are employed,
i.e. $\exp(x) = \cosh(x) + \sinh(x)$, $\cosh(x) = \frac{\exp(x)+\exp(-x)}{2}$ and $\tanh(x) = \frac{\sinh(x)}{\cosh(x)}$.

$$
\begin{aligned}
\dot{b} &= (1-b-c)\,\exp(f_b) \;-\; b\,\exp(-f_b) \\
&= (1-c)\,\exp(f_b) \;-\; 2b\,\tfrac{\exp(f_b)+\exp(-f_b)}{2} \\
&= (1-c)\,\cosh(f_b) \;+\; (1-c)\,\sinh(f_b) \;-\; 2b\,\cosh(f_b) \\
&= (1-c)\,\sinh(f_b) \;-\; (\,2b+c-1)\,\cosh(f_b) \\
&= [\,(1-c)\,\tfrac{\sinh(f_b)}{\cosh(f_b)} \;-\; (\,2b+c-1)]\,\cosh(f_b) \\
&= [\,(1-c)\,\tanh(f_b) \;-\; (\,2b+c-1)]\,\cosh(f_b)\,.
\end{aligned}
$$

It is straightforward to show the identity for the differential equation $\dot{c}$.

B.1.1.2 Derivation of Discriminant (12)

$$
\begin{aligned}
\Delta &= tr(J)^2 - 4\,det(J) \\
&= \big(\,2\phi(1-c) - 2 - 2\phi(\,2b + c - 1\,)\tanh(f_b)\,\big)^2\cosh^2(f_b) \\
&\quad + \big(\,2\phi(1-b) - 2 - 2\phi(\,2c + b - 1\,)\tanh(f_c)\,\big)^2\cosh^2(f_c) \\
&\quad + 2\cdot\cosh(f_b)\cosh(f_c)\cdot\big(\,2\phi(1-c) - 2 - 2\phi(\,2b + c - 1\,)\tanh(f_b)\,\big) \\
&\qquad\qquad \cdot\big(\,2\phi(1-b) - 2 - 2\phi(\,2c + b - 1\,)\tanh(f_c)\,\big) \\
&\quad - 4\cdot\cosh(f_b)\cosh(f_c)\cdot\big[\,3\phi^2(1-b)(1-c) - 3\phi(1-b) \\
&\qquad\qquad -3\phi(1-c) + 3 \\
&\qquad\qquad + \tanh(f_b)\big(\,-3\phi^2(\,2b + c - 1\,)(1-b) \\
&\qquad\qquad\qquad + 3\phi(\,2b + c - 1\,) \\
&\qquad\qquad\qquad + \phi(1-b) - 1\,\big) \\
&\qquad\qquad + \tanh(f_c)\big(\,-3\phi^2(\,2c + b - 1\,)(1-c) \\
&\qquad\qquad\qquad + 3\phi(\,2c + b - 1\,) \\
&\qquad\qquad\qquad + \phi(1-c) - 1\,\big) \\
&\qquad\qquad + \tanh(f_b)\tanh(f_c)\big(\,3\phi^2(\,2b + c - 1\,) \\
&\qquad\qquad\qquad\qquad \cdot(\,2c + b - 1\,) \\
&\qquad\qquad\qquad\qquad - \phi(\,2b + c - 1\,) \\
&\qquad\qquad\qquad\qquad - \phi(\,2c + b - 1\,) - 1\,\big)\big]
\end{aligned}
$$

$$
\begin{aligned}
= \quad & \big(\,2\phi(1-c)-2-2\phi(\,2b+c-1\,)\tanh(f_b)\,\big)^2\cosh^2(f_b) \\
& +\big(\,2\phi(1-b)-2-2\phi(\,2c+b-1\,)\tanh(f_c)\,\big)^2\cosh^2(f_c) \\
& +\,\cosh(f_b)\cosh(f_c)\cdot\big[\,-4\phi^2(1-b)(1-c)+4\phi(1-b) \\
& \qquad\qquad +4\phi(1-c)-4 \\
& \qquad\qquad +\tanh(f_b)\big(\,4\phi^2(\,2b+c-1\,)(1-b)-4\phi(1-b) \\
& \qquad\qquad\qquad -4\phi(\,2b+c-1\,)+4\,\big) \\
& \qquad\qquad +\tanh(f_c)\big(\,4\phi^2(\,2c+b-1\,)(1-c)-4\phi(1-c) \\
& \qquad\qquad\qquad -4\phi(\,2c+b-1\,)+4\,\big) \\
& \qquad\qquad +\tanh(f_b)\tanh(f_c)\big(\,-4\phi^2(\,2b+c-1\,) \\
& \qquad\qquad\qquad\qquad \cdot(\,2c+b-1\,) \\
& \qquad\qquad\qquad\qquad +4\phi(\,2b+c-1\,) \\
& \qquad\qquad\qquad\qquad +4\phi(\,2c+b-1\,)+4\,\big)\big] \\
= \quad & \big(\,2\phi(1-c)-2-2\phi(\,2b+c-1\,)\tanh(f_b)\,\big)^2\cosh^2(f_b) \\
& +\big(\,2\phi(1-b)-2-2\phi(\,2c+b-1\,)\tanh(f_c)\,\big)^2\cosh^2(f_c) \\
& -\,\cosh(f_b)\cosh(f_c)\cdot\Big[\big(\,2\phi(1-b)-2\,\big)\big(\,2\phi(1-c)-2\,\big) \\
& \qquad\qquad -\tanh(f_b)\big[\,2\phi(\,2b+c-1\,)\big(\,2\phi(1-b)-2\,\big) \\
& \qquad\qquad\qquad -2\big(\,2\phi(1-b)-2\,\big)\big] \\
& \qquad\qquad -\tanh(f_c)\big[\,2\phi(\,2c+b-1\,)\big(\,2\phi(1-c)-2\,\big) \\
& \qquad\qquad\qquad -2\big(\,2\phi(1-c)-2\,\big)\big] \\
& \qquad\qquad +\tanh(f_b)\tanh(f_c)\big(\,2\phi(\,2b+c-1\,) \\
& \qquad\qquad\qquad\qquad \cdot 2\phi(\,2c+b-1\,)\big) \\
& \qquad\qquad -\tanh(f_b)\tanh(f_c)\big(\,4\phi(\,2b+c-1\,) \\
& \qquad\qquad\qquad\qquad +4\phi(\,2c+b-1\,)+4\,\big)\Big]
\end{aligned}
$$

$$
\begin{aligned}
= \quad & \big(\,2\phi(1-c)-2-2\phi(\,2b+c-1\,)\tanh(f_b)\,\big)^2\cosh^2(f_b) \\
& +\big(\,2\phi(1-b)-2-2\phi(\,2c+b-1\,)\tanh(f_c)\,\big)^2\cosh^2(f_c) \\
& -\cosh(f_b)\cosh(f_c)\cdot\Big[\big(\,2\phi(1-b)-2\,\big)\big(\,2\phi(1-c)-2\,\big) \\
& \qquad -\tanh(f_b)\big[\big(\,2\phi(1-b)-2\,\big) \\
& \qquad\qquad \cdot\big(\,2\phi(\,2b+c-1\,)-2\,\big)\big] \\
& \qquad -\tanh(f_c)\big[\big(\,2\phi(1-c)-2\,\big) \\
& \qquad\qquad \cdot\big(\,2\phi(\,2c+b-1\,)-2\,\big)\big] \\
& \qquad +\tanh(f_b)\tanh(f_c)\big(\,2\phi(\,2b+c-1\,) \\
& \qquad\qquad \cdot 2\phi(\,2c+b-1\,)\big) \\
& \qquad -\tanh(f_b)\tanh(f_c)\big(\,4\phi(\,2b+c-1\,) \\
& \qquad\qquad +4\,\phi(\,2c+b-1\,)+4\,\big)\Big] \\
= \quad & \big(\,2\phi(1-c)-2-2\phi(\,2b+c-1\,)\tanh(f_b)\,\big)^2\cosh^2(f_b) \\
& +\big(\,2\phi(1-b)-2-2\phi(\,2c+b-1\,)\tanh(f_c)\,\big)^2\cosh^2(f_c) \\
& -\cosh(f_b)\cosh(f_c)\cdot\big[\big(\,2\phi(1-b)-2-2\phi(\,2b+c-1\,)\tanh(f_b)\,\big) \\
& \qquad \cdot\big(\,2\phi(1-c)-2-2\phi(\,2c+b-1\,)\tanh(f_c)\,\big) \\
& \qquad +2\big(\,2\phi(1-b)-2\,\big)\tanh(f_b) \\
& \qquad +2\big(\,2\phi(1-c)-2\,\big)\tanh(f_c) \\
& \qquad -\tanh(f_b)\tanh(f_c)\big(\,4\phi(\,2b+c-1\,) \\
& \qquad\qquad +4\,\phi(\,2c+b-1\,)+4\,\big)\big]
\end{aligned}
$$

$$
\begin{aligned}
= \quad & \big[\big(\,2\phi(1-c)-2-2\phi(\,2b+c-1\,)\tanh(f_b)\,\big)\cosh(f_b) \\
& -\big(\,2\phi(1-b)-2-2\phi(\,2c+b-1\,)\tanh(f_c)\,\big)\cosh(f_c)\big]^2 \\
& +\cosh(f_b)\cosh(f_c)\cdot\Big[\big(\,2\phi(1-b)-2\,\big)\big(\,2\phi(1-c)-2\,\big) \\
& \qquad -\tanh(f_b)\big[\big(\,2\phi(1-b)-2\,\big)\cdot 2\phi(\,2b+c-1\,)\big] \\
& \qquad -\tanh(f_c)\big[\big(\,2\phi(1-c)-2\,\big)\cdot 2\phi(\,2c+b-1\,)\big] \\
& \qquad +\tanh(f_b)\tanh(f_c)\big(\,2\phi(\,2b+c-1\,) \\
& \qquad\qquad \cdot 2\phi(\,2c+b-1\,)\big)\Big] \\
& +\cosh(f_b)\cosh(f_c)\cdot\big[\,-2\tanh(f_b)\big(\,2\phi(1-b)-2\,\big) \\
& \qquad -2\tanh(f_c)\big(\,2\phi(1-c)-2\,\big) \\
& \qquad +\tanh(f_b)\tanh(f_c)\big(\,4\phi(\,2b+c-1\,) \\
& \qquad\qquad +4\,\phi(\,2c+b-1\,)+4\,\big)\big] \\
= \quad & \big[\big(\,2\phi(1-c)-2-2\phi(\,2b+c-1\,)\tanh(f_b)\,\big)\cosh(f_b) \\
& -\big(\,2\phi(1-b)-2-2\phi(\,2c+b-1\,)\tanh(f_c)\,\big)\cosh(f_c)\big]^2 \\
& +\cosh(f_b)\cosh(f_c)\cdot\Big[\big(\,2\phi(1-b)-2\,\big)\big(\,2\phi(1-c)-2\,\big) \\
& \qquad -\tanh(f_b)\big[\big(\,2\phi(1-b)-2\,\big) \\
& \qquad\qquad \cdot\big(\,2\phi(\,2b+c-1\,)+2\,\big)\big] \\
& \qquad -\tanh(f_c)\big[\big(\,2\phi(1-c)-2\,\big) \\
& \qquad\qquad \cdot\big(\,2\phi(\,2c+b-1\,)+2\,\big)\big] \\
& \qquad +\tanh(f_b)\tanh(f_c)\big[\big(\,2\phi(\,2b+c-1\,)+2\,\big) \\
& \qquad\qquad \cdot\big(\,2\phi(\,2c+b-1\,)+2\,\big)\big]\Big] \\
= \quad & \big[\big(\,2\phi(1-c)-2-2\phi(\,2b+c-1\,)\tanh(f_b)\,\big)\cosh(f_b) \\
& -\big(\,2\phi(1-b)-2-2\phi(\,2c+b-1\,)\tanh(f_c)\,\big)\cosh(f_c)\big]^2 \\
& +\cosh(f_b)\cosh(f_c)\cdot\big[\,2\phi(1-c)-2-\big(\,2\phi(\,2b+c-1\,)+2\,\big)\tanh(f_b)\big] \\
& \qquad\qquad \cdot\big[\,2\phi(1-b)-2-\big(\,2\phi(\,2c+b-1\,)+2\,\big)\tanh(f_c)\big]
\end{aligned}
$$

B.1.2 Proofs

B.1.2.1 Proof of Proposition 1

We consider

$$\begin{aligned} \dot{b} &= F_b(\, b,\, c;\, \phi) = [\,(1-c)\, \tanh(f_b) \,-\, (\,2b + c - 1)]\, \cosh(f_b) \\ &= 0. \end{aligned}$$

Using $cosh(x) \geq 1$, $c \in [\,0, 1)$ and the feedback index f_b, the differential equation is reduced to

$$\tanh(\phi\,(\,2b + c - 1)) = \frac{(\,2b + c - 1)}{(1-c)}.$$

For the following approximations we employ the assumption $\phi < 1$. Additionally two cases are examined.

Case 1: $2b + c - 1 > 0$

$$\begin{aligned} 2b + c - 1 &< \tfrac{(\,2b+c-1)}{(1-c)} \\ &= \tanh(\phi\,(\,2b + c - 1)) < \tanh(\,2b + c - 1). \end{aligned}$$

But $\tanh(x)$ is a strictly monotonic increasing function and furthermore $\tanh(x) < x$ holds $\forall x \in (0, 1]$ with $x = 2b + c - 1$. Therefore $2b + c - 1 \not> 0$ is valid.

Case 2: $2b + c - 1 < 0$

$$\begin{aligned} \tanh(\,2b + c - 1) &< \tanh(\phi\,(\,2b + c - 1)) \\ &= \tfrac{(\,2b+c-1)}{(1-c)} < 2b + c - 1. \end{aligned}$$

But $\tanh(x)$ is a strictly monotonic increasing function and $\tanh(x) > x$ holds $\forall x \in [-1, 0)$ with $x = 2b + c - 1$. Therefore $2b + c - 1 \not< 0$ is valid. The case-by-case analysis leads to $2b + c - 1 = 0$ which is equivalent to LI_b.

□

It is straightforward to show the implication for the linear isocline LI_c.

B.1.2.2 Proof of Proposition 2

For the first statement we consider the trace, $tr(J) = -4+\frac{8}{3}\phi < 0$, and the determinant of the Jacobian, $det(J) = \frac{4}{3}(\phi - \frac{3}{2})^2 > 0$. The discriminant, $\Delta = \frac{16}{9}(\phi - \frac{3}{2})^2$, reveals monotonic limit behavior for $\phi \neq \frac{3}{2}$. For statement 2 and 3 see Proposition 1.

□

B.1.2.3 Proof of Proposition 3

1. See Eq. (10).
2. We consider Eq. (8) $= 0$, plug in $c = 0$ and $\phi = 1$ and apply $cosh(x) \geq 1$. This results in $\tanh(2b-1) - (2b-1) = 0$. Since $\tanh(x) = x$ leads to $x = 0$ we obtain $2b - 1 = 0 \Leftrightarrow b_0 = 0.5$.
3. For $c = 0$ assume that b_1 is a solution of Eq. (8) $= 0$. We apply $cosh(x) \geq 1$ and get $\tanh(\phi(2b_1-1)) - (2b_1-1) = 0$. Since $\tanh$ is symmetric with respect to the origin this leads to

$$\begin{aligned} 0 &= -\tanh(-\phi(2b_1-1)) - (2b_1-1) \\ &= \tanh(\phi(1-2b_1)) - (1-2b_1) \\ &= \tanh(\phi(2(1-b_1)-1)) - (2(1-b_1)-1) \\ &= \tanh(\phi(2b_2-1)) - (2b_2-1). \end{aligned}$$

4. For $b_1 > 0.5$ $\lim_{\phi\to\infty} \tanh(\phi(2b_1-1)) - (2b_1-1) = 1 - (2b_1-1)$ holds.
   Since b_1 is a b-axis intercept we know $1-(2b_1-1) = 0 \Leftrightarrow \lim_{\phi\to\infty} b_1 = 1$.
   Furthermore $\lim_{\phi\to\infty} b_2 = \lim_{\phi\to\infty} 1 - b_1 = 0$.

□

B.1.3 Bifurcation Types

Consider a two-dimensional continuous-time system depending on one parameter

$$\dot{x} = f(x, \phi), x \in \mathbb{R}^2, \phi \in \mathbb{R},$$

where f is smooth with respect to both x and ϕ. Assume that a bifurcation of the dynamical system occurs at $\phi = \phi^e$ for the equilibrium $x = x^e$ and the corresponding Jacobian matrix J^e has two eigenvalues λ_1^e and λ_2^e.

The following annotations are based on definitions in Kuznetsov (2004), Strogatz (1994) and Wiggins (2003).

B.1.3.1 Saddle-node Bifurcation

A saddle-node bifurcation is a local bifurcation in which two equilibria of a dynamical system are created. The Jacobian matrix J^e has an eigenvalue $\lambda_1^e = 0$ evaluated at the bifurcation point (x^e, ϕ^e).

For all the other values of $\phi \neq \phi^e$ the behavior of the system is distinct. For $\phi < \phi^e$ there are no equilibria in the system. For $\phi > \phi^e$ the system has two equilibria, one is stable, while the other one is unstable, more specifically it is a saddle-point equilibrium.

The equation $f(x, \phi) = 0$ defines an equilibrium manifold in the bifurcation diagram. This particular type of bifurcation is referred to as a supercritical saddle-node bifurcation. A subcritical saddle-node bifurcation exhibits two equilibrium points for $\phi < \phi^e$ and no equilibrium for $\phi > \phi^e$.

B.1.3.2 Pitchfork Bifurcation

A dynamical system exhibiting a pitchfork bifurcation is a particular type of local bifurcation where the system transitions from one equilibrium to three equilibria. So the system has an equilibrium for all ϕ. This equilibrium is stable for $\phi < \phi^e$ and unstable for $\phi > \phi^e$. For $\phi > \phi^e$, there are two additional equilibria branching from the

bifurcation point (x^e, ϕ^e) which are stable. This is a supercritical pitchfork bifurcation.

A subcritical pitchfork bifurcation is detected in a system with three equilibria for all ϕ. One equilibrium is stable for $\phi < \phi^e$ and unstable for $\phi > \phi^e$. For $\phi < \phi^e$, there are two additional equilibria branching to the bifurcation point (x^e, ϕ^e) which are unstable.

Continuous dynamical and symmetrical systems generically feature pitchfork bifurcations.

B.1.3.3 Transcritical Bifurcation

A transcritical bifurcation is a particular kind of local bifurcation, meaning that it is characterized by an equilibrium having an eigenvalue whose real part passes through zero.

A transcritical bifurcation is one in which a fixed point exists for all values of a parameter and is never destroyed. However, such a fixed point interchanges its stability with another fixed point as the parameter is varied. In other words, both before and after the bifurcation, there is one unstable and one stable fixed point. However, their stability is exchanged when they collide. So the unstable fixed point becomes stable and vice versa.

For $\phi < \phi^e$, there are two equilibria, the first one is stable and the second one is unstable. These two equilibria coalesce at $\phi = \phi^e$ and exchange their stability behavior. Hence for $\phi > \phi^e$, the first equilibrium is unstable and the second one is stable.

A transcritical saddle-source bifurcation is defined as a transcritical bifurcation with one unstable (source) manifold and one saddle manifold.

B.2 Discrete Choice Approach

In this section mathematical derivations of equations are provided for the discrete choice approach.

B.2.1 Derivations

The deterministic adjustment equations that governs the changes in the fractions b_t of bold agents c_t of cautious agents are

$$\begin{aligned} b_{t+\Delta t} &= b_t + \Delta t \cdot [\pi_t^b(f_b) - b_t], \\ c_{t+\Delta t} &= c_t + \Delta t \cdot [\pi_t^c(f_c) - c_t]. \end{aligned}$$

B.3 A Stochastic Model of Investor Sentiment

B.3.1 Sentiment Dynamics

The following *Taylor series expansion* around (x, y) is needed to derive the *Fokker-Planck-equation*:

$$
\begin{aligned}
\frac{\partial p\left(x,y;t\right)}{\partial t} \;=\; & p\left(x,y\right)\cdot\big[w_{0c}\left(xN+1,yN-1\right)-w_{0c}\left(xN,yN\right)\\
& \quad +w_{c0}\left(xN-1,yN+1\right)-w_{c0}\left(xN,yN\right)\\
& \quad +w_{0b}\left(xN+1,yN-1\right)-w_{0b}\left(xN,yN\right)\\
& \quad +w_{b0}\left(xN-1,yN+1\right)-w_{b0}\left(xN,yN\right)\\
& \quad +w_{bc}\left(xN,yN\right)+w_{cb}\left(xN,yN\right)\big]\\
& +\frac{\partial p\left(x,y;t\right)}{\partial x}\cdot\Big[\frac{1}{N}\big(w_{0b}\left(xN+1,yN-1\right)\\
& \quad -w_{b0}\left(xN-1,yN+1\right)\\
& \quad +w_{cb}\left(xN+1,yN\right)\\
& \quad -w_{bc}\left(xN-1,yN\right)\big)\Big]\\
& +\frac{\partial p\left(x,y;t\right)}{\partial y}\cdot\Big[\frac{1}{N}\big(-w_{0c}\left(xN+1,yN-1\right)\\
& \quad +w_{c0}\left(xN-1,yN+1\right)\\
& \quad -w_{0b}\left(xN+1,yN-1\right)\\
& \quad +w_{b0}\left(xN-1,yN+1\right)\big)\Big]\\
& +\ldots
\end{aligned}
$$

$$
\begin{aligned}
&\dots \\
&+ \frac{\partial^2 p\left(x,y;t\right)}{\partial x^2} \cdot \Big[\frac{1}{2N^2}\big(w_{0c}\left(xN+1,yN-1\right) \\
&\qquad\qquad + w_{c0}\left(xN-1,yN+1\right) \\
&\qquad\qquad + w_{0b}\left(xN+1,yN-1\right) \\
&\qquad\qquad + w_{b0}\left(xN-1,yN+1\right)\big)\Big] \\
&+ \frac{\partial^2 p\left(x,y;t\right)}{\partial y^2} \cdot \Big[\frac{1}{2N^2}\big(w_{0c}\left(xN+1,yN-1\right) \\
&\qquad\qquad + w_{c0}\left(xN-1,yN+1\right) \\
&\qquad\qquad + w_{0b}\left(xN+1,yN-1\right) \\
&\qquad\qquad + w_{b0}\left(xN-1,yN+1\right)\big)\Big] \\
&+ \frac{\partial^2 p\left(x,y;t\right)}{\partial y \partial x} \cdot \Big[\frac{1}{N^2}\big(-w_{0c}\left(xN+1,yN-1\right) \\
&\qquad\qquad - w_{c0}\left(xN-1,yN+1\right) \\
&\qquad\qquad - w_{0b}\left(xN+1,yN-1\right) \\
&\qquad\qquad - w_{b0}\left(xN-1,yN+1\right)\big)\Big]
\end{aligned}
$$

B.3.2 Sensitivity Analysis

	Model XI	Model XII
Parameter estimates		
ν_0	2.8246 (0.0101)	2.8244 (0.001)
ν_1	4.0005 (0.0171)	4.0 (0.0)
α_0	-	-
α_1	-	0.6742 (0.0006)
α_2	0.1626 (0.0107)	-
β_0	-0.512 (0.0118)	-0.5127 (0.0696)
β_1	-0.23 (0.0887)	-0.2244 (0.5049)
β_2	1.2352 (0.183)	1.2367 (0.0001)
Goodness-of-fit measures		
Log L	-456.9092	-498.8798
AIC	925.8184	1009.7596
BIC	943.0236	1026.9648

Table 9: Parameter estimates, corresponding standard errors in brackets and goodness-of-fit measures for two additional restricted bi-variate stochastic models of investor sentiment regarding the parameters α_0 and α_1, respectively α_0 and α_2.

Declaration

I hereby affirm that I have completed my doctoral thesis entitled, ”Three-State Sentiment Dynamics” entirely on my own and unassisted, and that I have specially marked all of the quotes I have used from other authors as well as these passages in my work that are extremely close to the thoughts presented by other authors, and listed the sources in accordance with the regulations I have been given.

Veronika Penner